ABSTRACT

FRICK, KONOR L. Coupling and Design of a Thermal Energy Storage System for Small Modular Reactors. (Under the direction of Dr. J. Michael Doster).

The contribution of intermittent (renewable) energy sources such as wind and solar continues to increase as renewables improve in both efficiency and price-point. However, the variability of renewables generates additional challenges for the electric grid in the form of rapidly varying electric loads.

Proposed options for accommodating this load have included operating nuclear reactors in a load follow mode, or operating the reactor at or near steady state and bypassing steam directly to the condenser. Both of these strategies result in lost energy potential. In addition to lost energy potential, load follow operation can result in increased stress on the fuel and other mechanical components. A more attractive approach is to operate the reactor at or near steady state and bypass excess steam to a thermal energy storage system. The thermal energy can then be recovered, either for electric generation during periods of peak electric demand, or for use in ancillary applications such as desalination and hydrogen production.

Sensible Heat Thermal Energy Storage is a mature technology currently used in solar energy systems. This research focuses on the design and coupling of such a system to Small Modular Reactors (SMRs), typical of Integral Pressurized Water Reactor (IPWR) designs currently under development.

Coupling and Design of a Thermal Energy Storage System for Small Modular Reactors

by
Konor L Frick

A thesis submitted to the Graduate Faculty of
North Carolina State University
in partial fulfillment of the
requirements for the degree of
Masters of Science

Nuclear Engineering

Raleigh, North Carolina

2016

APPROVED BY:

_____   _____
Dr. Stephen Terry   Dr. Mohamed A. Bourham

_____
Dr. J. Michael Doster,
Committee Chair

BIOGRAPHY

Konor Frick, an avid sports fan, was born 17 March 1993. He grew up across the eastern seaboard, having started school in North Carolina and ultimately graduating Shenendehowa High School in Upstate New York.

He earned his undergraduate degree at North Carolina State University (NCSU) in Nuclear Engineering during the spring of 2014. The following fall he began his graduate studies at NCSU under the direction of Dr. J. M. Doster in the hybrid energy field. Konor's research interests lie in the efficient storage and usage of thermal energy from nuclear reactors.

Among his more redeeming qualities is his infatuation with haunted attractions. While in high school he became acquainted with the haunted attraction industry by assisting with the design of haunted attractions at major theme parks and hours of hands-on experience, honing the craft. Konor often remarks when asked about his haunted house experience, "There is no better job in world. I am paid to scare people; only downhill from here."

ACKNOWLEDGMENTS

I would first like to thank my thesis advisor Dr. J. Michael Doster of the Nuclear Engineering Department at North Carolina State University. The door to Dr. Doster's office was always open whenever I ran into a trouble spot or had a question about my research or writing. He always provided useful comments, remarks and engagement through the learning process of this master thesis.

I would also like to acknowledge Dr. Mohamed Bourham and Dr. Stephen Terry as committee members. I am gratefully indebted to them for their valuable comments on this thesis.

iii

TABLE OF CONTENTS

LIST OF TABLES

LIST OF FIGURES

NOMENCLATURE

A	area
ACV	auxiliary control valve
BOP	balance of plant
c_p	specific heat
FCV	flow control valve
GHG	greenhouse gas
h	enthalpy
H	height
HTSE	high temperature steam electrolysis
IHX	intermediate heat exchanger
IPWR	integral pressurized water reactor
K	loss coefficient
M	mass
MSF	multistage flash desalination
MWe	megawatts electric
OTSG	once through steam generator
P	pressure
ρ	density
PRV	pressure relief valve
ΔP	pressure drop
$\dot{Q}$	heat transfer rate
R	universal gas constant
RO	reverse osmosis
t	time
T	temperature
$T_{IHXexit}$	temperature at exit of IHX (tube side)
TBV	turbine bypass valve
TES	thermal energy storage
u	internal energy
UA	overall heat transfer coefficient
V	volume

Subscripts

Amb	ambient
Cond	condenser
CT	cold tank
f	saturated liquid
feed	feed flow
g	saturated vapor
HDR	header
HT	hot tank
IHX	intermediate heat exchanger
Line	losses in lines
Sat	saturation value
SG	steam generator

Chapter 1 Introduction

1.1 Current State of Grid/Hybrid Energy Field

Renewable energy technologies continue to become more attractive with improvements in efficiency and price-point. However, the variability and increased penetration of renewables creates additional challenges for the electric grid. The most common forms of installed renewable energy are wind and solar. Wind and solar energy, while zero carbon footprint energy sources, have energy outputs which cannot be directly controlled and instead are subject to the variability found in nature. This implies the energy production side of the equation is no longer 100% controllable, and depending on the amount of solar and wind installed on the grid could mean large, uncontrolled variations in energy production. This can lead to mismatches between energy demand and energy production and ultimately system instabilities and blackouts.

Society has benefited from the reliability afforded by base load operation of the current production fleet. To maintain our current lifestyle, base load plants will likely still be required. However, as the penetration of renewables increases, base load plants may need to be more flexible in their operation as illustrated in Figure 1.1 and Figure 1.2. Figure 1.1 gives a representative load profile for a hot summer day in in an area with mixed commercial and residential characteristics [1]. Figure 1.2 shows representative energy profiles for wind and solar [2] and the energy output required of a plant operating in load follow mode if 65% of the peak energy demand can be provided by standard base load units. Without a plant designed to mitigate the load variability, the base load plants would need the ability to quickly increase and decrease power. An example of the relative load profile that might be experienced by the base load plants with upwards of 35% renewable penetration is illustrated in Figure 1.3.

1
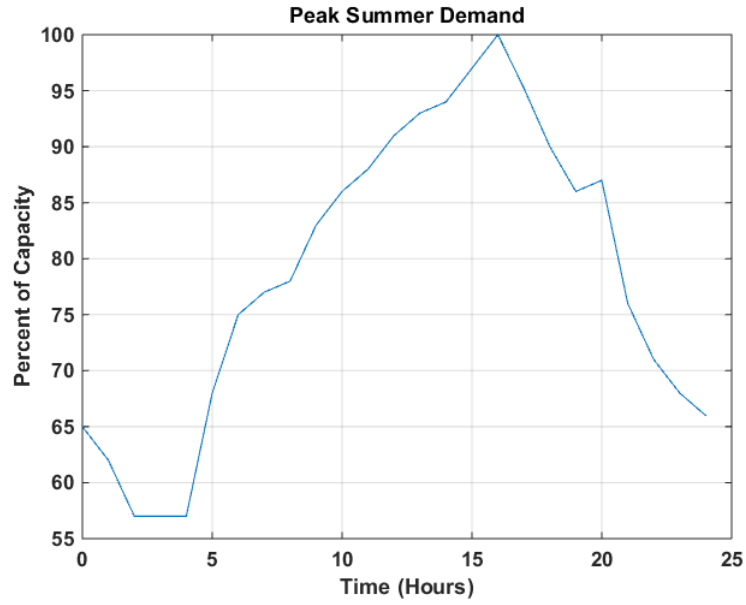
Figure 1.1: Peak Summer Day Load Profile
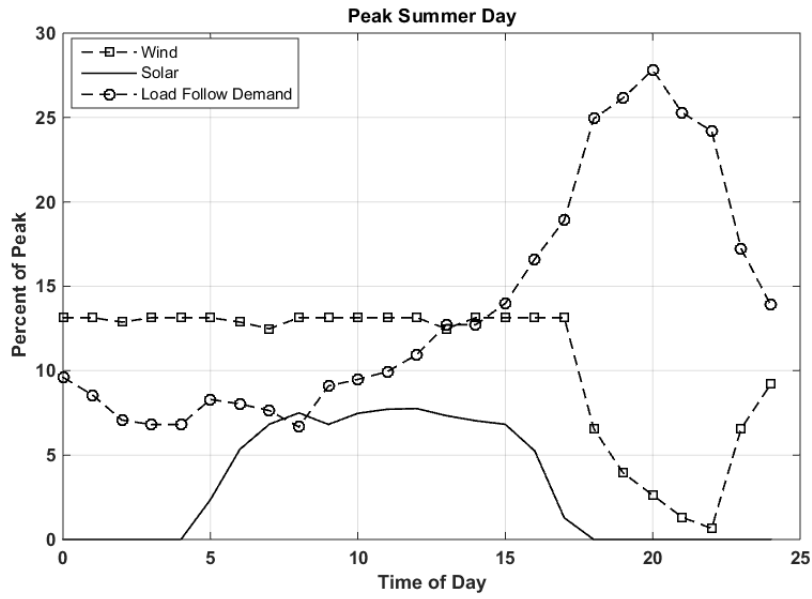
Figure 1.2: Peak Summer Day hourly demand with 65% power from base load units and 35% power from intermittent and load follow capacity.
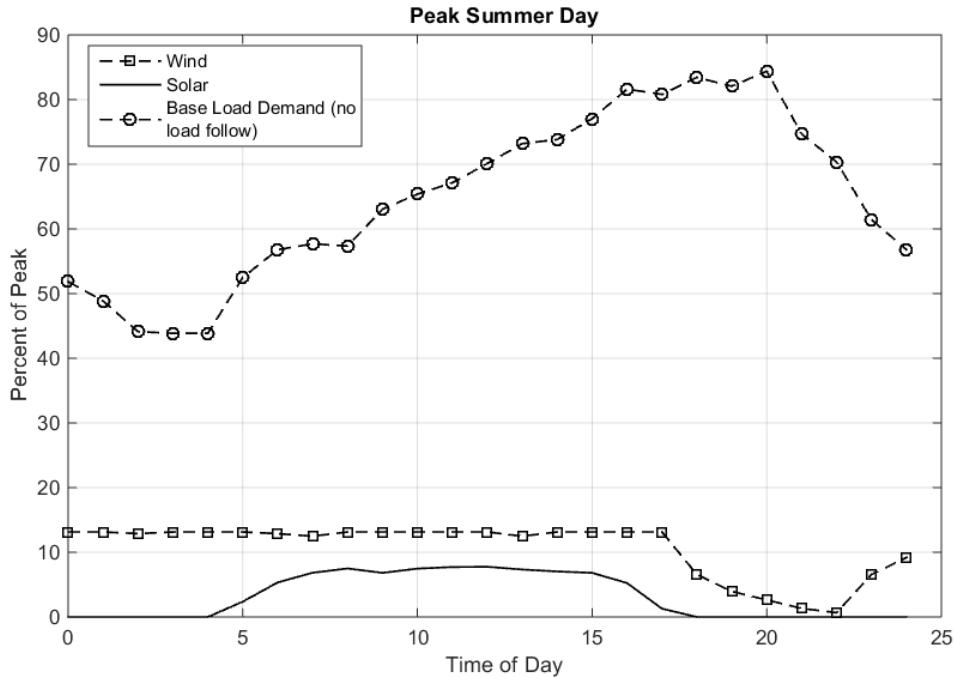
Figure 1.3: Peak summer day including intermittents of up to 35% penetration.

As the penetration of renewable technologies increases, scenarios will arise where base load units could be called upon to operate in a reduced or load follow mode. During these times it would be beneficial from both an economic and mechanical standpoint to keep the plants at 100% power and store/use the excess energy in either a thermal energy storage unit (TES) or alternative applications. Economically, it is generally beneficial to run nuclear plants at full power at all times. Further, operating nuclear plants in load follow mode increases the mechanical and thermal stresses on the fuel and other system components. A way to accommodate both the economic advantages of operating the plant at 100% power at all times and addressing the intermittency seen with renewables is to employ alternative applications of the energy provided by the nuclear plant.

1.2 Candidate Alternative Energy Applications

1.2.1 Desalination of brackish/Sea Water

A promising alternative energy application is the desalination of sea water. This would be a particularly useful application in areas such as Southern California or the Southwest United States where availability of potable drinking water is an increasing concern. To insure adequate water

3

supplies, desalination plants are being brought online yearly in Southern California, with the most recent in Carlsbad near San Diego in December 2015 [3], [4].

For desalination plants with a capacity of 4000 m^3/d and above the two main desalination technologies are multistage flash desalination (MSF) (69%) and reverse osmosis (RO) (23%) [5]. The process mechanics and energy requirements of the two are vastly different. Multistage flash desalination is based on heating seawater in a brine heater to around 90-110 degrees Celsius. The hot brine then enters a flash chamber which is held at vacuum. Since the water entering the chamber is above the boiling temperature at vacuum, part of the water flashes to steam. This steam rises to condensing coils where it condenses into fresh water. A diagram of this process is shown in Figure 1.4.
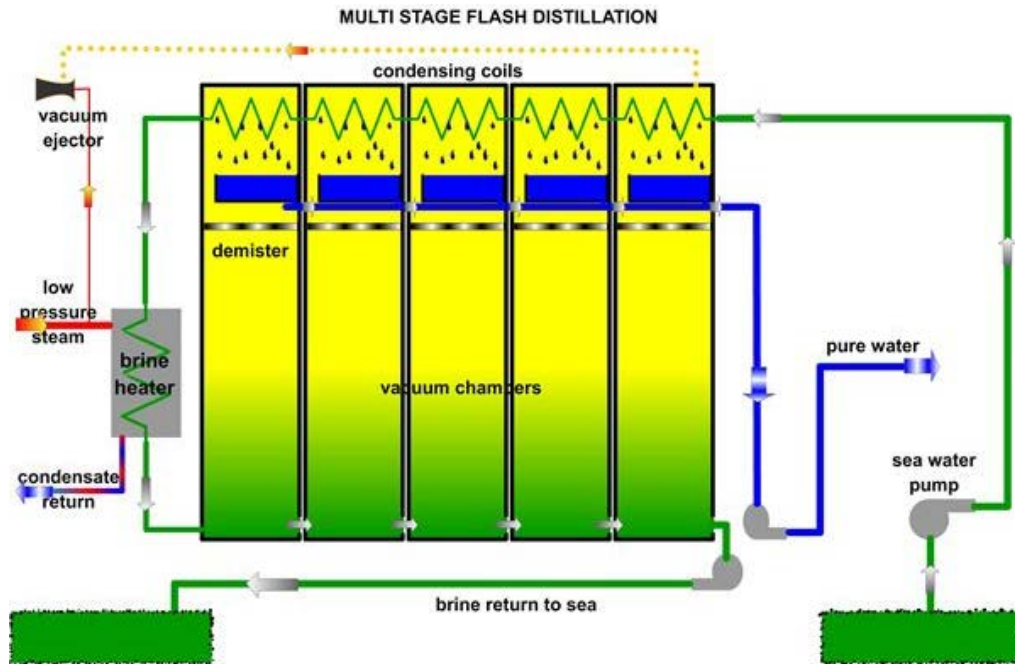
Figure 1.4: Example of a multistage flash desalination plant [6]

Reverse Osmosis is the main competitor to multistage flash desalination. The RO process works by passing water at high pressures through fine membranes that only allow water molecules to pass. A typical reverse osmosis plant works in two stages, the first being a pretreatment stage where chlorine and other chemical additives are used to remove biological organisms and control both the pH and hardness of the water. The water is then sent to the membrane filtration system where high pressure

4

forces the water molecules through the membranes into an inner collection tube [7]. A representative diagram of an RO system is shown in Figure 1.5.
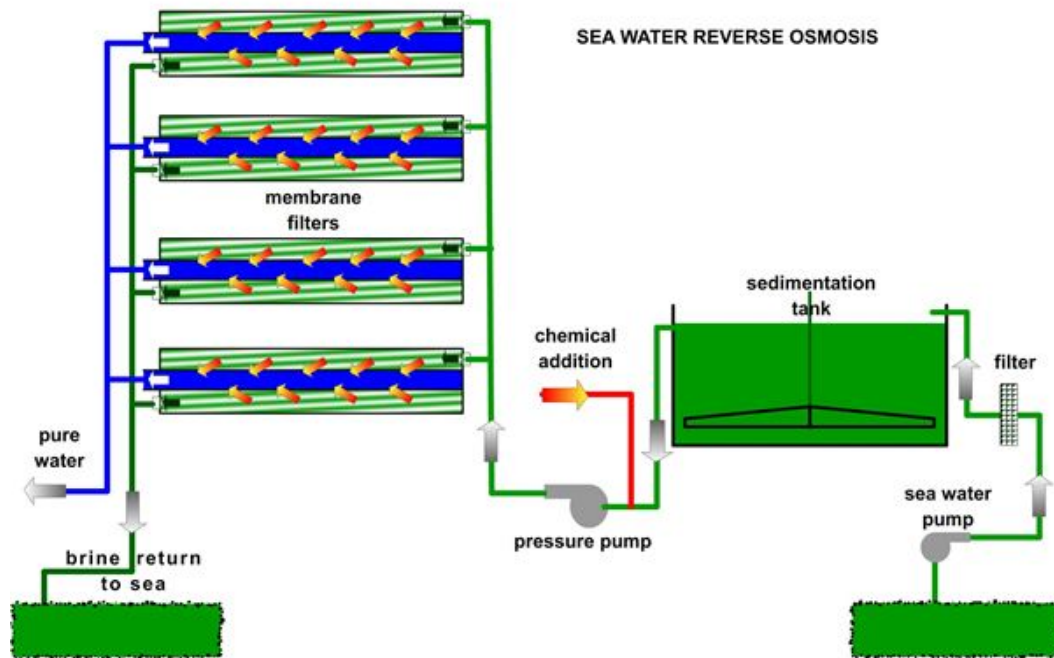
Figure 1.5: Example of a Reverse Osmosis (RO) plant. [7]

MSF is a proven technology for water desalination. It is a simple and extremely reliable process that requires no moving parts other than pumps. Unfortunately, MSF is more energy intensive than current RO plants, requires a direct steam connection to the power plant, and typically runs at full capacity to limit potential system instabilities [8]. These challenges limit MSF applications when steam shedding is being used as a load leveling strategy.

Reverse Osmosis has the benefit of consuming less energy than MSF. RO also does not need a direct steam connection to the power plant as it only requires electric energy to run pumps and has simple start/stop operating capability [8]. Since RO is operated in modules, operation can be staged to take advantage of available excess energy instead of the all or nothing operation of MSF. These properties make RO a highly attractive secondary energy application for hybrid energy technologies.

5

1.2.2 Hydrogen Production

Excess thermal and electrical energy can be used for a wide range of alternative applications. One of the most intriguing currently is hydrogen production. The anticipated development and deployment of fuel cell technology and infrastructure into the transportation sector will create substantial additional demand for hydrogen. One of the motivations to switch to a Hydrogen based infrastructure is to reduce greenhouse gas (GHG) emissions. However, significant GHG reduction will only occur if the hydrogen is produced from carbon-free sources.

Current large scale hydrogen production is produced by stripping hydrocarbon fuel via steam-methane reforming [9]. In steam-methane reforming, methane reacts with steam in the presence of a catalyst to produce hydrogen and carbon monoxide. In a subsequent "water-gas shift reaction" the carbon monoxide and steam are reacted using a catalyst to produce carbon dioxide and hydrogen.

Steam methane reforming reaction:

$$CH_4 + H_2O + (\text{heat}) \rightarrow CO + 3H_2$$

Water-gas shift reaction:

$$CO + H_2O \rightarrow CO_2 + H_2 \ (+ \text{ small amount of heat})$$
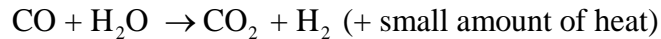
A byproduct of this reaction is CO_2 which does not meet the current GHG reduction standards. Fortunately, an alternative clean source of hydrogen, meaning no CO_2 emission, comes from the disassociation of water into hydrogen and oxygen via electrolysis. Currently, there are two ways of disassociating water via electrolysis, conventional electrolysis and High Temperature Steam Electrolysis [10]. HTSE is ~40% more efficient than conventional electrolysis but requires temperatures of $\sim 800^oC$ [11], [10].

A case study recently completed by NuScale [10] to establish a baseline cost for producing hydrogen through the HTSE process [10] showed that one 160MWth NuScale module could optimally produce 1,310 lb/hr of hydrogen using one matched HTSE module. The hydrogen would be 99% pure with no greenhouse gas emissions. The results of their economic analysis showed natural gas reforming to be more economical due to natural gas costs and the overall maturity of reforming technology. However, it also stated a coupled hybrid technology plant for hydrogen production could become competitive

6

depending on different economic factors including increased natural gas prices, carbon emission penalties, and optimization of the HTSE process.

1.3 Region Selection

Since renewable energy tends to be highly region specific, it is important to determine the most economically feasible region in which to build a hybrid energy system. Three of the most promising regions for deploying a hybrid energy system are presented below.

1.3.1 Southern California

The implementation of a nuclear hybrid energy system relies on three things: 1) sufficient renewable resources (wind, solar, etc.), 2) a use for the excess energy, and 3) availability of energy transmission lines to supply customers. The California Renewable Portfolio Standard set a goal of 33% of electricity generation to come from eligible renewable resources by 2020 [12]. Currently California leads the nation in energy production from solar and biomass. As further evidence of their commitment to renewables, California recently completed the world's largest solar thermal plant. The Ivanpah Solar Power Facility, located in San Bernardino County became operational on February 13, 2014 and is capable of producing upwards of 392MWe [13]. Excess energy created during times of non-peak demand or times of high renewable output could be put to use by desalination plants or for hydrogen production.

As of February 2014 there were 17 proposed desalination plants in Southern California alone [14]. With the population density and recent extreme drought experienced in this area, the need for potable water is undeniable. Unfortunately, desalination of ocean water is an extremely energy intensive process that uses on average 15,000 KW-hr of power per million gallons of fresh water produced. This is compared to an estimated 3,300-8,300 KW-hr for potable water production by wastewater treatment [15]. The energy intensiveness of desalination creates opportunities for hybrid energy plants not only from an efficiency standpoint, but also from the environmental standpoint of little to no added carbon emissions.

By 2020 automakers expect to have thousands of hydrogen fuel cell based vehicles in California [16]. This transition to a hydrogen fuel cell based infrastructure will require hydrogen production facilities. The ability to produce hydrogen during times of low electric demand would add value to the facility.

7

Lastly, Southern California is upgrading their grid transmission system. The recent installation of an extra 800 MW of transmission lines across southern California connecting renewable resources in southeast California to San Diego is a major step [17].

1.3.2 Southwest

Renewable energy resources in the southwest include wind, geothermal and photovoltaics. . Arizona currently has the one of the world's largest solar photovoltaic facilities located in Yuma County, AZ completed in 2014 [18]. With the addition of these photovoltaic facilities a stronger case could be made for an integrated nuclear-renewable system as the demand for grid flexibility increases with increased penetration of photovoltaics.

As in Southern California, drought conditions in the southwest illustrate the need for additional sources of potable water. While current resources from the upper Colorado River Basin are sufficient, recent studies have shown this water supply to be dwindling [19]. With the population density and drought levels not seen in 1,250 years [19], the need for potable water is real.

The availability of transmission lines is another advantage the southwest has over other regions. Due to the possible closure of existing coal plants, the availability of an existing grid would be conducive to installing an integrated nuclear-renewable system.

1.3.3 Agricultural Midwest

The Agricultural Midwest is considered to be the best opportunity for integrated nuclear-renewable systems [20]. The region has abundant wind energy supplies over the Great Plains. Second to Texas, Iowa is the leading producer of wind energy in the nation [21]. This combined with the recent closures of coal fired power plants in the Midwest [22] could lead to a higher demand for renewables making integrated nuclear-renewable systems more attractive.

Renewable energy technologies combined with industrial processes such as ammonia/fertilizer production adds additional benefit to these systems. During times of peak wind output or low electric demand, excess capacity could be diverted to ammonia production. An existing transmission infrastructure left over from coal plant closures also makes the Agricultural Midwest an extremely attractive option for these integrated nuclear-renewable systems.

1.4 TES System Configuration

Thermal Energy Storage (TES) systems have been proposed as a way to store energy during periods of excess capacity and have already been employed in concentrated solar plants in the southwest [23]. Thermal energy storage can be classified into three main types; sensible heat storage, thermochemical storage, and latent heat storage. Sensible heat storage (SHS) systems work by raising the temperature of a storage medium, usually a solid or a liquid. The storage materials undergo no change in phase over the temperature range of the storage process. A good sensible heat storage material has high heat capacity, relative molecular stability and durability over the temperature range of interest. Latent heat storage is an approximately isothermal process which takes advantage of the heat of fusion of the storage material as it changes phase. Thermochemical storage is a newer technology that relies on heat to drive reversible chemical reactions [24].

For the application proposed here, a sensible heat system was chosen. This allows for the simple bypass of steam to an intermediate heat exchanger, which transfers thermal energy to a thermal energy storage fluid. A two-tank direct system was chosen for this work. The two tank system can accommodate molten salts or synthetic oils that are highly stable over the expected operating range of the system. Currently, the two tank storage system is the most commercially mature technology [24].

9

Chapter 2   Thermal Energy Storage System

2.1 Design

The proposed Thermal Energy Storage System is shown in Figure 2.1. An outer loop interfaces with the reactor's Balance of Plant (BOP) directly through four parallel auxiliary turbine bypass valves connected at the pressure equalization header. Bypass steam is directed through an intermediate heat exchanger (IHX) and discharged to the main condenser. An inner loop containing a TES fluid consists of two large storage tanks along with several pumps to transport the TES fluid between the tanks, the IHX and a steam generator. Therminol-66 is chosen to be the TES fluid as it is readily available, can be pumped at low temperatures, and offers thermal stability over the range $(27^{o}F - 650^{o}F)$ which covers the anticipated operating range of the TES system $(350^{o}F - 500^{o}F)$. Other considered TES fluids are given in Table 2.1.

Table 2.1: Properties of Possible TES fluids at ~500 degrees Fahrenheit

Heat Transfer Fluid	Boiling Point ($\circ$F)	Heat Storage (W*hr/m³$\circ$F)	Operating Range ($\circ$F)
Therminol®-66 [25]	678	576.95	27 to 650
Therminol®-68 [26]	586	563.03	-14 to 680
Therminol®-75 [27]	649	551.54	175 to 725

The TES system is designed to allow the reactor to run continuously at ~100% power over a wide range of operating conditions. During periods of excess capacity, bypass steam is directed to the TES unit through the auxiliary bypass valves where it condenses on the shell side of the IHX. TES fluid is pumped from the Cold Tank to the Hot Tank through the tube side of the IHX at a rate sufficient to raise the temperature of the TES fluid to some set point. Condensate is collected in a hot well below the IHX and drains back to the main condenser. The TES fluid is then stored in the Hot Tank at constant temperature. The system is discharged during periods of peak demand, or when process steam is desired, by pumping the TES fluid from the Hot Tank through a boiler (steam generator) to the Cold Tank. This process steam can then be reintroduced into the power conversion cycle for electricity production or directed to some other application. While the boiler in Figure 2.1 implies a Once Through Steam Generator (OTSG) design, a U-Tube design could just as easily be substituted. Though not indicated in Figure 2.1, pressure relief lines connect the shell side of the IHX with the condenser to prevent over pressurization of the heat exchanger during periods of low condensation

rate. A nitrogen cover gas dictates the tank pressures during charging and discharging operation. For the purposes of this work we will focus only on the IHX system and the associated charging mode.
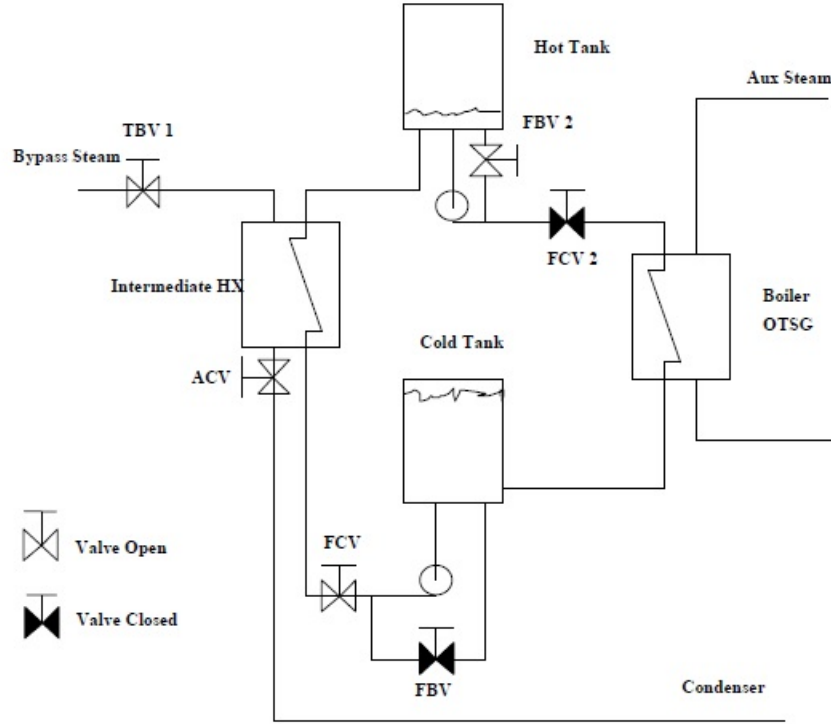
Figure 2.1: Thermal Energy Storage System (charging mode).

2.2 TES System Model

The time dependent behavior of the TES system is obtained by solving mass, energy and simple momentum balances on the Shell side of the IHX (Outer Loop), and the Tube side or Inner Loop.

System Equations for Shell Side (Outer Loop)

Energy Equation

$$V_{IHX} \frac{d(\rho u)}{dt} = \sum_n \dot{m}_{TBV_n} h_{SG} - \dot{m}_{IHX} h_f - \sum_m \dot{m}_{PRV_m} h_{IHX} - \dot{Q}_{IHX} \qquad (2.1)$$

For n=1,2,…,n$_{tbv}$ and m=1,2,…,m$_{prv.}$

11

Mass Equation

$$V_{IHX} \frac{d\rho}{dt} = \sum_n \dot{m}_{TBV_n} - \dot{m}_{IHX} - \sum_m \dot{m}_{PRV_m} \tag{2.2}$$

Momentum Equations

$$P_{HDR} = P_{IHX} + \frac{\left(K_{TBVline} + K_{TBV_n}\right)\dot{m}_{TBV_n}^2}{2A_{TBV_n}^2 \rho_g} \tag{2.3}$$

$$P_{IHX} = P_{Cond} + \frac{\left(K_{ACVline} + K_{ACV}\right)\dot{m}_{IHX}^2}{2A_{ACV}^2 \rho_f} \tag{2.4}$$

$$P_{IHX} = P_{Cond} + \frac{\left(K_{PRVline} + K_{PRV_m}\right)\dot{m}_{PRV_m}^2}{2A_{PRV_m}^2 \rho_g} \tag{2.5}$$

State Equations

$$\rho = \alpha_l \rho_l + \alpha_g \rho_g \tag{2.6}$$

$$\rho u = \alpha_l \rho_l u_l + \alpha_g \rho_g u_g \tag{2.7}$$

Equations for tube side (Inner Loop) charging mode

Hot Tank Mass Balance

$$\frac{dM_{HT}}{dt} = \dot{m}_{TES} = \rho_{TES} A_{HT} \frac{dH_{HT}}{dt} \tag{2.8}$$

Cold Tank Mass Balance

$$\frac{dM_{CT}}{dt} = -\dot{m}_{TES} = \rho_{TES} A_{CT} \frac{dH_{CT}}{dt} \tag{2.9}$$

Momentum Equation

$$P_{CT} + \Delta P_{pump} = P_{HT} + \frac{\left(K_{FCV} + K_{FCVline}\right)\dot{m}_{TES}^2}{2A_{FCV}^2 \rho_{TES}} \tag{2.10}$$

Hot tank energy balance

$$M_{HT} c_p \frac{dT_{HT}}{dt} = \dot{m}_{TES} c_p T_{IHX_{Exit}} - (UA)_{HT}\left(T_{HT} - T_{Amb}\right) \tag{2.11}$$

12

Hot Tank Pressure

$$P_{HT} = \rho_{HT} R T_{HT} \tag{2.12}$$

Cold Tank Pressure

$$P_{CT} = \rho_{CT} R T_{CT} \tag{2.13}$$

The energy transfer between the tube and shell side of the intermediate heat exchanger is based on the effectiveness technique.

The heat transfer rate from equation (2.1) can be written as

$$\dot{Q}_{IHX} = (UA)_{IHX} \left(T_{sat} - \overline{T}_{TES} \right) \tag{2.14}$$

where $\overline{T}_{TES}$ is the average TES fluid temperature within the IHX. To obtain the average TES temperature we solve a simple energy balance on the fluid.

$$\dot{m}_{TES} c_p \frac{dT_{TES}}{dz} = (UP_w)_{IHX} \left(T_{sat} - T_{TES} \right)$$

$$\frac{dT_{TES}}{dz} = \frac{(UP_w)_{IHX}}{\dot{m}_{TES} c_p} \left(T_{sat} - T_{TES} \right) \Rightarrow \frac{dT_{TES}}{dz} = \frac{\beta}{L} \left(T_{sat} - T_{TES} \right)$$

where, $\quad \beta = \dfrac{(UA)_{IHX}}{\dot{m}_{TES} c_p}$

$$\frac{dT_{TES}}{dz} + \frac{\beta}{L} T_{TES} = \frac{\beta}{L} T_{sat}$$

$$T_{TES}(z) e^{\frac{\beta z}{L}} = T_{c_1} + \int_0^z \frac{\beta}{L} T_{sat} e^{\frac{\beta z'}{L}} dz' \Rightarrow T_{TES}(z) e^{\frac{\beta z}{L}} = T_{c_1} + T_{sat} e^{\frac{\beta z'}{L}} \Big|_0^z$$

$$T_{TES}(z) = T_{c_1} e^{-\frac{\beta z}{L}} + T_{sat} \left\{ 1 - e^{-\frac{\beta z}{L}} \right\} \tag{2.15}$$

Now defining $\overline{T}_{TES}$ as

$$\overline{T}_{TES} = \frac{1}{L} \int_0^L T_{TES}(z) dz$$

Plugging in equation (2.15)

13

$$\overline{T}_{TES} = \frac{1}{L}\int_0^L T_{c_1}\,e^{-\frac{\beta z}{L}}\,dz + T_{sat} - \frac{T_{sat}}{L}\int_0^L e^{-\frac{\beta z}{L}}\,dz$$

$$\overline{T}_{TES} = T_{sat} + \frac{\left(T_{sat} - T_{c_1}\right)}{L}\int_0^L e^{-\frac{\beta z}{L}}\,dz$$

$$\overline{T}_{TES} = T_{sat} + \frac{\left(T_{sat} - T_{c_1}\right)}{L}\left(\frac{L}{\beta}\right) e^{-\frac{\beta z}{L}}\Bigg|_0^L$$

Rearranging gives the final equation.

$$\overline{T}_{TES} = T_{sat} - \frac{\left(T_{sat} - T_{c_1}\right)}{\beta}\left\{1 - e^{-\beta}\right\} \tag{2.16}$$

Further, the determination of Q_{IHX} requires the UA value

$$UA_{IHX} = \frac{2\pi n L}{\dfrac{1}{h_i r_i} + \dfrac{1}{k}\ln\left(\dfrac{r_o}{r_i}\right) + \dfrac{1}{h_o r_o}} \tag{2.17}$$

where an average condensation heat transfer coefficient is assumed for the shell side of the form,

$$h_o = h_{cond}\left(T_w\right) = 0.725\left[\frac{\rho_f\left(\rho_f - \rho_g\right)g h_{fg}' k_f^3}{\mu_f d\left(T_{sat} - T_w\right)}\right]^{\frac{1}{4}} \tag{2.18}$$

$$h_{fg}' = h_{fg}\left[1 + \frac{0.68 c_{p_f}\left(T_{sat} - T_w\right)}{h_{fg}}\right]$$

and T_w satisfies

$$h_{cond}\left(T_w\right) r_o\left(T_{sat} - T_w\right) = \left\{\frac{1}{k}\ln\left(\frac{r_o}{r_i}\right) + \frac{1}{h_i r_i}\right\}^{-1}\left(T_w - T_{c_{avg}}\right)$$

$$T_{c_{avg}} = \frac{T_{c_1} + T_{IHX_{exit}}}{2}$$

14

$$h_i = \frac{k_{TES} Nu_i}{De_{IHX}} \tag{2.19}$$

$$Nu_i = \max\left[0.023\,\mathrm{Re}^{0.8}\,\mathrm{Pr}^{0.4}, 4.66\right] \tag{2.20}$$

In the equations above, n=number of tubes, r_i = tube inner radius, r_o = tube outer radius, k=thermal conductivity of tube, L=length of tubes, and d=inner diameter of tube, T_{C_1} inlet temperature from cold tank. Equation (2.20) insures non zero heat transfer coefficients during periods of zero or very low TES flow rates.

2.3 Solution strategy

The TES system model requires solving a system of nonlinear equations. The solution method is outlined below.

<u>Shell Side of IHX</u>

A semi-implicit time discretization is chosen for the shell side equations of the form

Energy Equation

$$V_{IHX}\left\{\frac{\rho u^{t+\Delta t} - \rho u^t}{\Delta t}\right\} = \sum_n \dot{m}_{TBV_n}^{t+\Delta t} h_{SG}^t - \dot{m}_{IHX}^{t+\Delta t} h_f^t - \sum_m \dot{m}_{PRV_m}^{t+\Delta t} h_{IHX}^t - \dot{Q}_{IHX}^t \tag{2.21}$$

For n=1,2,…,n$_{tbv}$ and m=1,2,…,m$_{prv.}$

Mass Equation

$$V_{IHX}\left\{\frac{\rho^{t+\Delta t} - \rho^t}{\Delta t}\right\} = \sum_n \dot{m}_{TBV_n}^{t+\Delta t} - \dot{m}_{IHX}^{t+\Delta t} - \sum_m \dot{m}_{PRV_m}^{t+\Delta t} \tag{2.22}$$

Momentum Equations

$$P_{HDR}^{t+\Delta t} = P_{IHX}^{t+\Delta t} + \frac{\left(K_{TBVline} + K_{TBV_n}\right)\left(\dot{m}_{TBV_n}^2\right)^{t+\Delta t}}{2 A_{TBV_n}^2 \rho_g} \tag{2.23}$$

$$P_{IHX}^{t+\Delta t} = P_{Cond}^{t+\Delta t} + \frac{\left(K_{ACVline} + K_{ACV}\right)\left(\dot{m}_{IHX}^2\right)^{t+\Delta t}}{2 A_{ACV}^2 \rho_f} \tag{2.24}$$

15

$$P_{IHX}^{t+\Delta t} = P_{Cond}^{t+\Delta t} + \frac{\left(K_{PRVline} + K_{PRV_m}\right)\left(\dot{m}_{PRV_m}^2\right)^{t+\Delta t}}{2A_{PRV_m}^2 \rho_g} \tag{2.25}$$

State Equations

$$\rho^{t+\Delta t} = \alpha_l^{t+\Delta t} \rho_l^{t+\Delta t} + \alpha_g^{t+\Delta t} \rho_g^{t+\Delta t} \tag{2.26}$$

$$\rho u^{t+\Delta t} = \alpha_l^{t+\Delta t} \rho_l^{t+\Delta t} u_l^{t+\Delta t} + \alpha_g^{t+\Delta t} \rho_g^{t+\Delta t} u_g^{t+\Delta t} \tag{2.27}$$

These equations are nonlinear in the new time values. Applying a Newton-Iteration yields the following linear equations in the new iterate (k +1) values.

Energy Equation

$$V_{IHX}\left\{\frac{\rho u^{k+1} - \rho u^t}{\Delta t}\right\} = \sum_n \dot{m}_{TBV_n}^{k+1} h_{SG}^t - \dot{m}_{IHX}^{k+1} h_f^t - \sum_m \dot{m}_{PRV_m}^{k+1} h_{IHX}^t - \dot{Q}_{IHX}^t \tag{2.28}$$

For n=1,2,…,n$_{tbv}$ and m=1,2,…,m$_{prv.}$

Mass Equation

$$V_{IHX}\left\{\frac{\rho^{k+1} - \rho^t}{\Delta t}\right\} = \sum_n \dot{m}_{TBV_n}^{k+1} - \dot{m}_{IHX}^{k+1} - \sum_m \dot{m}_{PRV_m}^{k+1} \tag{2.29}$$

Momentum Equations

$$P_{HDR}^{t+\Delta t} = P_{IHX}^{k+1} + \frac{\left(K_{TBVline} + K_{TBV_n}\right)}{2A_{TBV_n}^2 \rho_g^t}\left(2\dot{m}_{TBVn}^{k+1} - \dot{m}_{TBn}^k\right)\dot{m}_{TBn}^k \tag{2.30}$$

$$P_{IHX}^{k+1} = P_{Cond}^{t+\Delta t} + \frac{\left(K_{ACVline} + K_{ACV}\right)}{2A_{ACV}^2 \rho_f^t}\left(2\dot{m}_{IHX}^{k+1} - \dot{m}_{IHX}^k\right)\dot{m}_{IHX}^k \tag{2.31}$$

$$P_{IHX}^{k+1} = P_{Cond}^{t+\Delta t} + \frac{\left(K_{PRVline} + K_{PRV_m}\right)}{2A_{PRV_m}^2 \rho_g^t}\left(2\dot{m}_{PRVm}^{k+1} - \dot{m}_{PRVm}^k\right)\dot{m}_{PRVm}^k \tag{2.32}$$

State Equations

$$\tilde{\rho}^k = \rho\left(\alpha_g^k, P_{IHX}^k\right) = \rho_f\left(P_{IHX}^k\right) + \alpha_g^k\left[\rho_g\left(P_{IHX}^k\right) - \rho_f\left(P_{IHX}^k\right)\right] \tag{2.33}$$

$$\widetilde{\rho u}^k = \rho u\left(\alpha_g^k, P_{IHX}^k\right) = \rho_f\left(P_{IHX}^k\right)u_f\left(P_{IHX}^k\right) + \alpha_g^k\left[\rho_g\left(P_{IHX}^k\right)u_g\left(P_{IHX}^k\right) - \rho_f\left(P_{IHX}^k\right)u_f\left(P_{IHX}^k\right)\right] \tag{2.34}$$

16

$$\rho^{k+1} = \tilde{\rho}^k + \delta\alpha_g \left.\frac{\partial \rho}{\partial \alpha_g}\right|_k + \delta P_{IHX} \left.\frac{\partial \rho}{\partial P}\right|_k \tag{2.35}$$

$$\rho u^{k+1} = \widetilde{\rho u}^k + \delta\alpha_g \left.\frac{\partial \rho u}{\partial \alpha_g}\right|_k + \delta P_{IHX} \left.\frac{\partial \rho u}{\partial P}\right|_k \tag{2.36}$$

Equations (2.28)-(2.36) can be reduced to a 4x4 matrix providing solutions for $\rho^{k+1}, \rho u^{k+1}, \delta\alpha_g, P_{IHX}^{k+1}$. From these variables direct solves for the mass flows can be performed. The equations are iterated to convergence based on the maximum relative difference for any single variable between iterations. The converged values become the solution for the new time values.

<u>Tube Side Equations</u>

Tube side Energy Equation

$$V_{IHX}\rho_{TES}c_{p_{TES}} \left\{ \frac{T_{IHX_{exit}}^{t+\Delta t} - T_{IHX_{exit}}^{t}}{\Delta t} \right\} + \dot{m}_{TES}^{t+\Delta t} c_{p_{TES}} \left\{ T_{IHX_{exit}}^{t+\Delta t} - T_{C_1} \right\} = \dot{Q}_{IHX}^{t+\Delta t} \tag{2.37}$$

$$\dot{Q}_{IHX}^{t+\Delta t} = (UA)_{IHX}^{t} \left(T_{sat} - \overline{T}_{TES}^{t+\Delta t} \right) \tag{2.38}$$

$$\overline{T}_{TES}^{t+\Delta t} = T_{sat_{IHX}} - \frac{\left(T_{sat_{IHX}} - T_{c_1} \right)}{\beta}\left\{ 1 - e^{-\beta} \right\}, \quad \beta = \frac{(UA)_{IHX}^{t}}{\dot{m}_{TES}^{t+\Delta t} c_{p_{TES}}} \tag{2.39}$$

Hot Tank Mass Balance

$$\dot{m}_{TES}^{t+\Delta t} = \rho_{TES}A_{HT} \left\{ \frac{H_{HT}^{t+\Delta t} - H_{HT}^{t}}{\Delta t} \right\} \tag{2.40}$$

Cold Tank Mass Balance

$$-\dot{m}_{TES}^{t+\Delta t} = \rho_{TES}A_{CT} \left\{ \frac{H_{CT}^{t+\Delta t} - H_{CT}^{t}}{\Delta t} \right\} \tag{2.41}$$

Momentum Equation

$$P_{CT}^{t+\Delta t} + \Delta P_{pump} = P_{HT}^{t+\Delta t} + \frac{K_{FCV}^{t} \left(\dot{m}_{TES}^{t+\Delta t} \right)^2}{2A_{FCV}^2 \rho_{TES}} \tag{2.42}$$

17

Hot tank energy balance

$$M_{HT}^{t} c_p \left\{ \frac{T_{HT}^{t+\Delta t} - T_{HT}^{t}}{\Delta t} \right\} = \dot{m}_{TES}^{t+\Delta t} c_{p_{TES}} \left(T_{IHX_{Exit}}^{t+\Delta t} - T_{HT}^{t+\Delta t} \right) - (UA)_{HT}^{t} \left(T_{HT}^{t+\Delta t} - T_{Amb} \right) \qquad (2.43)$$

Hot Tank Cover Gas

$$\rho_{HT}^{t+\Delta t} = \frac{M_{\text{Fillgas}_{HT}}^{o}}{A_{HT} \left(\text{Tank}_{\text{Height}} - H_{HT}^{t+\Delta t} \right)} \qquad (2.44)$$

Cold Tank Cover Gas

$$\rho_{CT}^{t+\Delta t} = \frac{M_{\text{Fillgas}_{CT}}^{o}}{A_{CT} \left(\text{Tank}_{\text{Height}} - H_{CT}^{t+\Delta t} \right)} \qquad (2.45)$$

Hot Tank Pressure (State Equation)

$$P_{HT}^{t+\Delta t} = \rho_{HT}^{t+\Delta t} R T_{HT}^{t+\Delta t} \qquad (2.46)$$

Cold Tank Pressure (State Equation)

$$P_{CT}^{t+\Delta t} = \rho_{CT}^{t+\Delta t} R T_{CT}^{t} \qquad (2.47)$$

Note: For the charging mode cold tank temperature is assumed constant and can always be assumed at past time.

The tube side equations also form a non-linear system that must be solved iteratively. A general Newton-Raphson iteration for this system had poor convergence characteristics due to the stiffness of the system. As an alternate approach, the equations were cast as a single non-linear equation in the TES flow rate that could be solved iteratively by Brent's algorithm [28]. This provides for a much more robust search.

Tube side nonlinear search strategy:

Guess $\dot{m}_{TES}^{k+1}$ and solve the tube side equations in the following order

$$\overline{T}_{TES}^{k+1} = T_{sat_{IHX}} - \frac{\left(T_{sat_{IHX}} - T_{c_1} \right)}{\beta} \left\{ 1 - e^{-\beta} \right\}, \quad \beta = \frac{(UA)_{IHX}^{t}}{\dot{m}_{TES}^{k+1} c_{p_{TES}}} \qquad (2.48)$$

Energy equation inside tubes

$$T_{IHX_{Exit}}^{k+1} = \frac{UA_{IHX}\left(T_{sat_{IHX}} - \overline{T}_{TES}^{k+1}\right) + \dot{m}_{TES}^{k+1}c_{p_{TES}}T_{CT} + \dfrac{V_{inner}c_{p_{TES}}\rho_{TES}T_{IHX_{Exit}}^{t}}{\Delta t}}{\dot{m}_{TES}^{k+1}c_{p_{TES}} + \dfrac{V_{inner}c_{p_{TES}}\rho_{TES}}{\Delta t}} \tag{2.49}$$

Hot tank energy

$$T_{HT}^{k+1} = \frac{\dfrac{M_{HT}^{t}c_{p_{TES}}T_{HT}^{t}}{\Delta t} + \dot{m}_{TES}^{k+1}c_{p_{TES}}T_{IHX_{Exit}}^{k+1} + UA_{HT}^{t}T_{Amb}}{\dot{m}_{TES}^{k+1}c_{p_{TES}} + (UA)_{HT}^{t} + \dfrac{M_{HT}^{t}c_{p_{TES}}}{\Delta t}} \tag{2.50}$$

Hot tank height

$$H_{HT}^{k+1} = \frac{\dot{m}_{TES}^{k+1}\Delta t}{\rho_{TES}A_{HT}} + H_{HT}^{t} \tag{2.51}$$

Cold tank height

$$H_{CT}^{k+1} = \frac{-\dot{m}_{TES}^{k+1}\Delta t}{\rho_{TES}A_{CT}} + H_{CT}^{t} \tag{2.52}$$

Hot tank density

$$\rho_{HT}^{k+1} = \frac{M_{\text{Fillgas}_{HT}}^{o}}{A_{HT}\left(\text{Tank}_{\text{Height}} - H_{HT}^{k+1}\right)} \tag{2.53}$$

Cold tank density

$$\rho_{CT}^{k+1} = \frac{M_{\text{Fillgas}_{CT}}^{o}}{A_{CT}\left(\text{Tank}_{\text{Height}} - H_{CT}^{k+1}\right)} \tag{2.54}$$

Hot tank pressure

$$P_{HT}^{k+1} = \rho_{HT}^{k+1}RT_{HT}^{k+1} \tag{2.55}$$

Cold tank pressure

$$P_{CT}^{k+1} = \rho_{CT}^{k+1}RT_{CT}^{t} \tag{2.56}$$

The momentum equation is used to determine how closely the equations are satisfied with the guess value of $\dot{m}_{TES}^{k+1}$

19

$$P_{CT}^{k+1} + \Delta P_{pump} - P_{HT}^{k+1} - \frac{K_{FCV}^t \left(\dot{m}_{TES}^2\right)^{k+1}}{2 A_{FCV}^2 \rho_{TES}} = error \qquad (2.57)$$

When the error is within some specified tolerance the (k+1) iteration values become new time (t+Δt) values. Otherwise, a new guess value for $\dot{m}_{TES}^{k+1}$ is chosen according to Brent's algorithm.

For this algorithm it is necessary to bound the possible solution. To do this we consider the natural solution for the mass flow rate.

$$\dot{m}_{TES}^{t+\Delta t} = \sqrt{\frac{2 \rho_{TES} \left(P_{CT}^{t+\Delta t} + \Delta P_{pump} - P_{HT}^{t+\Delta t}\right)}{K_{FCV} / A_{FCV}^2}} \qquad (2.58)$$

The minimum flow possible is when the pressure of the cold tank is 0 psi. Likewise, the maximum possible flow is when pressure in the hot tank is 0 psi. Using the past time pressures as estimates of the new time values, gives an estimate of the bounds for the new time flow rate.

$$\dot{m}_{TES}^{t+\Delta t}\Big|_{min} \approx \sqrt{\frac{2 \rho_{TES} \left(\Delta P_{pump} - P_{HT}^t\right)}{K_{FCV} / A_{FCV}^2}} \qquad (2.59)$$

$$\dot{m}_{TES}^{t+\Delta t}\Big|_{max} \approx \sqrt{\frac{2 \rho_{TES} \left(P_{CT}^t + \Delta P_{pump}\right)}{K_{FCV} / A_{FCV}^2}} \qquad (2.60)$$

The nonlinear solver then does a number line search on a value of m_{TES}^{k+1} such that all of the equations associated with the tube side are satisfied. Once this value has been determined, m_{TES}^{k+1} is the solution for $m_{TES}^{t+\Delta t}$. This value is directly substituted into the tube side equations to determine $T_{IHX_{Exit}}^{t+\Delta t}, T_{HT}^{t+\Delta t}, H_{HT}^{t+\Delta t}, H_{CT}^{t+\Delta t}, \rho_{HT}^{t+\Delta t}, \rho_{CT}^{t+\Delta t}, P_{HT}^{t+\Delta t}, P_{CT}^{t+\Delta t}, Q_{IHX}^{t+\Delta t}, \overline{T}_{TES}^{t+\Delta t}$

A schematic of the Thermal Energy System solution strategy is illustrated in Figure 2.2.

20

```
┌─────────────────────────────────────────┐
│            Time Advancement             │
└─────────────────────────────────────────┘
                    │
                    ▼
┌─────────────────────────────────────────┐
│             Advance Valves              │
└─────────────────────────────────────────┘
                    │
                    ▼
┌─────────────────────────────────────────┐
│          Advance Shell Side of IHX      │
│      After Newton Iteration Converges   │
│                  Gives                  │
└─────────────────────────────────────────┘
                    │
                    ▼
┌─────────────────────────────────────────┐
│   Advance Heat Exchanged Between Two    │
│                 Sides                   │
└─────────────────────────────────────────┘
                    │
                    ▼
┌─────────────────────────────────────────┐
│          Advance Tube Side of IHX       │
│           Nonlinear Search Gives        │
└─────────────────────────────────────────┘
```

Advance Shell Side of IHX

After Newton Iteration Converges Gives

$$\rho^{t+\Delta t}, \rho u^{t+\Delta t}, \delta\alpha_g, \mathrm{P}_{IHX}^{t+\Delta t}, \dot{m}_{TBV_n}^{t+\Delta t}, \dot{m}_{ACV}^{t+\Delta t}, \dot{m}_{PRV_m}^{t+\Delta t}$$

Advance Heat Exchanged Between Two Sides

$$\dot{\mathrm{Q}}_{IHX}^{t+\Delta t}$$

Advance Tube Side of IHX

Nonlinear Search Gives

$$T_{IHX_{Exit}}^{t+\Delta t}, T_{HT}^{t+\Delta t}, H_{HT}^{t+\Delta t}, H_{CT}^{t+\Delta t}, \rho_{HT}^{t+\Delta t}, \rho_{CT}^{t+\Delta t}, \mathrm{P}_{HT}^{t+\Delta t}, \mathrm{P}_{CT}^{t+\Delta t}, \overline{T}_{TES}^{t+\Delta t}$$

Figure 2.2: Thermal Energy Storage System Time Advancement Scheme

2.4 Control

The TES system has four valves used to control the system parameters: auxiliary bypass valves, TES flow control valve, auxiliary control valve, and pressure relief valves.

To test the system in a stand-alone mode prior to connecting the reactor system model, the auxiliary bypass valves are operated based on a single element controller where the error signal is generated from the difference between normalized nominal steam flow and the sum of the bypass flow and turbine steam flow. Steam flow to the turbine is related to the electric demand from the grid. The

21

difference between the nominal steam flow rate and the turbine flow rate is a measure of the excess capacity in the system. The bypass valves have individual opening set points, based on the total steam demand.

$$Signal_{TBV} = \frac{(\dot{m}_{nominal} - (\dot{m}_{turbine} + \dot{m}_{bypass}))}{\dot{m}_{nominal}} \tag{2.61}$$

Flow from the cold tank to the hot tank is via a TES flow control valve. The TES flow control valve operates off a single element controller that modulates to maintain the TES fluid temperature leaving the Intermediate Heat Exchanger at some reference value.

$$Signal_{FCV} = \frac{T_{IHX_{Exit}} - T_{IHX_{Exitref}}}{T_{IHX_{Exitref}}} \tag{2.62}$$

The auxiliary control valve (ACV) is used to control the IHX hot well level. This valve operates on a three element controller based on the level of the IHX and the difference in mass flows into and out of the IHX as shown in equations (2.63)-(2.65) where G_1 and G_2 are error weighting gains.

$$Signal_{ACV} = G_1 E_1 + G_2 E_2 \tag{2.63}$$

$$E_1 = Level\text{-}Level_{Ref} \tag{2.64}$$

$$E_2 = \dot{m}_{bypass} - \dot{m}_{ACV} \tag{2.65}$$

Pressure relief valves (PRV's) have been installed in the IHX to mitigate pressure increases. Should pressure reach an upper set point the valves will open according to equation (2.66) and will not close until the pressure falls below a lower set point.

$$Signal_{PRV} = \frac{P_{IHX} - P_{IHX_{Setpoint}}}{P_{IHX_{Setpoint}}} \tag{2.66}$$

The only variables directly controlled in the charging mode of the TES system are the IHX exit temperature on the inner loop and the level in the IHX. All other variables including IHX pressure, tank levels, inner loop mass flow rate, and heat transfer across the IHX are indirectly controlled variables calculated from the mass, energy and momentum balances on the system.

A stop valve is placed in the flow line between the cold tank and hot tank to ensure tank pressure and level stay below designated set points. Should either the pressure or level set points be exceeded the stop valve will close and TES fluid flow between the tanks will cease. A redundant control on level is that the volume of Therminol-66 in the system is less than the total volume of either tank.

Chapter 3   Condenser Model

3.1 Design

The presence of the TES system places additional demands on the condenser, and its time dependent behavior is necessary to predict overall system performance.   The condenser model is sufficient to handle all foreseeable operating modes. Included in the Condenser model are flows from the turbine and the TES system's ACV and PRVs. The condenser model will provide the time varying condenser pressure and associated system dynamics.
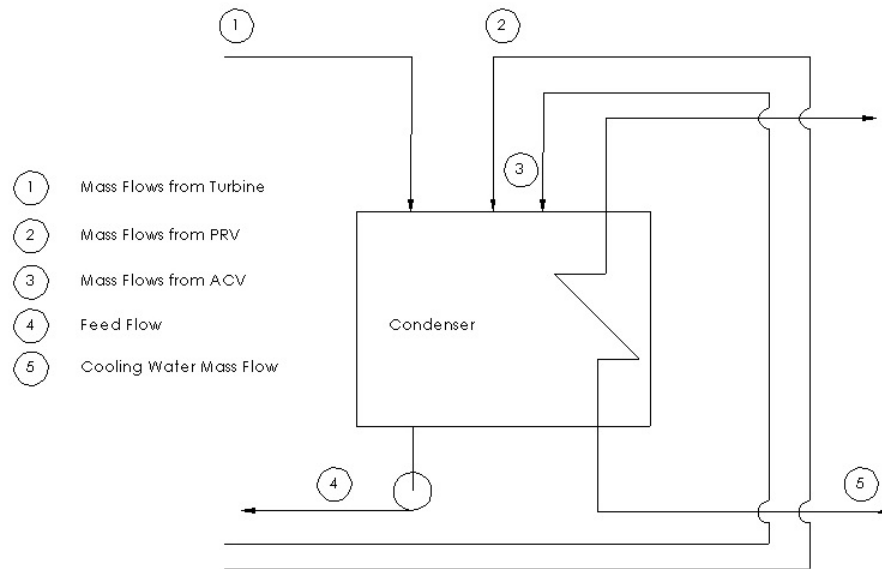
Figure 3.1: Condenser Configuration

3.2 Condenser equation set

To model the Condenser, an equation set similar to that for the Intermediate heat exchanger is used.

Energy Equation

$$V_{cond} \frac{d\rho u}{dt} = \sum_n \dot{m}_{IHX} h_{f_{@ P_{IHX}}} + \sum_m \dot{m}_{PRV_{IHX}} h_{g_{@ P_{IHX}}} + \sum_l \dot{m}_{turb_{exh}} h_{exh_l} - \dot{m}_{Feed} h_{f_{@ P_{Cond}}} - \dot{Q}_{Cond} \quad (3.1)$$

23

Mass Equation

$$V_{cond}\frac{d\rho}{dt} = \sum_n \dot{m}_{IHX} + \sum_m \dot{m}_{PRV_{IHX}} + \sum_l \dot{m}_{turb_{exh}} - \dot{m}_{Feed} \tag{3.2}$$

State Equations

$$\rho = \alpha_l\rho_l + \alpha_g\rho_g \tag{3.3}$$

$$\rho u = \alpha_l\rho_l u_l + \alpha_g\rho_g u_g \tag{3.4}$$

Differencing in time gives

$$V_{cond}\left\{\frac{\rho u^{t+\Delta t} - \rho u^t}{\Delta t}\right\} = \sum_n \dot{m}_{IHX}^{t+\Delta t} h_{f_{@\,P_{IHX}}}^{t+\Delta t} + \sum_m \dot{m}_{PRV_{IHX}}^{t+\Delta t} h_{g_{@\,P_{IHX}}}^{t+\Delta t} + \sum_l \dot{m}_{turb_{exh}}^{t+\Delta t} h_{exh_l}^{t+\Delta t} - \dot{m}_{Feed}^{t+\Delta t} h_{f_{@\,P_{Cond}}}^{t+\Delta t} - \dot{Q}_{Cond}^t \tag{3.5}$$

$$V_{cond}\left\{\frac{\rho^{t+\Delta t} - \rho^t}{\Delta t}\right\} = \sum_n \dot{m}_{IHX}^{t+\Delta t} + \sum_m \dot{m}_{PRV_{IHX}}^{t+\Delta t} + \sum_l \dot{m}_{turb_{exh}}^{t+\Delta t} - \dot{m}_{Feed}^{t+\Delta t} \tag{3.6}$$

State Equations

$$\rho^{t+\Delta t} = \alpha_l^{t+\Delta t}\rho_l^{t+\Delta t} + \alpha_g^{t+\Delta t}\rho_g^{t+\Delta t} \tag{3.7}$$

$$\rho u^{t+\Delta t} = \alpha_l^{t+\Delta t}\rho_l^{t+\Delta t}u_l^{t+\Delta t} + \alpha_g^{t+\Delta t}\rho_g^{t+\Delta t}u_g^{t+\Delta t} \tag{3.8}$$

Assuming the inlet flows and enthalpies are known, casting the problem as a Newton Iteration gives for the new iterate values

$$V_{cond}\left\{\frac{\rho u^{k+1} - \rho u^t}{\Delta t}\right\} = \sum_n \dot{m}_{IHX}^{t+\Delta t} h_{f_{@\,P_{IHX}}}^{t+\Delta t} + \sum_m \dot{m}_{PRV_{IHX}}^{t+\Delta t} h_{g_{@\,P_{IHX}}}^{t+\Delta t} + \sum_l \dot{m}_{turb_{exh}}^{t+\Delta t} h_{exh_l}^{t+\Delta t} - \dot{m}_{Feed}^{t+\Delta t} h_{f_{@\,P_{Cond}}}^{t+\Delta t} - \dot{Q}_{Cond}^t \tag{3.9}$$

$$V_{cond}\left\{\frac{\rho^{k+1} - \rho^t}{\Delta t}\right\} = \sum_n \dot{m}_{IHX}^{t+\Delta t} + \sum_m \dot{m}_{PRV_{IHX}}^{t+\Delta t} + \sum_l \dot{m}_{turb_{exh}}^{t+\Delta t} - \dot{m}_{Feed}^{t+\Delta t} \tag{3.10}$$

$$\tilde{\rho}^k = \rho\left(\alpha_g^k, P_{Cond}^k\right) = \rho_f\left(P_{Cond}^k\right) + \alpha_g^k\left[\rho_g\left(P_{Cond}^k\right) - \rho_f\left(P_{Cond}^k\right)\right] \tag{3.11}$$

$$\widetilde{\rho u}^k = \rho u\left(\alpha_g^k, P_{Cond}^k\right) = \rho_f\left(P_{Cond}^k\right)u_f\left(P_{Cond}^k\right) + \alpha_g^k\left[\rho_g\left(P_{Cond}^k\right)u_g\left(P_{Cond}^k\right) - \rho_f\left(P_{Cond}^k\right)u_f\left(P_{Cond}^k\right)\right] \tag{3.12}$$

$$\rho^{k+1} = \tilde{\rho}^k + \delta\alpha_g\left.\frac{\partial\rho}{\partial\alpha_g}\right|_k + \delta P_{Cond}\left.\frac{\partial\rho}{\partial P}\right|_k \tag{3.13}$$

$$\rho u^{k+1} = \widetilde{\rho u}^k + \delta\alpha_g\left.\frac{\partial\rho u}{\partial\alpha_g}\right|_k + \delta P_{Cond}\left.\frac{\partial\rho u}{\partial P}\right|_k \tag{3.14}$$

24

The system of equations can be rewritten as a direct solve for $\rho u^{k+1}, \rho^{k+1}, \delta\alpha_g, \delta P_{Cond}$. Upon convergence, the heat transfer rate for the next time step ($\dot{Q}^t_{Cond}$) can be obtained from $\dot{Q}_{Cond} = UA_{cond}\Delta T_m$ where

$$\Delta T_m = \frac{\left(T_{sat} - T_{Cond_{exit}}\right) - \left(T_{sat} - T_{Cond_{inlet}}\right)}{\ln\left[\dfrac{T_{sat} - T_{Cond_{exit}}}{T_{sat} - T_{Cond_{inlet}}}\right]} \tag{3.15}$$

$$UA_{cond} = \frac{2\pi nL}{\dfrac{1}{h_i r_i} + \dfrac{1}{k}\ln\left(\dfrac{r_o}{r_i}\right) + \dfrac{1}{h_o r_o}} \tag{3.16}$$

The condensing heat transfer rates h_i and h_o are obtained in the same manner as in the intermediate heat exchanger equations (2.18) and (2.19).

It will be assumed that the mass flow rate of the cooling water is constant and known along with the cooling water inlet temperature and pressure. This gives $T_{Cond_{inlet}}$. To calculate $T_{Cond_{exit}}$ an energy balance can be applied between the tube and shell side of the condenser.

$$V_{Cond}\rho_{flow}c_{p_{flow}}\left\{\frac{T^{t+\Delta t}_{Cond_{exit}} - T^t_{Cond_{exit}}}{\Delta t}\right\} + \dot{m}_{Cond}c_{p_{flow}}\left\{T^{t+\Delta t}_{Cond_{exit}} - T_{Cond_{inlet}}\right\} = \dot{Q}^t_{Cond} \tag{3.17}$$

Rearranging gives for $T^{t+\Delta t}_{Cond_{exit}}$

$$T^{t+\Delta t}_{Cond_{exit}} = \frac{\dot{Q}^t_{Cond}}{\zeta} + \frac{\dot{m}_{Cond}c_{p_{flow}}T_{Cond_{inlet}}}{\zeta} + \frac{T^t_{Cond_{exit}}\dfrac{V_{Cond}\rho_{flow}c_{p_{flow}}}{\Delta t}}{\zeta} \tag{3.18}$$

Where, $\zeta = \dfrac{V_{Cond}\rho_{flow}c_{p_{flow}}}{\Delta t} + \dot{m}_{Cond}c_{p_{flow}}$.

3.3 Simulation

To test the condenser model, a 100 second null transient was run. The initial conditions and sizing of the condenser are shown below in Table 3.1.

25

Table 3.1: Condenser Parameters

Parameter	Value
Number of Tubes	76824
Length of Tubes	24.1 feet
Thermal conductivity	10.3 Btu/hr-ft-F
Cooling Water Temperature	50F
Pressure of Cooling Water	14.7psi
Cooling Water Mass Flow Rate	34,110,000 lbm/hr
Condenser Design Pressure	0.7 psi
Cross Sectional Area of Shell Side	114.611 ft^2
Cross Sectional Area of Tube Side	116.4 ft^2
Tube Inner Radii	0.022 ft
Tube Outer Radii	0.029 ft
Turbine exhaust mass flow	1,146,000 lbm/hr
Flow out of Condenser	1,146,000 lbm/hr
Design Heat Transfer Rate	350 MW
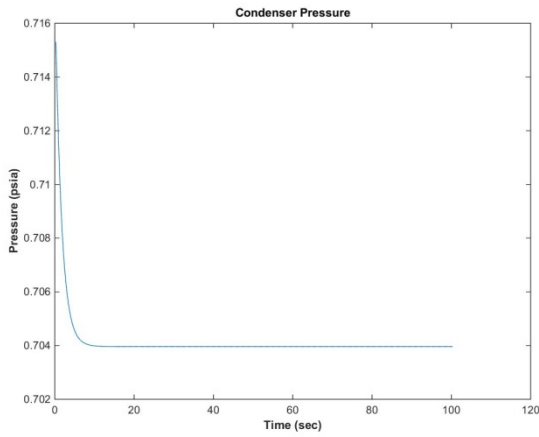
Figure 3.2: Condenser Pressure
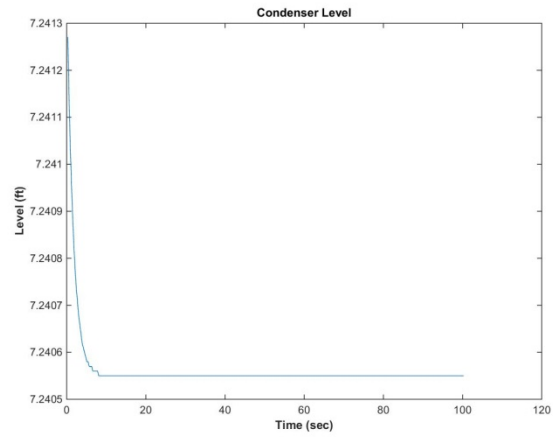
Figure 3.3: Condenser Level

26
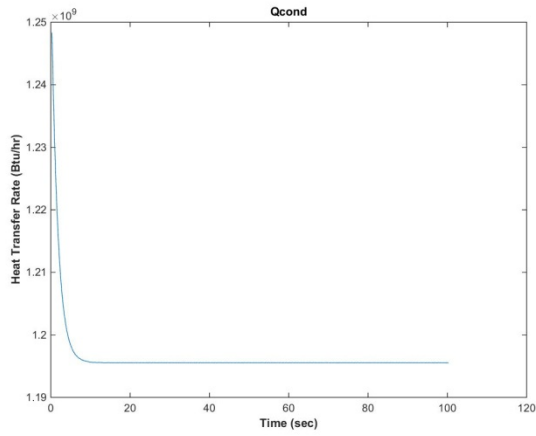
Figure 3.4: Condenser Heat Transfer Rate

As illustrated in Figure 3.2-Figure 3.4 the condenser model quickly goes to steady state. The system stabilizes at a pressure of 0.7 psi and is rejecting about 350MW of power.

Chapter 4   TES Standalone System Response

4.1 NuScale Size System

The system was designed to accommodate 85% steam dump from a NuScale size system for 24 hours. To accommodate this demand, large storage tanks were installed. To ensure that neither tank over pressurizes the combined amount of TES fluid in both the hot and cold tanks is slightly less than what either one could hold on their own. System design parameters are given in Table 4.1.

Table 4.1: NuScale Size System Parameters

Parameter	Value
TES Fluid	Therminol®-66
Hot tank Volume	2,000,000 ft^3
Cold Tank Volume	2,000,000 ft^3
IHX reference Exit Temperature	500F
Number of TBV's	4
TES maximum steam accommodation	85% Nominal conditions of NuScale size reactor
Pressure Relief Valve Upper Setpoint	780 psi
Pressure Relief valve Lower Setpoint	735 psi
Turbine Header Pressure	825 psi
Shell Side (outer loop) IHX Volume	755.443 ft^3
Number of tubes	12190
Length of tubes	36 ft
Tube Inner Diameter	0.044 ft
Tube Outer Diameter	0.058 ft
Mass of Hot Tank Fill Gas	1.122×10^5 lbm
Mass of Cold Tank Fill Gas	1.309×10^5 lbm
Temperature of Cooling Water	50F
Volume of Condenser (Shell Side)	7607 ft^3
Number of tubes in Condenser	76824
Length of tubes in Condenser	24.1ft
Mass Flow of Cooling Water	3.411×10^7 lbm/hr
Condenser Tube Inner Diameter	0.044 ft
Condenser Tube Outer Diameter	0.058 ft

4.1.1 Aggressive Load Profile

To test the robustness of the TES system an aggressive load profile was made for the system ranging from 85% bypass all the way down to 30% bypass over a sixteen hour run. This load profile is not typical of standard electrical demand profiles and is only used to test the robustness of the TES system model. If this demand can be met then it stands to reason that other less aggressive profiles should be easily accommodated given proper sizing of the system.
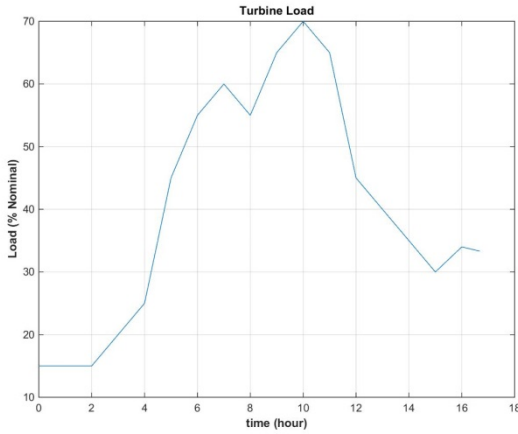
Figure 4.1: Aggressive Load Profile
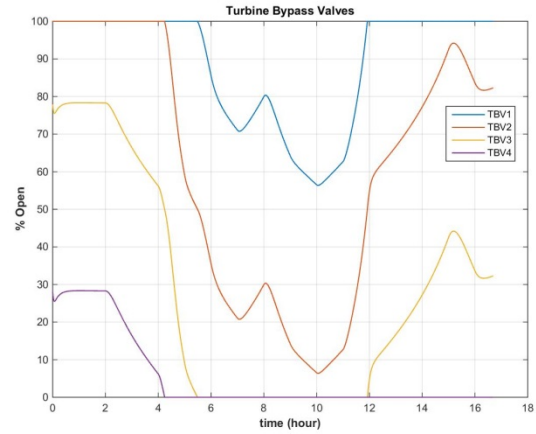
Figure 4.2: Auxiliary Bypass Valve Position
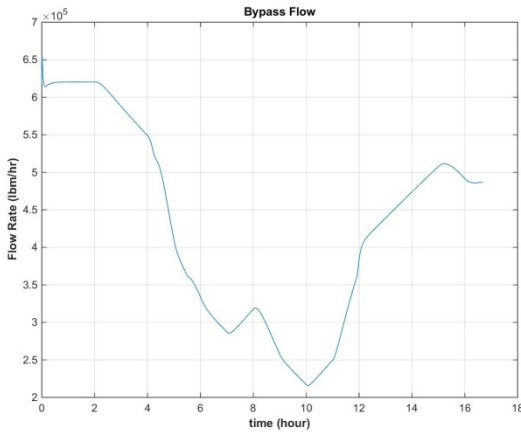
Figure 4.3: Bypass Flow
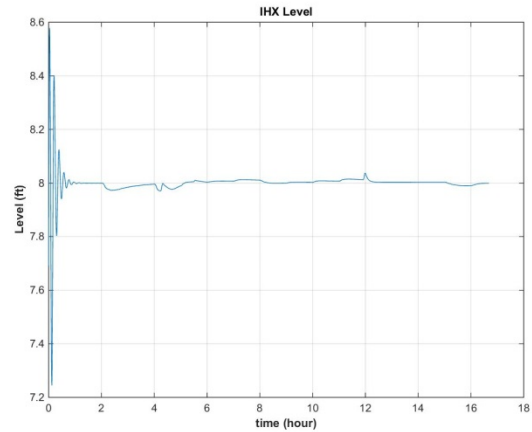
Figure 4.4: Level in the Intermediate Heat Exchanger

29
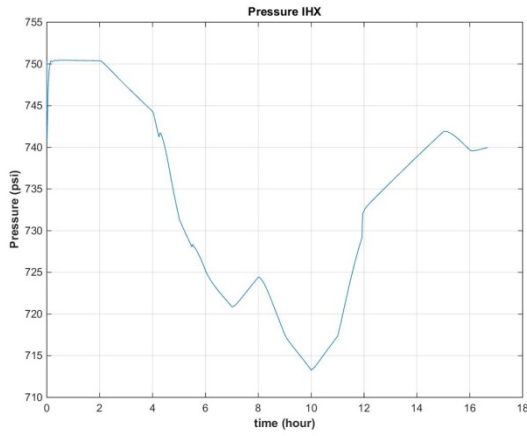
Figure 4.5: Pressure in the Intermediate Heat Exchanger
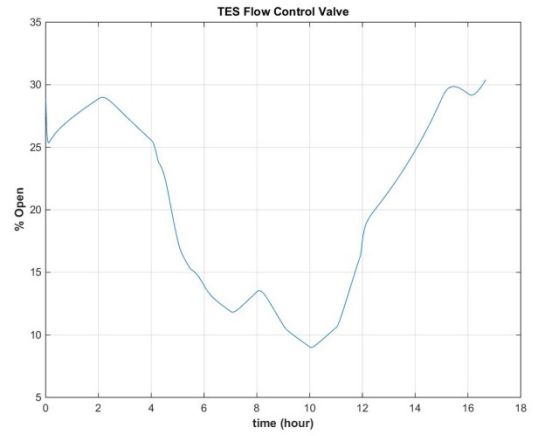
Figure 4.6: TES Flow Control Valve Position
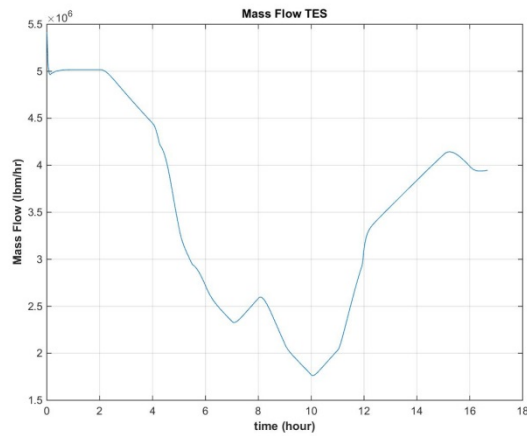
Figure 4.7: Mass Flow of the Therminol-66 from the cold tank to the hot tank
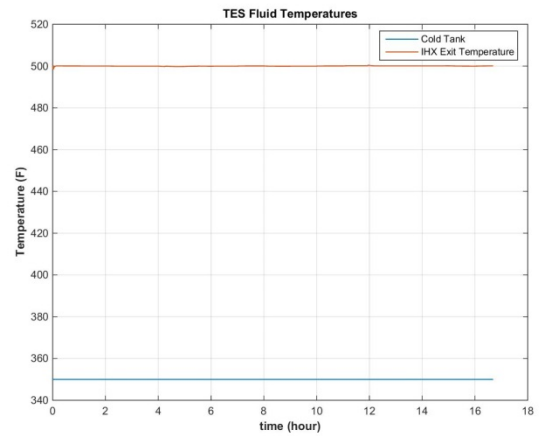
Figure 4.8 TES Fluid Temperature at exit of IHX

30
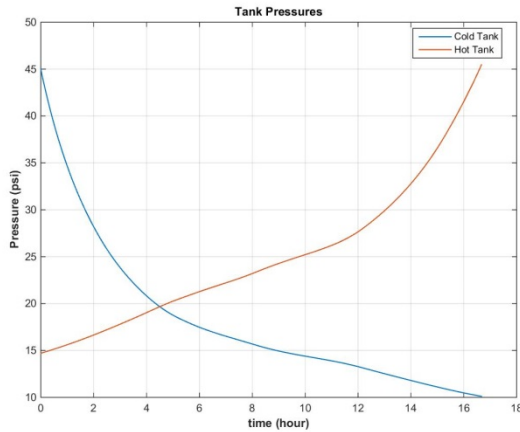
Figure 4.9 Hot and Cold Tank Pressures   Figure 4.10: Hot and Cold Tank Levels
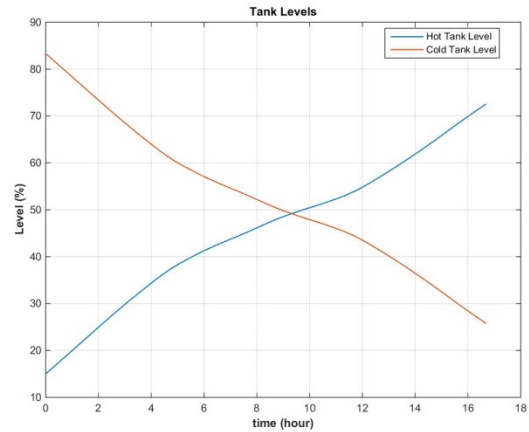
The system has a nominal output of ~160 MWth. As seen in Figure 4.1 the system initially starts with about 15% load on the turbine. This small turbine load means that the TES system is in full charging mode as 85% of the net reactor capacity is being pushed through the TES system. At this demand level all four of the auxiliary turbine bypass valves are open to allow steam into the IHX.

As the turbine load increases the bypass valves begin to close and subsequently the heat transfer rate to the inner loop decreases. When the heat transfer rate decreases so does the TES fluid exit temperature causing the FCV to close to keep the temperature at the set point value. The closing of the FCV reduces the charging rate between the hot and cold tanks as seen in Figure 4.7. At the end of the run the cold tank has gone from 82% full down to about 26% full while the hot tank has gone from 15% full up to about 72% full.

At the full design criteria of 85% steam dump with the cold tank relatively full, the FCV is ~25% open. This extra 75% capacity in the FCV is to accommodate full 85% steam dump when the hot tank approaches its design capacity.

4.2 mPower Size System

In the next scenario, a TES system designed to handle bypass from a mPower size reactor was simulated. mPower has an electric output of 180MWe with a 530MWth operating power [29]. The

TES system bypass lines have been designed to accommodate ~45%-50% bypass from the reactor at an IHX shell side operating pressure of 750psi. The Condenser for this model has been designed to accommodate 530MW.

Table 4.2: Design Parameters for a mPower size TES system.

Parameter	Value
TES Fluid	Therminol®-66
Hot tank Volume	8,000,000 ft³
Cold Tank Volume	8,000,000 ft³
IHX reference Exit Temperature	500F
Number of TBV's	4
TES maximum steam accommodation	~45% Nominal
Pressure Relief Valve Upper Setpoint	780 psi
Pressure Relief valve Lower Setpoint	760 psi
Turbine Header Pressure	825 psi
Shell Side (outer loop) IHX Volume	1171 ft³
Number of tubes	19140
Length of tubes	36.9 ft
Tube Inner Diameter	0.044 ft
Tube Outer Diameter	0.058 ft
Mass of Hot Tank Fill Gas	5.235×10^5 lbm
Mass of Cold Tank Fill Gas	4.489×10^5 lbm
Temperature of Cooling Water	50F
Volume of Condenser (Shell Side)	7607 ft³
Number of tubes in Condenser	76824
Length of tubes in Condenser	24.1ft
Mass Flow of Cooling Water	3.411×10^7 lbm/hr
Condenser Tube Inner Diameter	0.044 ft
Condenser Tube Outer Diameter	0.058 ft

4.2.1 Typical Summer Day
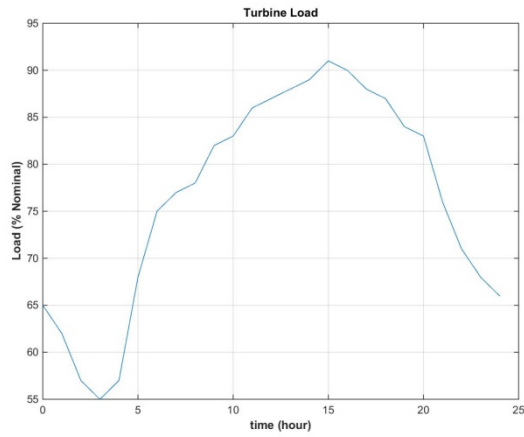
Figure 4.11: Summer Day Load Profile
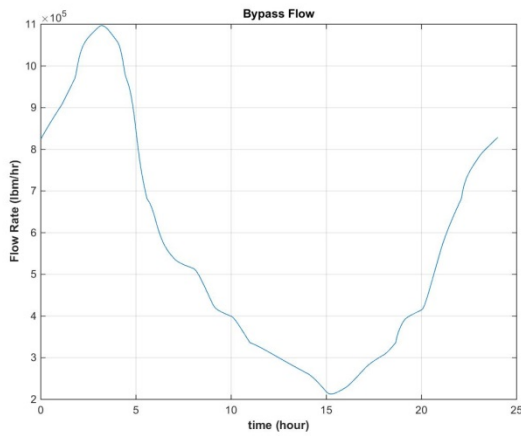
Figure 4.12: Bypass Flow
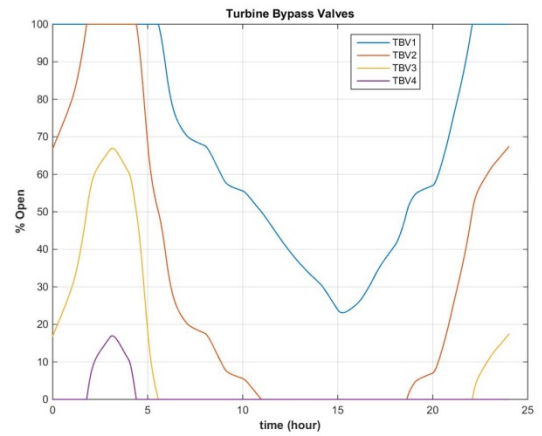
Figure 4.13: Position of TES Bypass Valves

33
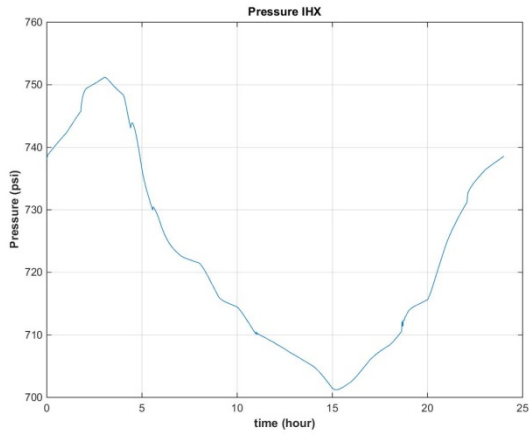
Figure 4.14: Intermediate Heat Exchanger Pressure
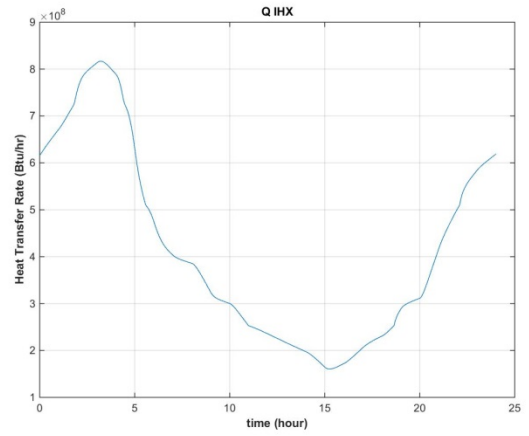
Figure 4.15: Heat Transfer Rate Across the Intermediate Heat Exchanger
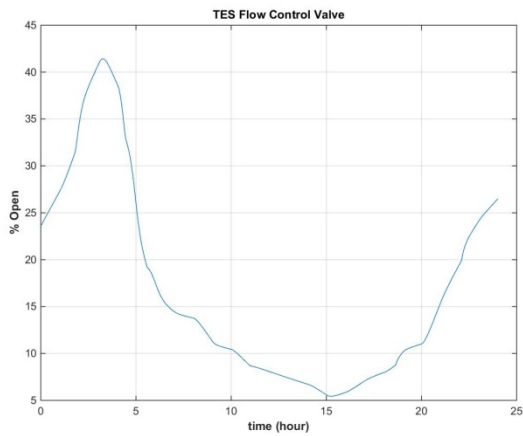
Figure 4.16: Position of TES Flow Control Valve
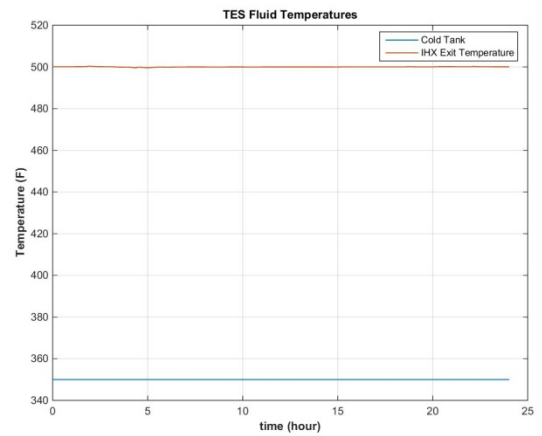
Figure 4.17: Temperature of the TES fluid leaving the IHX.

34
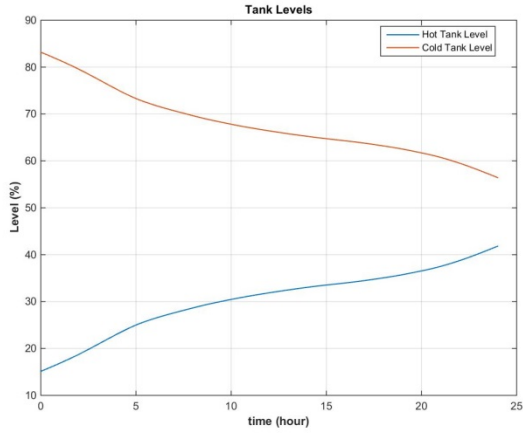
Figure 4.18: Hot and Cold Tank Levels
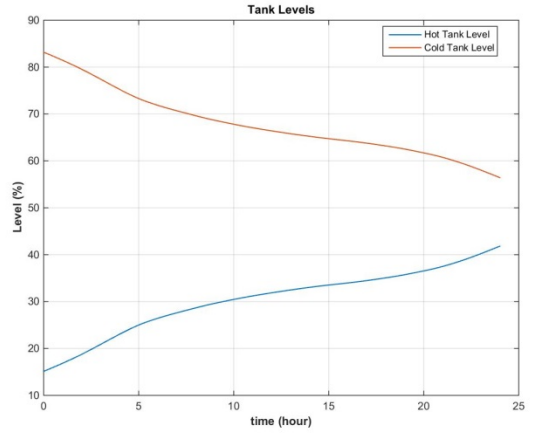
Figure 4.19: Hot and Cold Tank Pressures
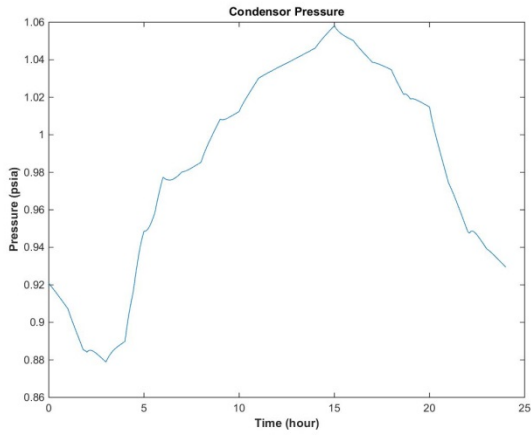
Figure 4.20: Condenser Pressure
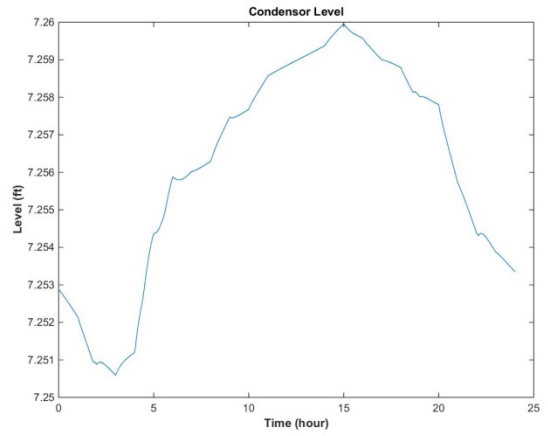
Figure 4.21: Condenser Level

35
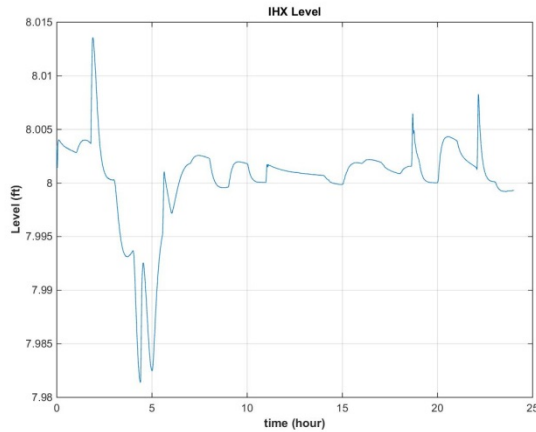
Figure 4.22: Level in the IHX.

The reactor system was assumed to have sufficient capacity to meet 100% load on the most extreme summer day. The run shown above is representative of a typical summer day [1]. As a result, there will always be some bypass demand. Bypass demand goes as nominal reactor output-turbine demand. For the run shown we have bypass ranging from ~45% bypass down to ~7-8% bypass. Figure 4.13 shows that we are able to meet bypass demand as the valves never fully open or shut. Figure 4.14 shows the operating pressure at 45% bypass at the 750 psi design pressure, and over the course of the run reaches a minimum of ~700psi. As the pressure does not fall below 680psi, the shell side saturation temperature remains above the tube side set point temperature of 500F. Should the pressure in the IHX fall below this value the set point temperature on the tube side could not be reached. Further, the pressure in the IHX never reaches the setpoint of 780psi at which point the Pressure Relief Valves would open. Since the Pressure Relief Valves do not open this means zero energy is bypassing the TES system through the PRV's.

As shown in Figure 4.16 the flow control valve is ~24% open at the beginning of the simulation, it continues to move to ~42% open as bypass into the IHX increases. It then begins to close down to ~8% open as the amount of bypass flow into the IHX decreases later in the simulation. Figure 4.17 shows the flow control valve is able to maintain TES exit temperature at ~500F over the entire 24 hour simulation.

As the hot tank fills and the cold tank empties, the pressures in the tanks change due to compression and expansion of the cover gases. As the pressures change the relative position of the FCV required to

36

achieve the same mass flow rate of TES fluid changes. As a result, the FCV is more open towards the end of the 24-hour run than the beginning despite the same demand levels.

Over the course of the day condenser pressures vary from 0.86psi to 1psi, despite the condenser cooling water temperatures and flows remaining constant. The level of the IHX remains steady about the reference value of 8 feet.

4.2.2 Typical Winter Day

During the winter months there tends to be two peaks in the load profile. One associated with morning activities around 8-10am and a second when people are returning home for the evening [1]. Given that bypass flow goes as 1-relative demand, the overall bypass demand on the system is larger in the winter than in the summer months.
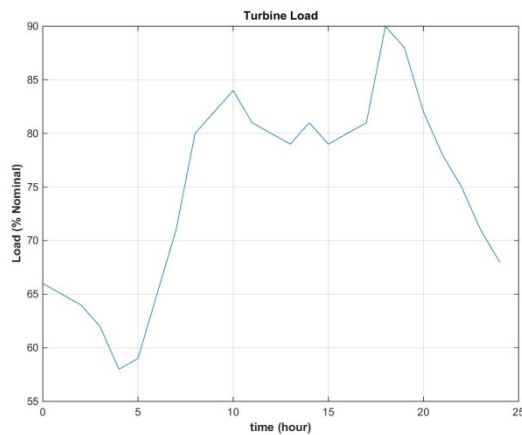
Figure 4.23: Winter Day Load Profile
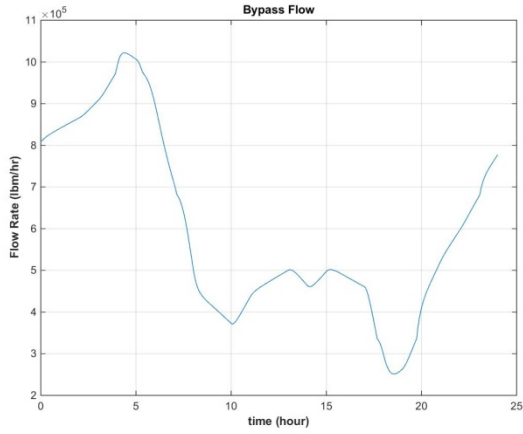
Figure 4.24: Bypass Flow
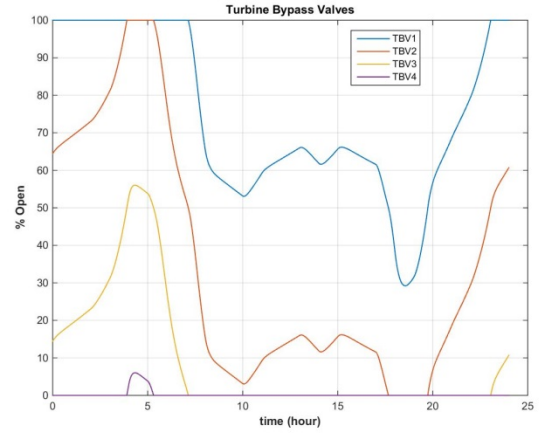
Figure 4.25: Position of TES Turbine Bypass Valves
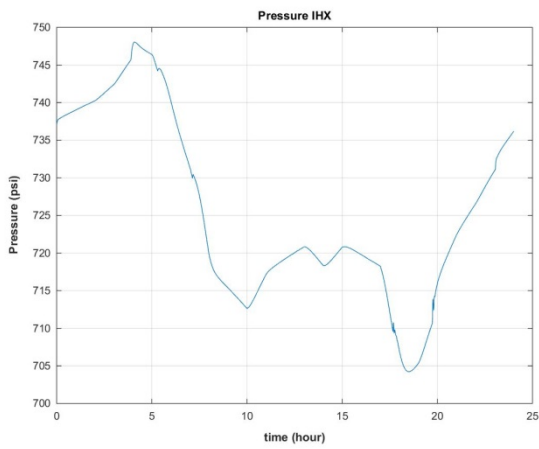
Figure 4.26: Pressure on the shell side of the IHX.
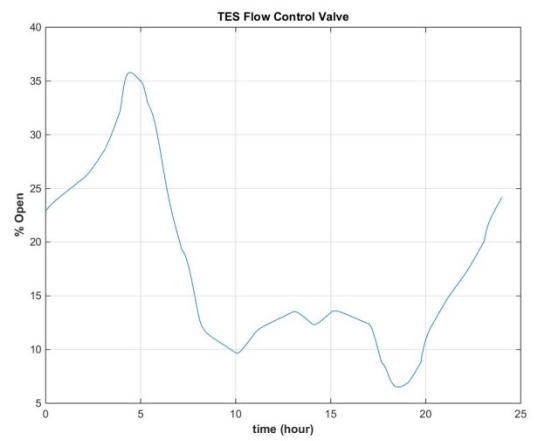
Figure 4.27: TES Flow Control Valve Position.

38
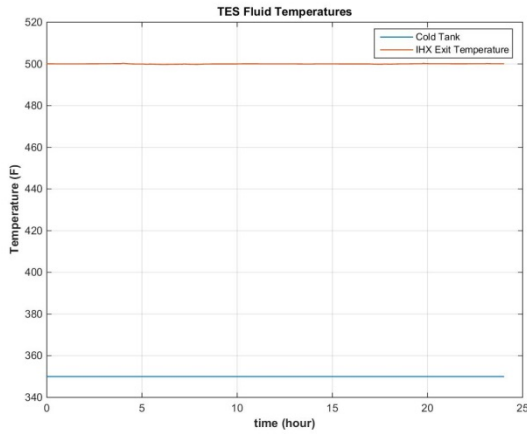
Figure 4.28: Temperature of TES fluid at exit of IHX.
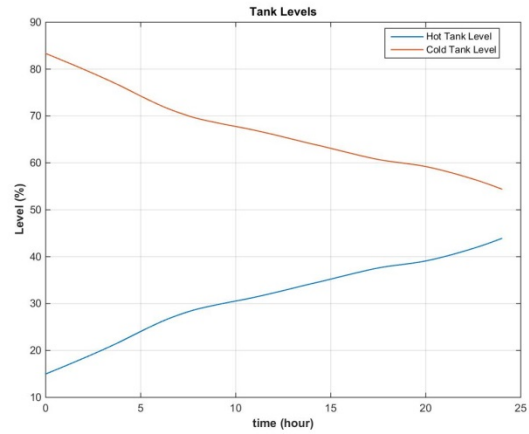
Figure 4.29: Hot and Cold Tank Levels.

As indicated in Figure 4.23 the turbine load goes from a minimum of ~57% up to 90% demand. This means the bypass demand is ranging from 43% nominal flow down to 10% nominal flow. In Figure 4.25 we see the turbine bypass valves never all go full open or full shut. This means we are never getting into a situation where the bypass demand is not met. Pressure in the IHX can be seen in Figure 4.26 and over the course of the run never falls below the target saturation pressure of 680psi or goes above the PRV set point of 780psi. With the pressure staying above 680psi the saturation temperature in the IHX stays above the reference temperature of 500F. Likewise, the pressure remaining below 780psi over the course of the entire 24 hour run ensures the PRV's remain closed. With the PRV's remaining closed all of the potential heat from the reactor is transferred into the TES fluid rather than bypassing straight to the condenser. From Figure 4.27 the flow control valve can be seen to never fully open or fully close. This means the system is never at the limits of its capacity and should be able to maintain the temperature at the top of the IHX over the course of the entire 24 hour run. This can be seen in Figure 4.28. As the flow control valve modulates flow to maintain the TES fluid temperature, the hot tank begins to fill as seen in Figure 4.29 .

4.2.3 Summer Day –Including Solar

The summer day load profile was modified to reflect upwards of 40MWe installed solar capacity. The reactor system was again assumed to have sufficient capacity to meet 100% load on the most extreme summer day. When applied to a standard summer day as in the previous example the output from

39

solar influences the load drastically. Figure 4.31 shows the overall load from 3am in the morning through 3am the following morning. Over the course of the day the solar output increases from zero power from midnight to 4am to near full power from 8am to 3pm [2]. Since solar generation tends to have grid priority in most areas this directly affects the demand profile seen by the nuclear plant. This difference in load can be seen in Figure 4.31 when comparing the overall demand with the demand on the reactor. The reactor demand curve is the result of taking the overall demand and subtracting the solar output from Figure 4.30.
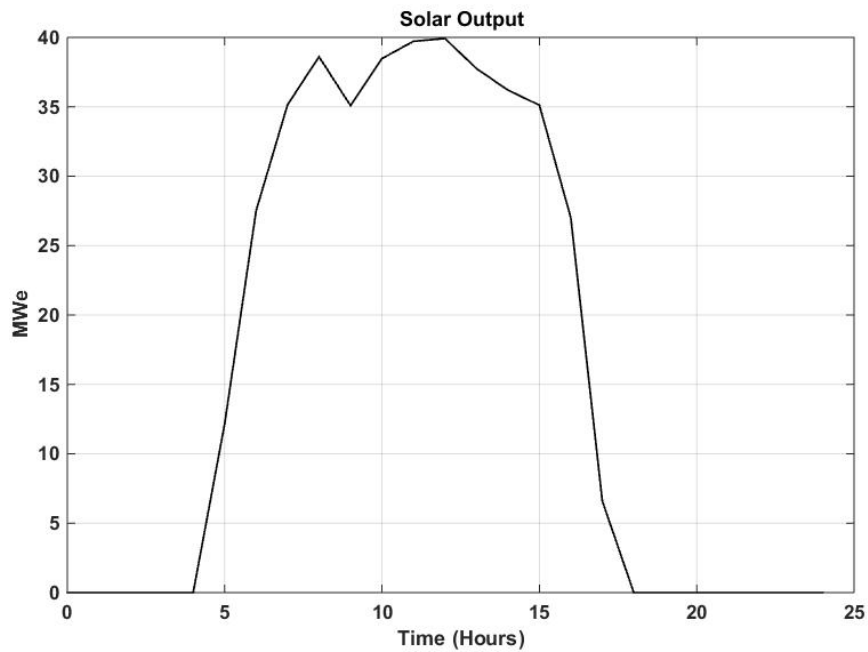
Figure 4.30: Typical Solar Output for a Summer Day

Typical Summer Day Demand
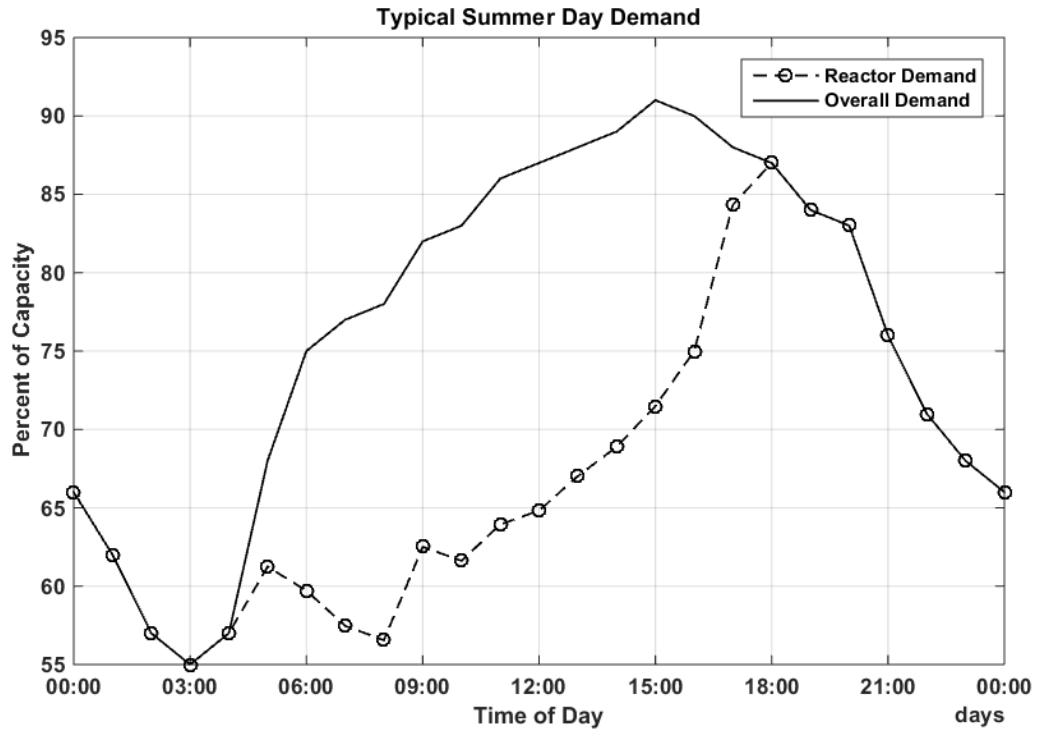
Figure 4.31: Demand profiles of a typical summer day with and without solar
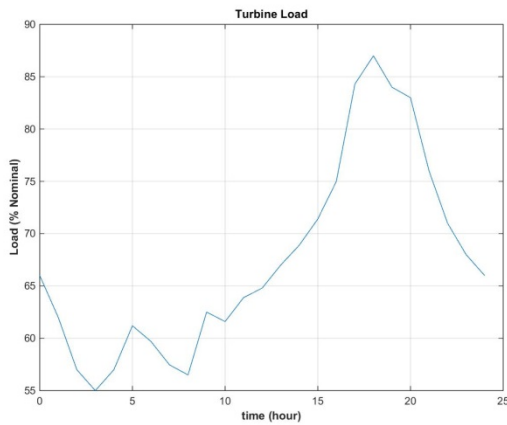
Figure 4.32: Summer Load Profile With Solar Generation
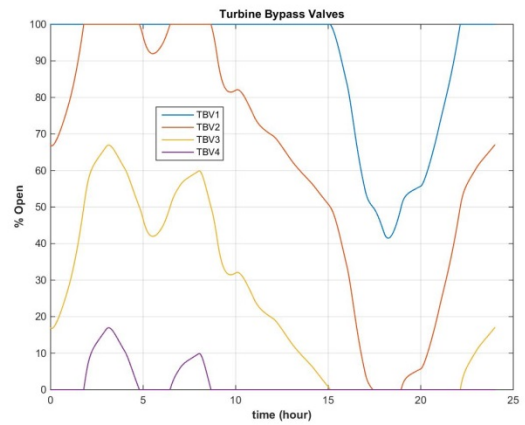
Figure 4.33: TES Bypass Valve Position

41
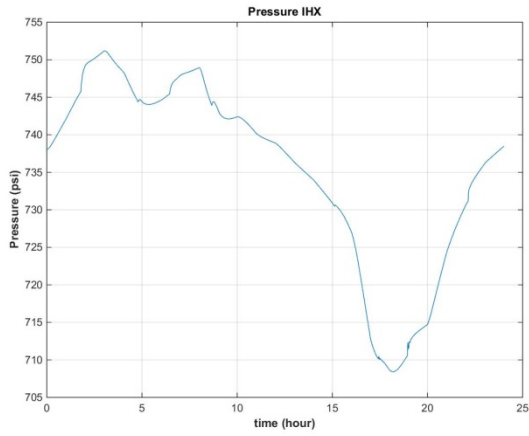
Figure 4.34: Pressure in the IHX.
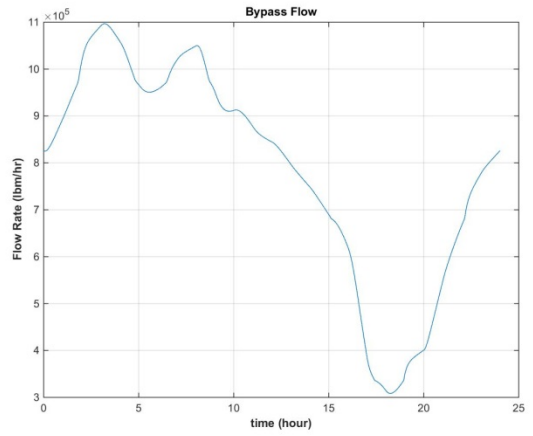
Figure 4.35: Bypass Flow
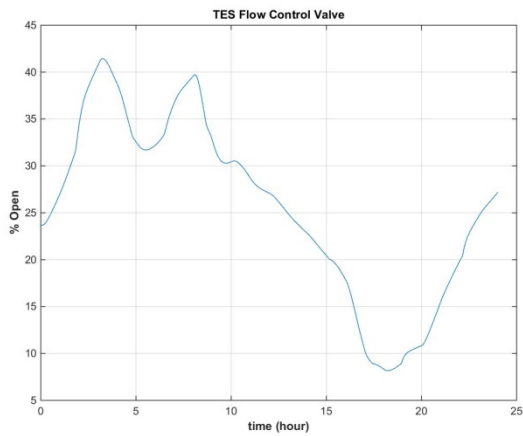
Figure 4.36: Flow Control Valve Position
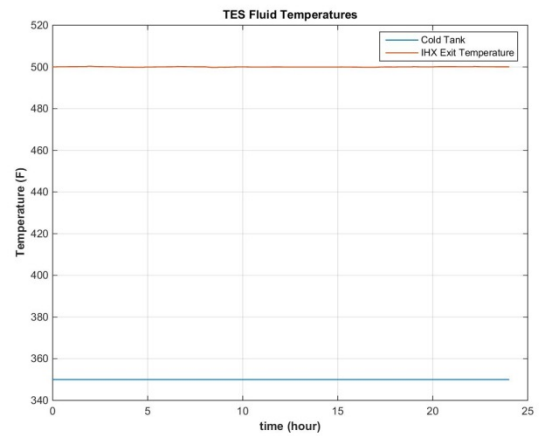
Figure 4.37: Temperature of TES fluid exiting the IHX.
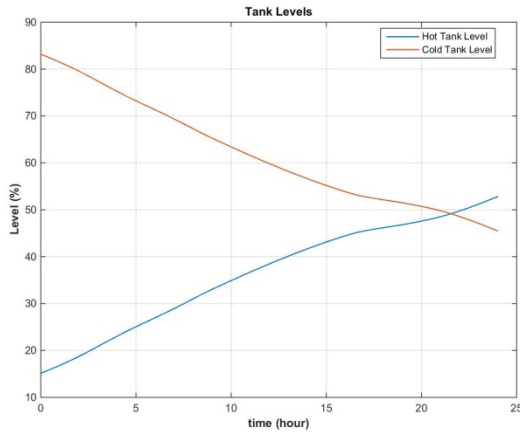
Figure 4.38: Hot and Cold Tank Levels.
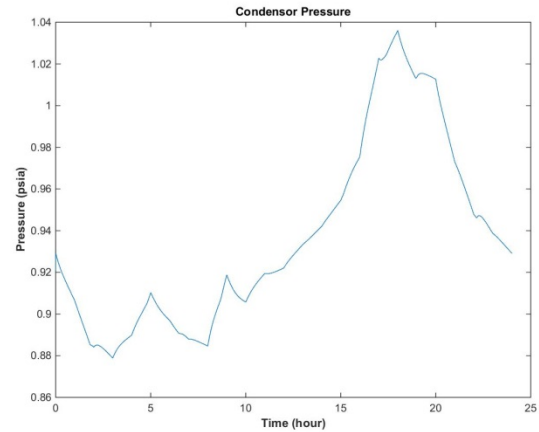
Figure 4.39: Condenser Pressure

Over the course of the simulation bypass flow ranges from 45% down to a bypass flow rate of ~13%. During this time Figure 4.33 shows the bypass valves initially start with one full open, two partially open, and one closed. The two partially open valves are at positions of ~17% and 67%. This 50% difference is due to a 50% overlap in the opening and closing set points for the valves. As the run progresses and the bypass demand is reduced, the valves close such that at 18 hours into the simulation all but one of the valves are completely closed. As the valves close and heat continues to be transferred from the shell side of the IHX to the tube side, shell side pressure decreases. Pressure ranges from 750psi to ~707psi, but remains above 680psi corresponding to the reference temperature of the IHX. Further, the pressure never reached the set point of 780psi that would open the PRV's.

As seen in Figure 4.36 and Figure 4.37 the flow control valve is moving to insure the temperature at the exit of the IHX is maintained at 500F. From Figure 4.38 the hot tank level increases and is able to accommodate the full 24 hour load cycle.

4.2.4   Summer Day –Including Wind

Solar generation is only available when the sun is shining. Wind power on the other hand is variable throughout the day. This inability to predict wind availability necessitates the need to lower the penetration level of wind power compared to solar power [2]. While solar generation tends to coincide with the highest power demand parts of the day, wind can be producing power at full capacity during times that demand is already low. If the wind penetration is sufficiently large this

43

could create a situation where the bypass valves are full open and the bypass demand cannot be met. In this situation, the reactor would likely be required to reduce power.
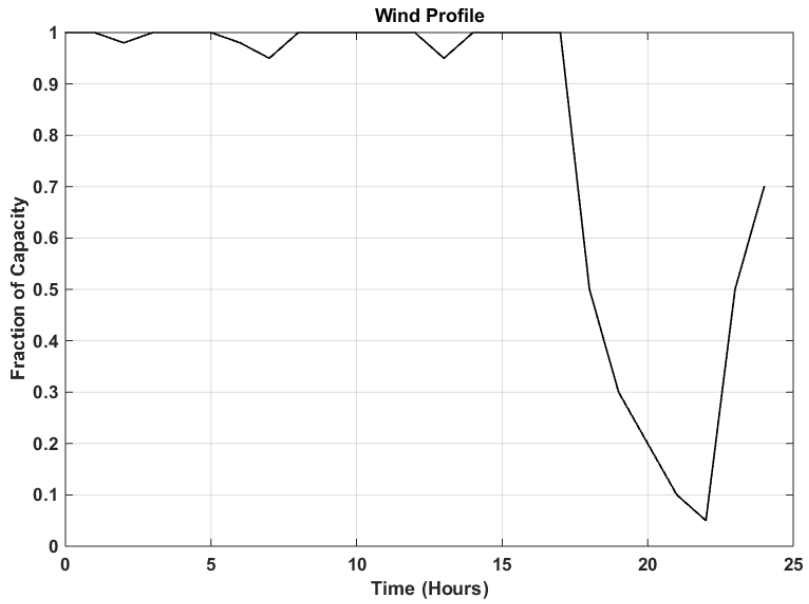
Figure 4.40: Wind availability profile.
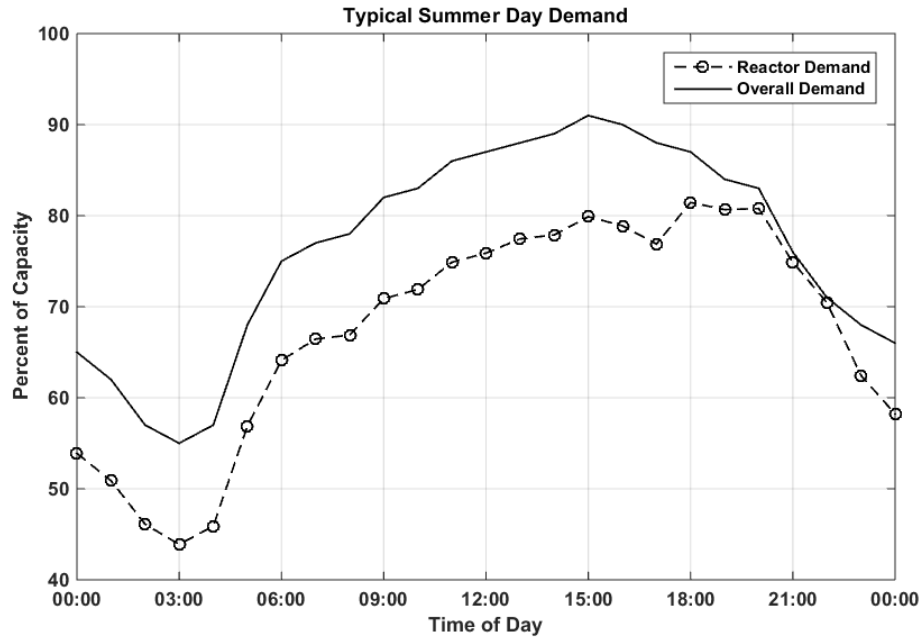
Figure 4.41: Typical summer day profile with 20MW wind capacity installed.

44

The demand on the reactor is the overall demand minus power provided by the wind plant. This decrease in turbine demand, seen in Figure 4.41, increases the amount of bypass flow allowed into the system. The bypass demand is upwards of 55% around 3am. This large amount of bypass is slightly more than the TES capacity, as seen in Figure 4.43.
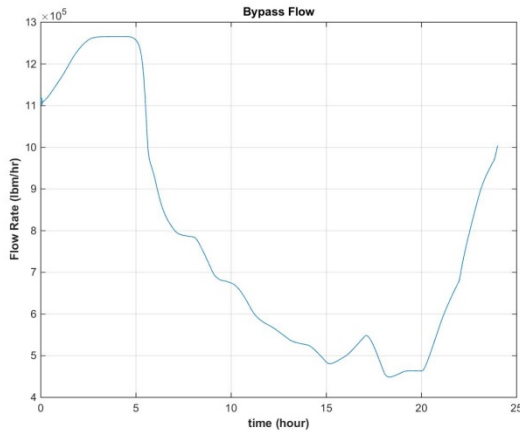
Figure 4.42: Bypass Flow
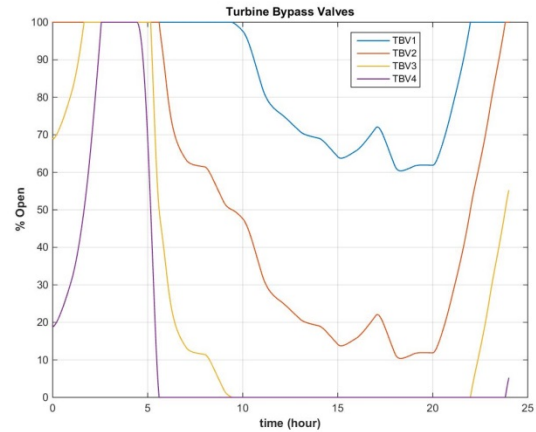
Figure 4.43: TES Turbine Bypass Valve Positions
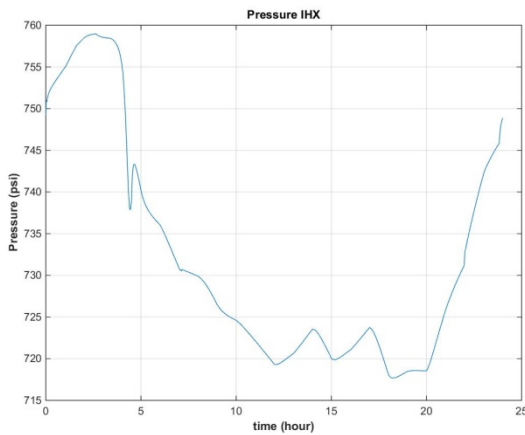
Figure 4.44: Pressure in the IHX.
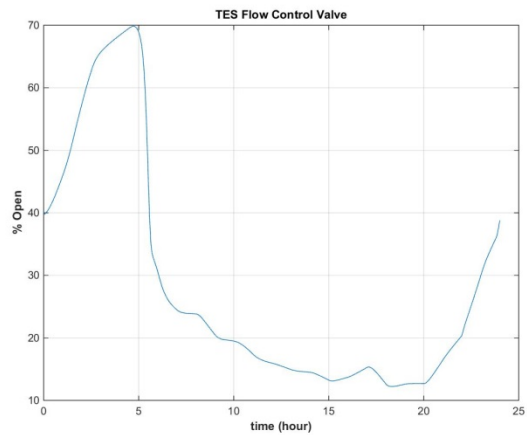
Figure 4.45: TES Flow Control Valve Position
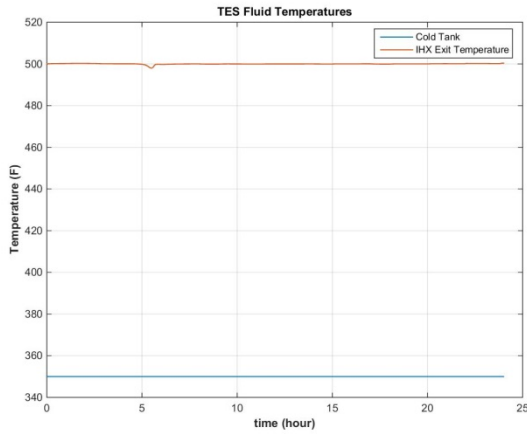
| Figure 4.46: Temperature at the exit of the IHX. | Figure 4.47: Hot and Cold Tank Levels |
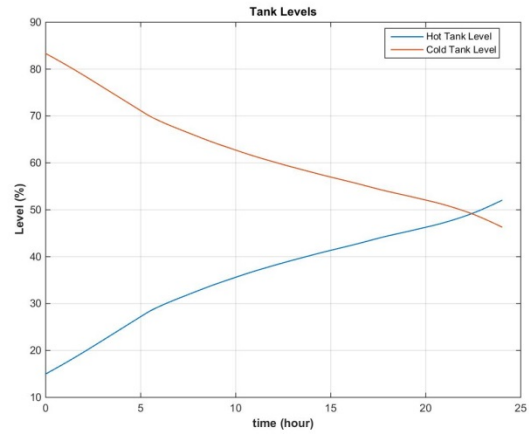
For the load profile considered above the bypass demand reaches around 55%. When attempting to accommodate this large bypass demand the bypass valves go full open. At their full open position, the valves are unable to provide the bypass flow necessary to keep the reactor at 100% power. In this situation the reactor would have to decrease power. While the bypass valves are full open the pressure in the IHX increases. Fortunately, over the course of the run the pressure stays below the PRV set point of 780psi meaning the PRV's are never forced to open. As bypass demand decreases later in the day, the bypass valves close and pressure in the IHX decreases. Figure 4.45 and Figure 4.46 show that over the course of the run the FCV went from 38% open up to 68% open as the FCV is modulating to maintain the reference temperature at the top of the IHX. For a brief period when the pressure in the IHX was dropping quickly the heat transfer rate across the IHX also drops. As the heat transfer rate across the IHX decreased rapidly the temperature at the exit of the IHX dropped significantly and it took the FCV a while to ultimately catch up. This is why there is a small period of time (~5-10 minutes) where the TES fluid temperature leaving the IHX is slightly less than the reference temperature.

4.2.5 Summer Day –Including Wind and Solar

Another potential configuration is with simultaneous wind and solar generation in an area.
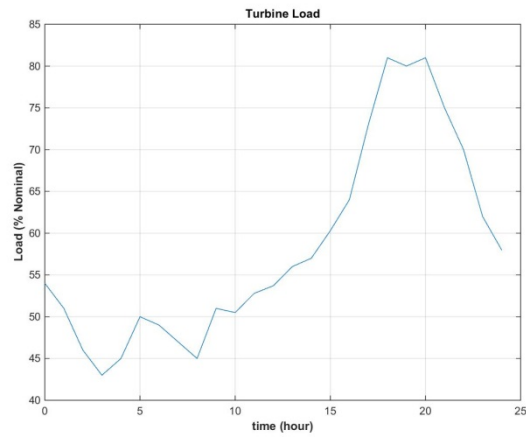
Figure 4.48: Summer Day Load Profile with Wind and Solar Generation
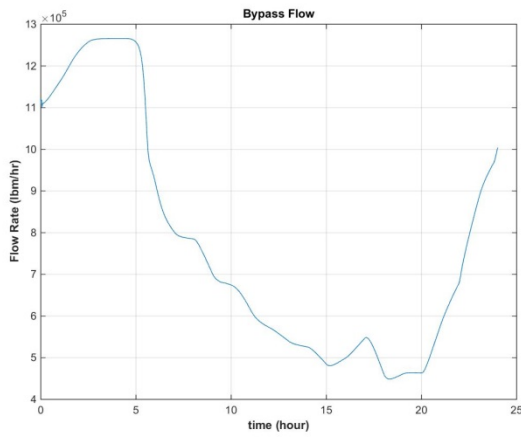
Figure 4.49: Bypass Flow
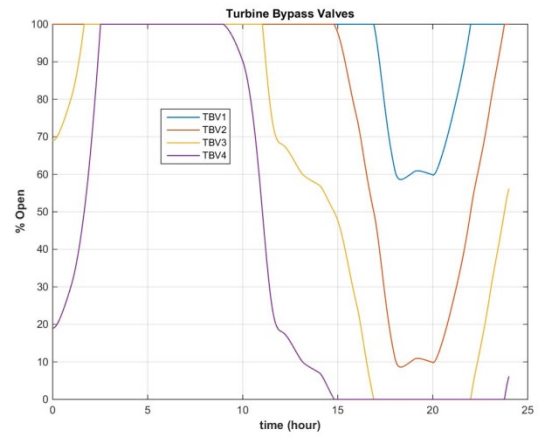
Figure 4.50: TES Turbine Bypass Valve Positions
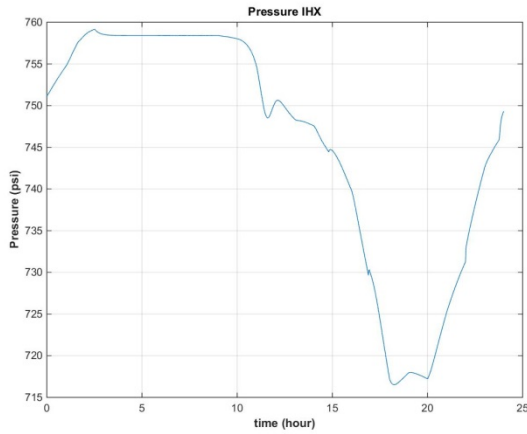
Figure 4.51: Pressure on the shell side of the IHX.
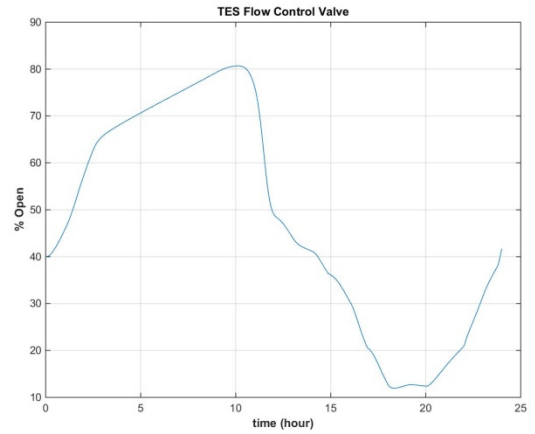
Figure 4.52: TES Flow Control Valve Position
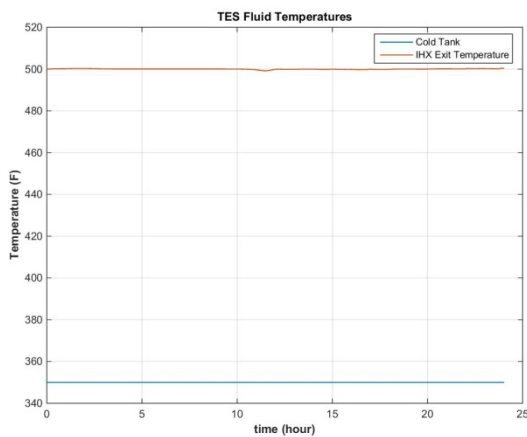
Figure 4.53: Temperature at the exit of the IHX
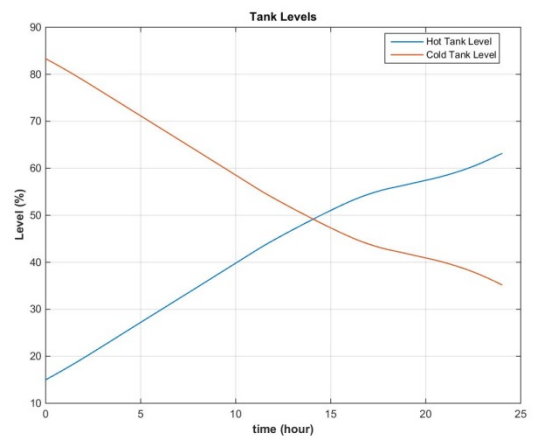
Figure 4.54: Hot and Cold Tank levels

The inclusion of both wind and solar produces a much more demanding load profile. With the increased demand on the TES system the bypass valves often go to their full open position. When full open the amount of bypass required to maintain the reactor at nominal 100% power is not met. This means the reactor will be required to decrease in power. Figure 4.50 shows that from hour 3 to about hour 8 the bypass valves are full open. Looking at Figure 4.51 the pressure in the IHX never decreases below 680psi and never goes above the 780 set point for PRV's to open. Over the course of the simulation the flow control valve oscillates between 10% open and 80% open to maintain the temperature at the exit of the IHX at the reference 500F as seen in Figure 4.52 and Figure 4.53.

48

Chapter 5 Reactor Simulator

5.1 Simulator Design

To further test the systems robustness, the TES system model was connected to a high fidelity time-dependent SMR systems code [30]. The systems code gives the time dependent behavior of the reactor, primary and secondary coolant loops, balance of plant and associated control systems. The modeled SMR was an Integral Pressurized Water Reactor with system parameters similar to B&W's mPower. The nodalization of the primary loop is illustrated in Figure 5.1.

Nodes	Description
1 – 4	Reactor Core
5	Lower Riser
6, 26	Upper Riser
7, 25	RCP Inlet Plenum
8 – 13, 19 – 24	Steam Generator
14, 18	Upper Downcomer
15,17	Lower Downcomer
16	Lower Plenum
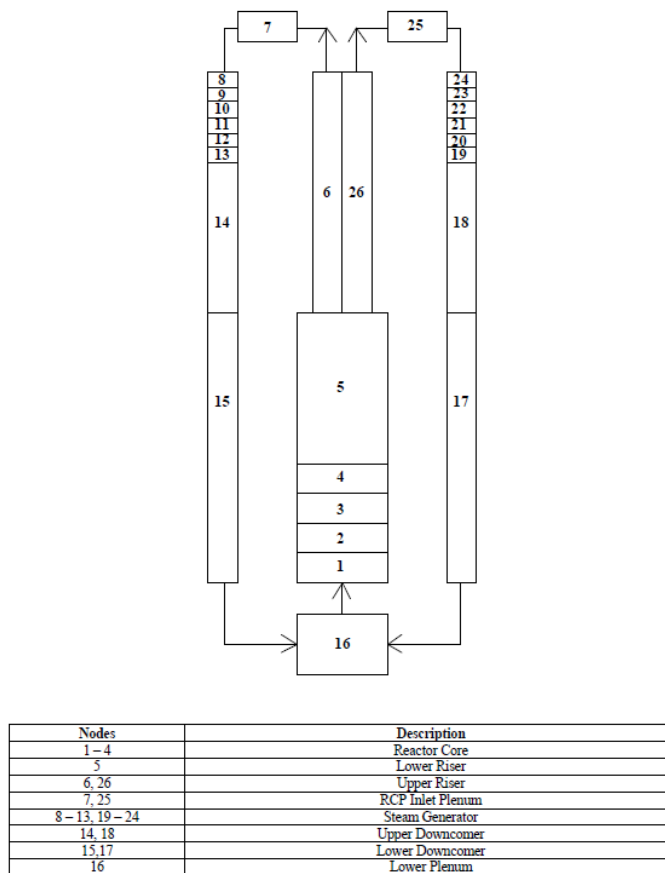
Figure 5.1: SMR Simulator Nodalization

The Steam Generator is a Once Through design where the tubes are located in the annulus between the Pressure Vessel Wall and the upper riser. The Steam Generator Tube length was designed such that there is ~50 F superheat at nominal conditions with a steam pressure of 825 psia.

Table 5.1: SMR Design Parameters

Parameter	Value
Reactor Thermal Output	530 Mwt
Electric Output	180 Mwe
Primary System Pressure	2050 psia
Core Inlet Temperature	566 F
Core Exit Temperature	611 F
Core Flow Rate	30 Mlbm/hr
Steam Pressure	825 psia
Steam Temperature	571 F
Feed Temperature	414 F
Steam Flow Rate	2.1Mlbm/hr
Number of Tubes	7048
Tube Material	Inconel-690
Tube Inner Diameter	0.523 inches
Tube Outer Diameter	0.687 inches
Pitch	0.824 inches

5.2 Connection Points

A typical main steam line configuration is illustrated in Figure 5.2. For plants incorporating Once Through Steam Generators (OTSG) the turbine control valve (TCV) acts as a pressure control valve to maintain Steam Generator pressure at some set point. With this in mind there are two options for bypassing steam to the TES system. Bypass can either be taken off the steam line at the pressure equalization header before the turbine control valves or after the turbine control valves prior to entering the high pressure turbine. For the TES system design described previously it is desired to have roughly constant steam conditions since the shell side pressure in the Intermediate Heat Exchanger directly affects the reference temperature at the top of the IHX. This constraint makes taking bypass steam from the pressure equalization header upstream of the turbine control valves the preferred operating mode. Taking bypass steam downstream of the turbine control valves would give highly varying steam pressures and temperatures that could result in low IHX pressures.
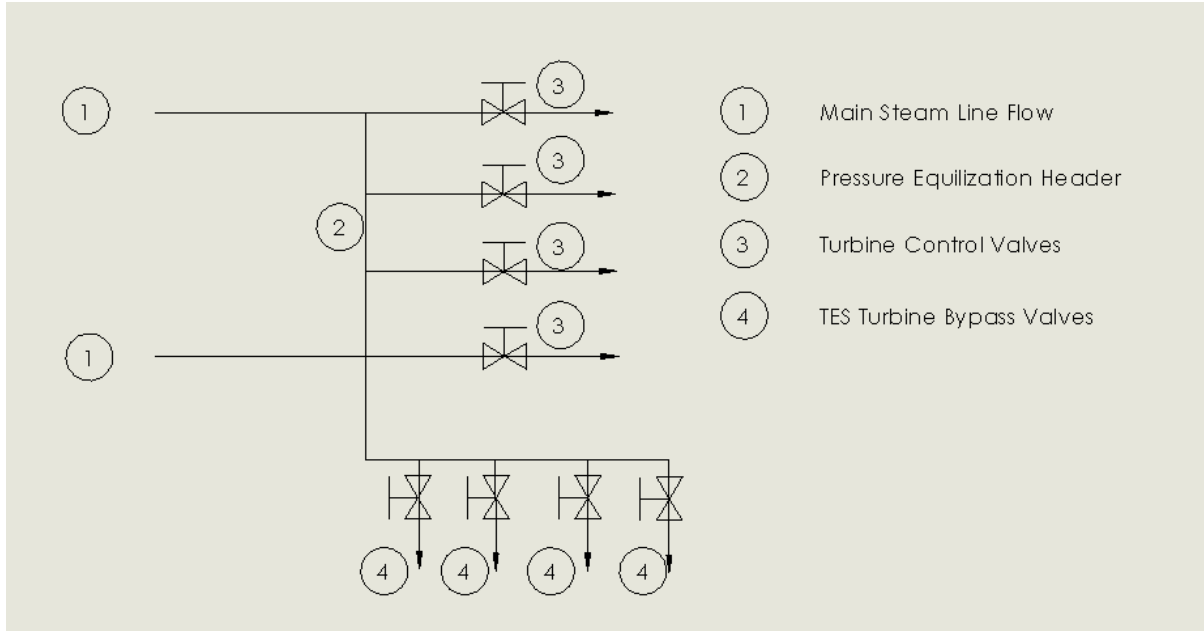
Figure 5.2: TES configuration with bypass taken prior to the Turbine Control Valves.

5.3 Control

The goal of the bypass flow controller is to provide bypass steam to the TES system at a rate sufficient to maintain the reactor at or near its nominal steady state value. This requires a more sophisticated control algorithm than that given previously as equation (2.61)

The new control algorithm is given below.

$$Signal_{TBV} = \frac{\dot{m}_{Bypass_{Demand}}}{\dot{m}_{Bypass_{Ref}}} - \frac{\dot{m}_{Bypass}}{\dot{m}_{Bypass_{Ref}}} \tag{5.1}$$

$$\dot{m}_{Bypass_{Demand}} = \dot{m}_{nominal} \frac{W_{Fullpower} - W_{load}}{W_{load}} + Shim_{TES} \tag{5.2}$$

$$Shim_{TES}^{t+\Delta t} = Shim_{TES}^{t} + \frac{K_{Shim}\dot{m}_{nominal}\left(Q_{Rx_{ref}} - Q_{Rx}\right)\Delta t}{Q_{Rx_{ref}}} \tag{5.3}$$

51

The new bypass valve controller generates an error signal based on the difference between measured bypass flow and a bypass flow demand signal. The bypass demand signal assumes the required bypass flow is proportional to the relative difference between the nominal full power turbine output and the instantaneous electric load plus a correction term (shim). The shim term modifies the demand signal such that reactor power is kept approximately constant.

Prior to connecting the Rx simulator to the TES system model, a series of stand-alone simulations were run to test the performance of the bypass controller and assess its impact on the reactor system behavior. Standard 24-hour summer and winter load profiles were run.

5.4 Standalone Reactor Response

5.4.1   Typical Summer Day

Throughout the full 24 hour run turbine load is dictated by the grid demand, shown in Figure 5.3. As illustrated in Figure 5.5 and Figure 5.7, as turbine load varies the bypass flow varies to match turbine load and keep the reactor power approximately constant. The TCV's modulate to maintain steam generator pressure at 825psi.
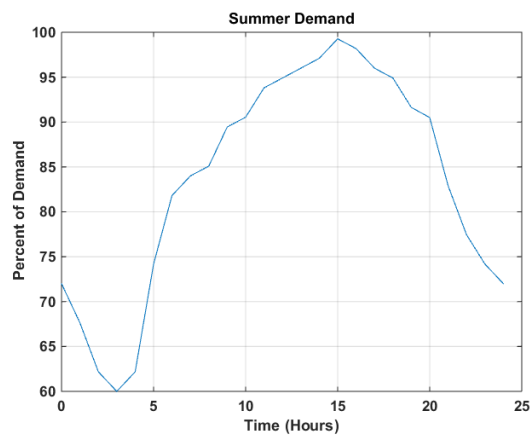
Figure 5.3: Typical Summer Demand Profile
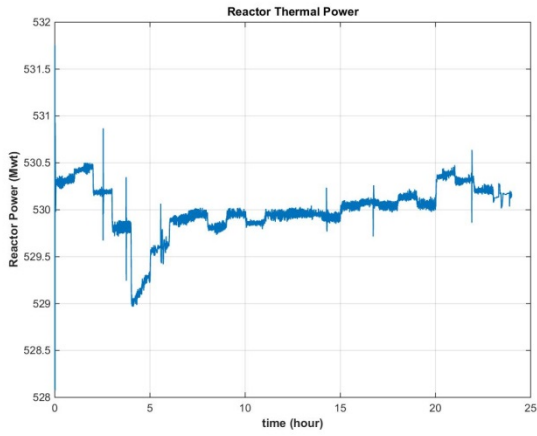
Figure 5.4: Reactor Power
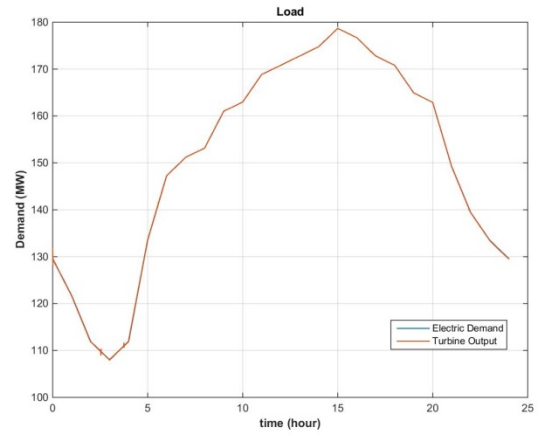
Figure 5.5: Turbine Load and Demand
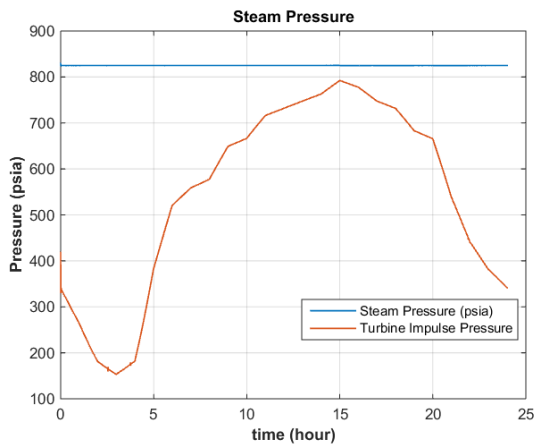
Figure 5.6: Steam Pressure
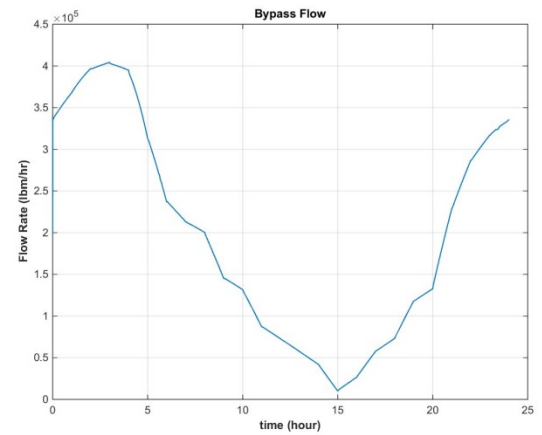
Figure 5.7: Bypass Flow

53

5.4.2   Typical Winter Day

Similar results are obtained when the reactor is subjected to the typical winter demand profile illustrated in Figure 5.8. As before the auxiliary bypass valves open to maintain reactor power while meeting electric demand.
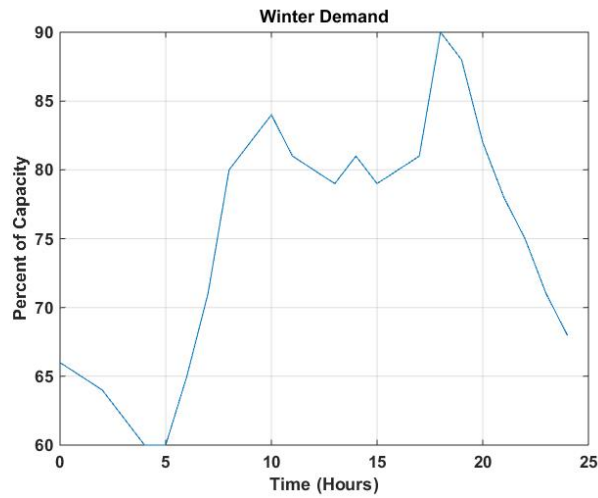
Figure 5.8: Typical Winter Demand Profile.
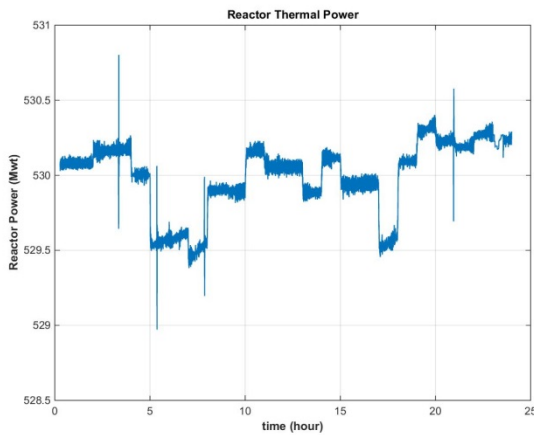
Figure 5.9: Reactor Power
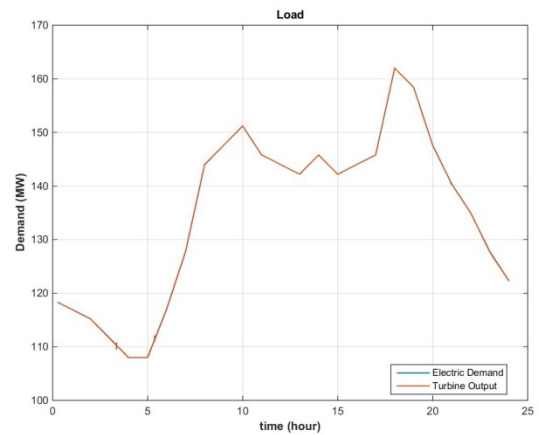
Figure 5.10: Turbine Output and Demand
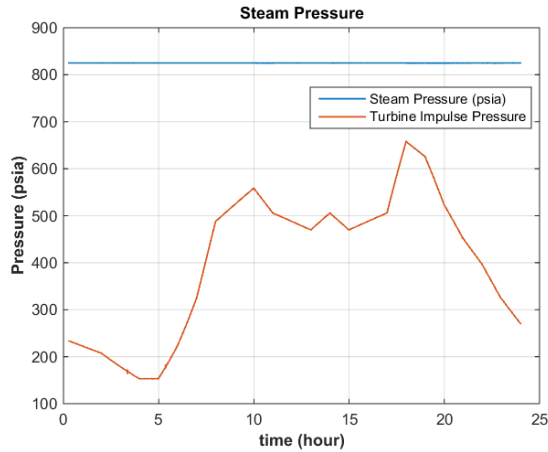
Figure 5.11: Steam Pressure
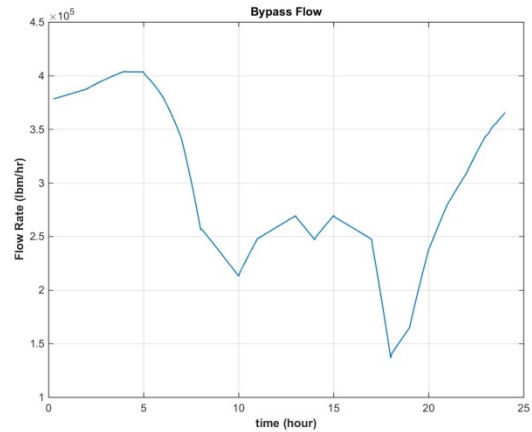
Figure 5.12: Bypass Flow

5.5 Load Follow Operation for a typical summer day

To show the benefits of bypassing steam to the TES system, a 24 hour simulation without bypass was run using the typical summer day load profile. Shown in Figure 5.14 and Figure 5.15, the system is able to maneuver such that turbine output matches load. Reactor thermal output also follows the load. Control rods are configured in four overlapping banks and move to match a specified T_{ave} program. As shown in Figure 5.17, banks A – C remain in their full out position and control bank D is sufficient to provide reactivity control for the maneuver.

Maneuvering the plant to follow load profiles of this nature can place additional stresses on the fuel and mechanical components that can limit plant lifetime.
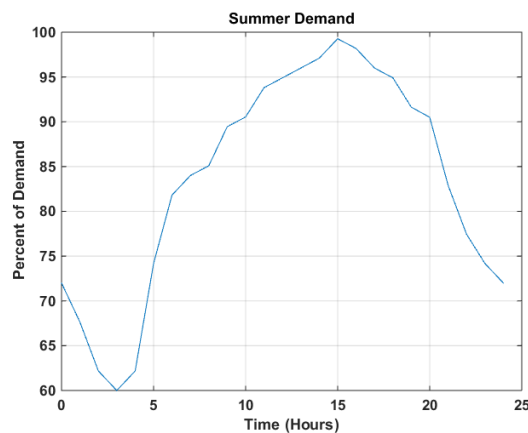
Figure 5.13: Typical Summer Demand Profile

55
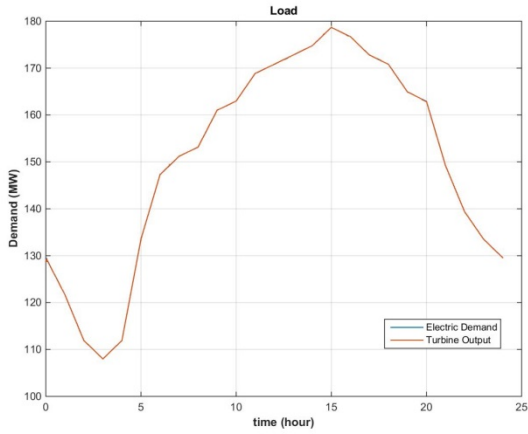
Figure 5.14: Turbine Output and Demand
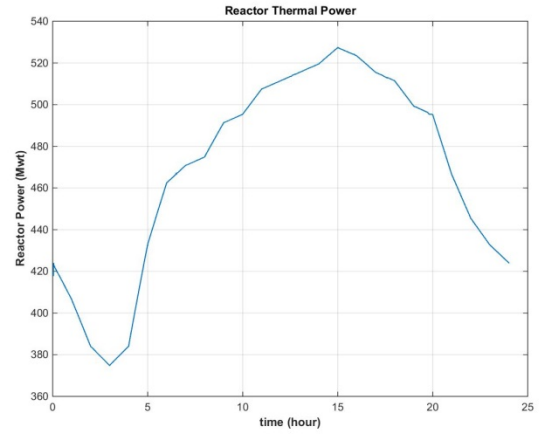
Figure 5.15: Reactor Power
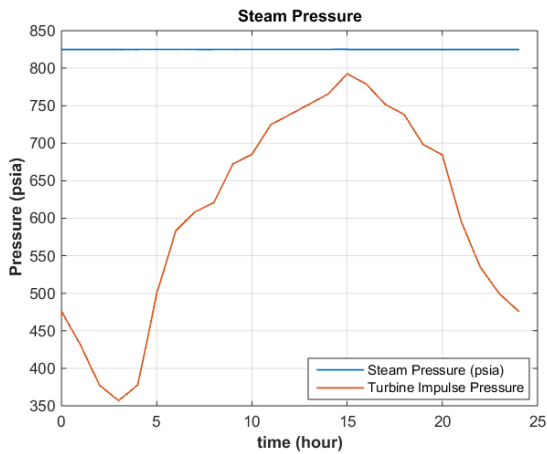
Figure 5.16: Steam Pressure
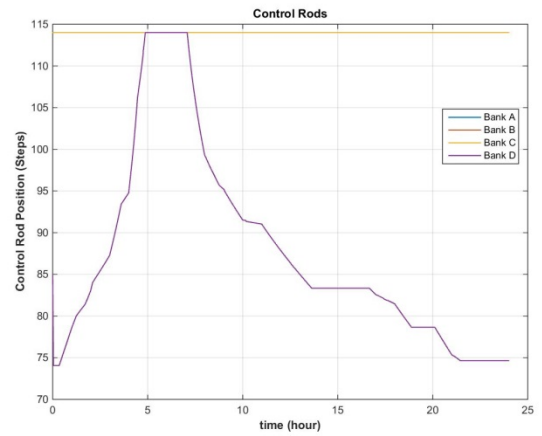
Figure 5.17: Control Rod Position

56

Chapter 6   Coupling the Reactor Simulator and TES System Model

It has been shown the stand alone TES and reactor systems models are able to accommodate the simulated load profiles and associated bypass flows. Of interest is how steam bypass coupled to a time varying TES system influences the reactor behavior. This requires accounting for the feedback between the two systems. The reactor simulator calculates the TES bypass valve positions and effective loss coefficients based on the assumed demand profile. It also passes the pressure equalization header pressure and steam enthalpy to the IHX. The TES routine uses these variables to compute the TES system behavior and returns bypass flow to the reactor model.

6.1 Additional Control Requirements

When connecting the TES system to the reactor simulator it was discovered that additional control of the TES flow control valve was required.

When the bypass control valves open and thermal energy is bypassed into the IHX, pressure begins to rise. During this time energy is conducted across the IHX tubes into the TES fluid. The TES Flow Control Valve, designed to maintain a reference temperature at the exit of the IHX, coupled with the pressure relief valve has an infinite number of solutions. Only one of which will match energy into the IHX with energy being transferred across it. A mismatch between energy into and across the IHX will lead to pressure changes in the IHX. To mitigate pressure changes and help match energy into and across the IHX a second signal was added to the TES Flow Control Valve controller. The second error signal is based on

$$
\begin{aligned}
Error_2 &= \frac{\dot{m}_{Bypass}}{\dot{m}_{Bypass_{Ref}}} - \frac{\dot{m}_{TES}}{\dot{m}_{TES_{Ref}}} \\
\dot{m}_{TES_{Ref}} &= \frac{\dot{m}_{Bypass_{Ref}} \left(h_{Steam} - h_f(P_{IHX}) \right)}{c_{p_{TES}} \left(T_{IHX_{Ref}} - T_{CT} \right)}
\end{aligned}
\tag{6.1}
$$

Where $\dot{m}_{Bypass_{Ref}}$ is the reference design bypass flow rate for the IHX. The TES Flow Control Valve now modulates according to a three-element controller.

$$
Signal_{FCV} = G_1 Error_1 + G_2 Error_2
\tag{6.2}
$$

Where,

$$Error_1 = \frac{T_{IHX_{Exit}} - T_{IHX_{Exitref}}}{T_{IHX_{Exitref}}}$$

This controller allows the system to match the Intermediate heat exchanger reference temperature and roughly match heat input into the TES fluid with the heat bypassed into the IHX.

6.2 Full Reactor TES simulations
6.2.1 Summer Day

To test the performance of the reactor when attached to the thermal energy storage system the typical summer day load profile, shown in Figure 6.1, was used. Time zero on the demand profile corresponds to midnight. The control strategy is for the reactor to run continuously at about 100% power, and during times of off peak demand bypass steam to the TES system.
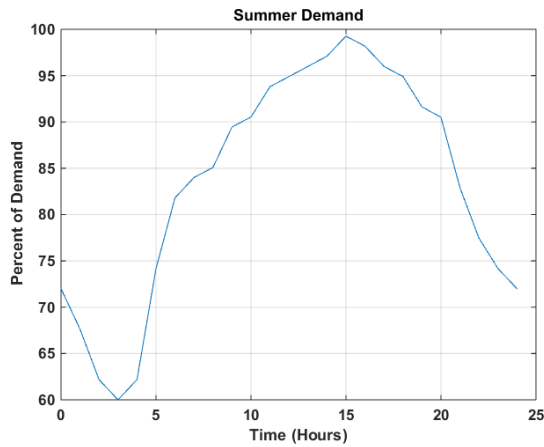
Figure 6.1: Summer Day Demand Profile
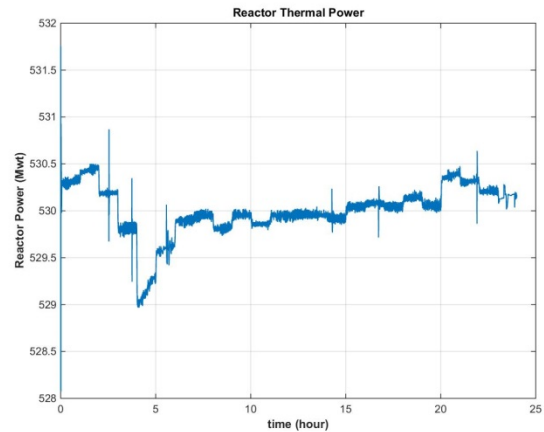
Figure 6.2: Reactor Power
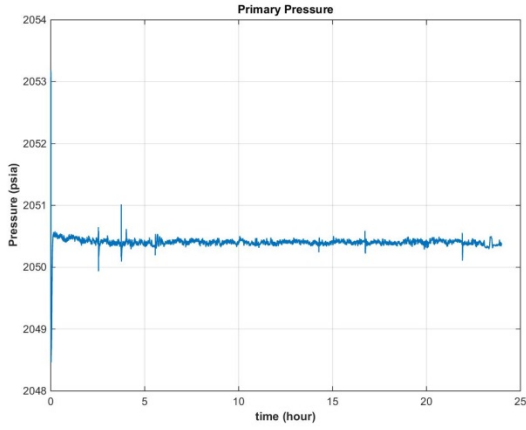
Figure 6.3: Primary Pressure
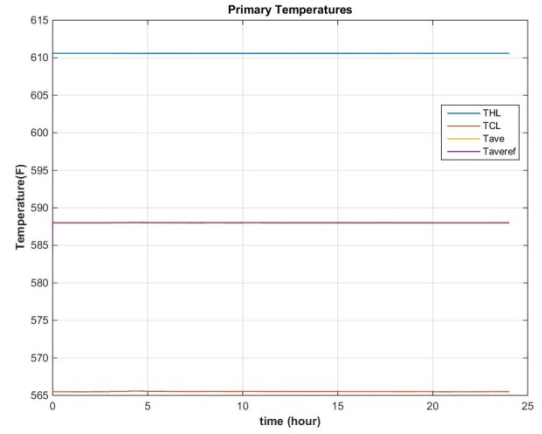
Figure 6.4: Primary Temperature
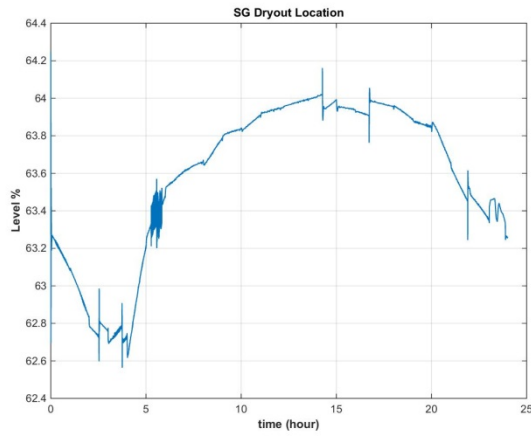
Figure 6.5: Boiling Length
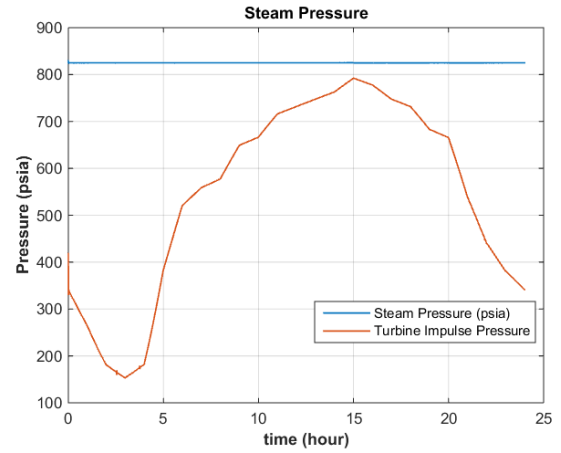
Figure 6.6: Steam Pressure

59
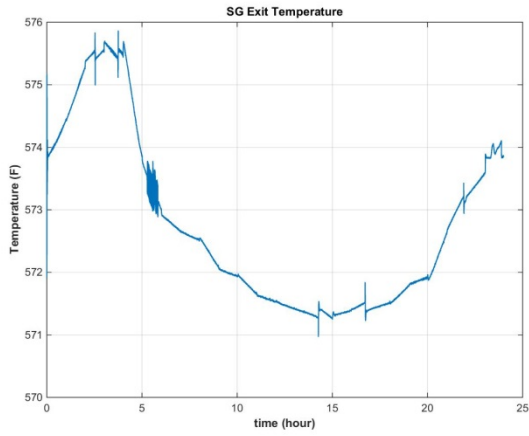
Figure 6.7: Steam Generator Exit Temperature
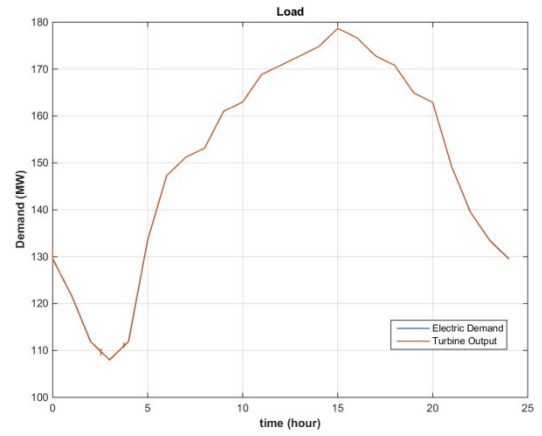
Figure 6.8: Turbine Load and Output
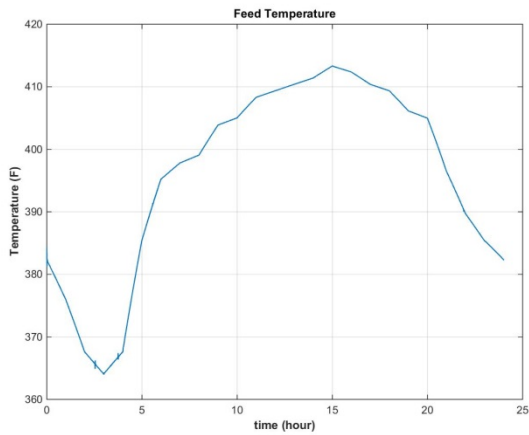
Figure 6.9: Feed Temperature
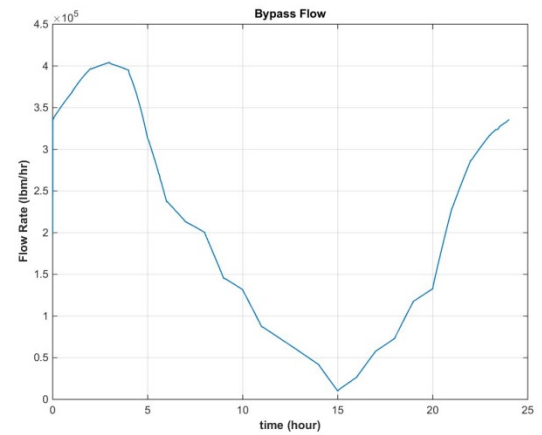
Figure 6.10: Bypass Demand

60
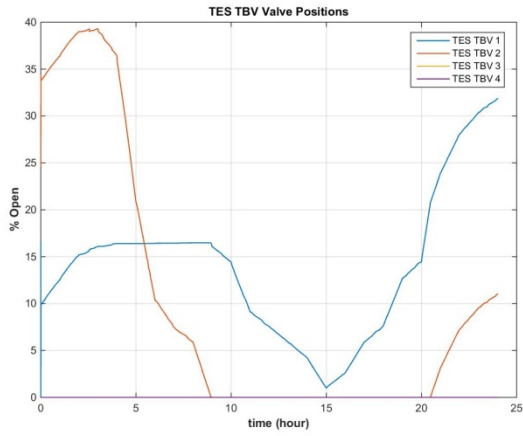
Figure 6.11: Auxiliary Bypass Valve Position
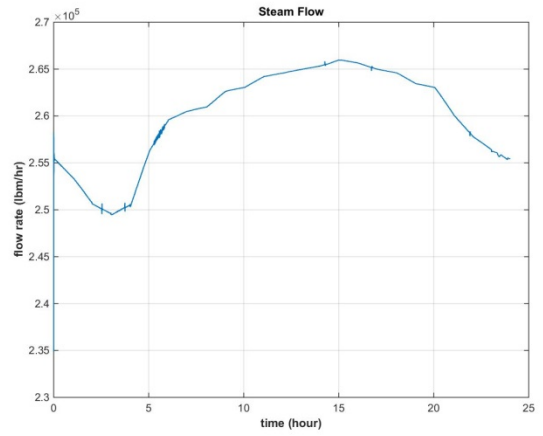
Figure 6.12: Steam Flow
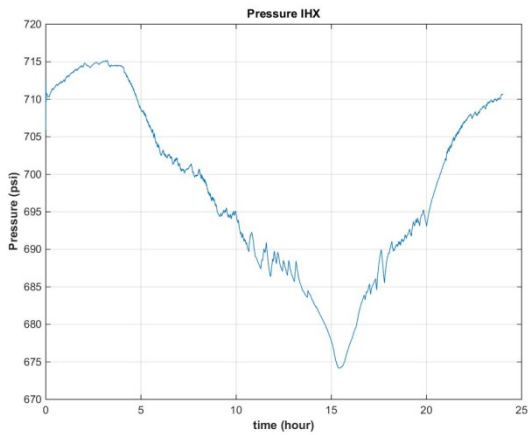
Figure 6.13: Intermediate Heat Exchanger Pressure
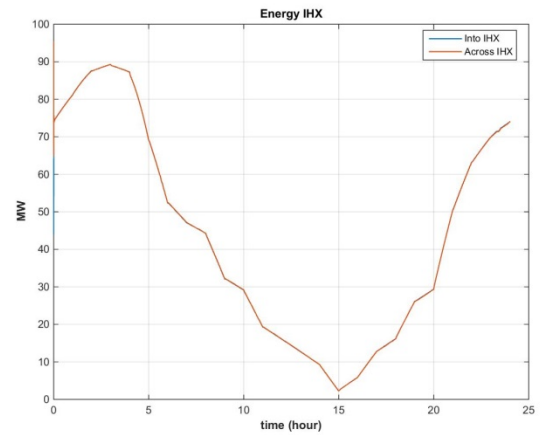
Figure 6.14: Energy into and across IHX

61
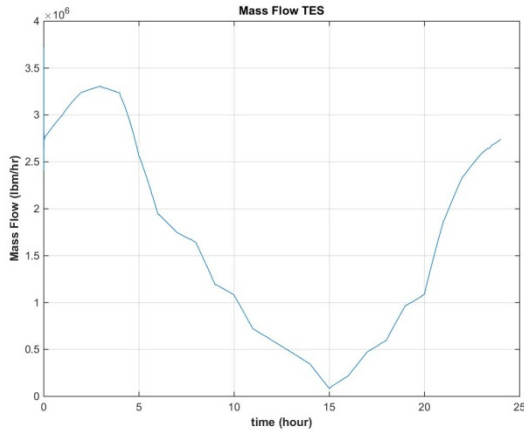
Figure 6.15: TES Fluid Flow Rate
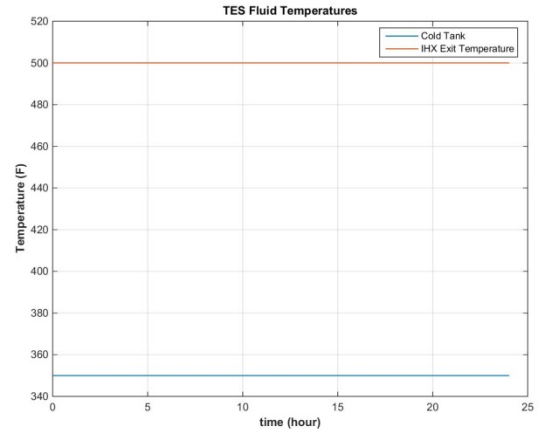
Figure 6.16: TES Fluid Temperatures
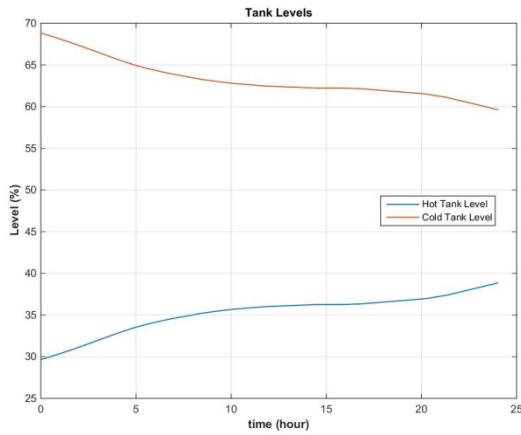
Figure 6.17: Hot and Cold Tank Levels
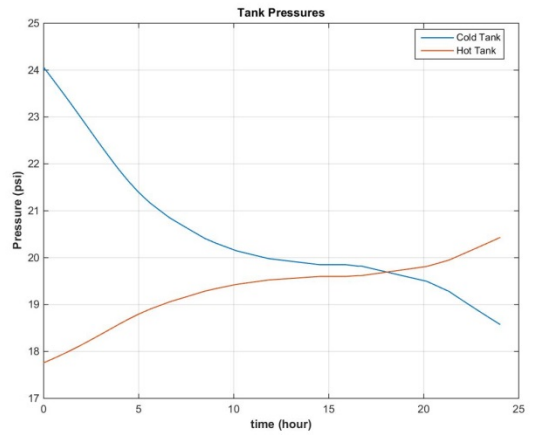
Figure 6.18: Hot and Cold Tank Pressures

As shown in Figure 6.8, turbine output matches the grid demand for the full 24 hour run. From Figure 6.10-Figure 6.12 the TES bypass valves modulate to keep the power of the reactor approximately constant and to match turbine load. As steam enters the IHX the TES flow control valve begins to move according to equation (6.2). Energy from the steam is transferred across the IHX tubes into the TES fluid pumped from the cold tank to the hot tank. As energy from the steam is transferred across the IHX, the steam condenses and is collected in the hot well below the IHX.

62

The flow control valve helps to match the energy transfer into the IHX with the energy transfer rate across the IHX. This controller helps keep the pressure swings in the IHX to a minimum and minimizes perturbations to the reactor system.

Initially, turbine demand decreases causing an increase in bypass demand, opening the bypass valves and allowing more steam to be bypassed into the TES system. To accommodate an increase in bypass the TCV's close to maintain steam generator pressure at 825psi as shown in Figure 6.6. This closing of the TCV's causes a decrease in the impulse pressure. As the impulse pressure decreases, so does turbine work. Reduction in the turbine impulse pressure also results in a decrease in the tap pressures used in feed heating, which causes a decrease in the feed temperature. The reduction in feed temperature decreases primary temperature which increases reactor power. This small increase in reactor power dials back the bypass demand based on the shim component of the bypass valve control algorithm.

This secondary shim control is why a 40% decrease in load does not equate to 40% thermal energy bypass into the TES system despite the reactor maintaining 100% power. This is due to a reduction in the cycle efficiency as the demand on the turbine is reduced. The reduction in cycle efficiency results from the reduction in feed temperature as well as the reduction in turbine impulse pressure as the TCV closes.

During the run the hot tank goes from 29% full to 38% full while the cold tank drops from 68% full down to 59%. This makes sense since the tanks are designed for upwards of 40% thermal bypass for 24 hours where during this simulation the maximum bypass only reached about 20%.

Of additional interest are the primary system temperatures and pressures. As illustrated in Figure 6.3 and Figure 6.4, primary temperature and pressure is effectively constant for the duration of the transient. In addition, as shown in Figure 6.5 – Figure 6.7 only small perturbations are seen in steam generator temperature, pressure and boiling length. Not shown are the control rod positions, which remained constant throughout the simulation. The small variations in these parameters lead to significant stress reductions in the fuel and other components which ultimately extend reactor lifetime.

6.2.2 Summer Day –Including Solar

An advantage of TES systems is the ability to accommodate the presence of intermittent energy sources on the grid, particularly solar energy penetration that can be varying depending on time of day or cloud cover. The amount of solar penetration is region and area specific but for the case considered below we will assume a combined profile matching that considered earlier but scaled such that the maximum turbine load is 60%. The load profile is given in Figure 6.19. Time zero corresponds to midnight. Over the course of the simulation, turbine load is met while thermal power stays approximately constant as illustrated in Figure 6.20 and Figure 6.21. The response of other system parameters is similar to that shown previously for the typical summer day. The TES system has the capacity to charge for the full 24 hour run as tank levels go from 26% to 45% as shown in Figure 6.23.
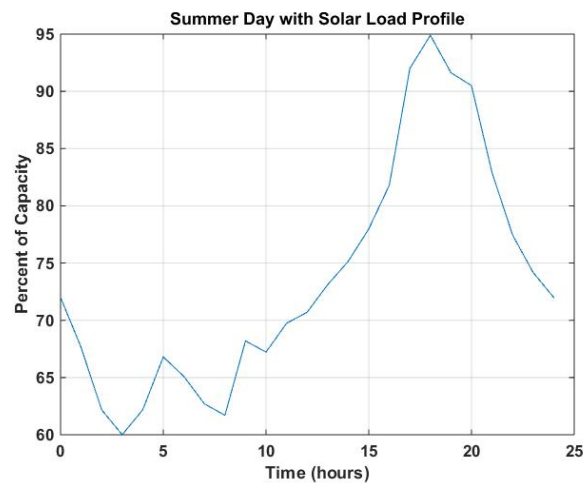
Figure 6.19: Summer Day Demand Profile with Solar Generation
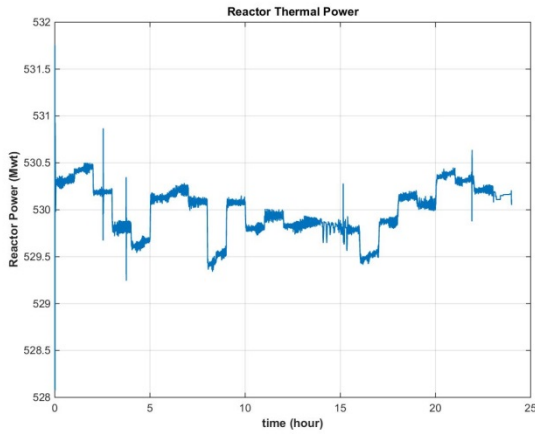
Figure 6.20: Reactor Power
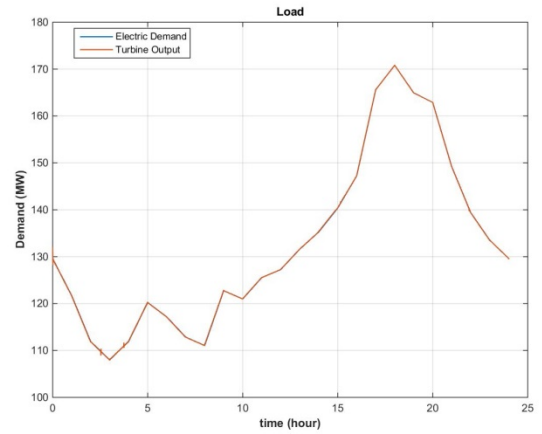
Figure 6.21: Turbine Load and Output
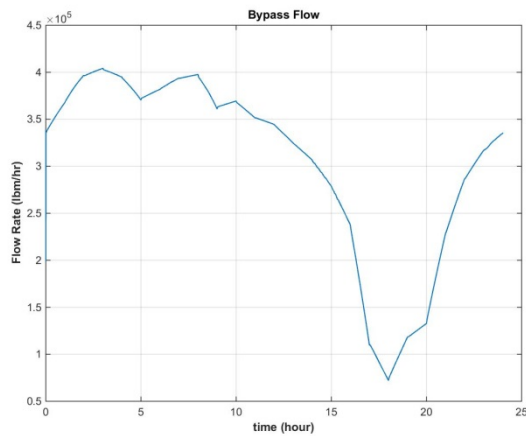
Figure 6.22: Auxiliary Bypass Flow
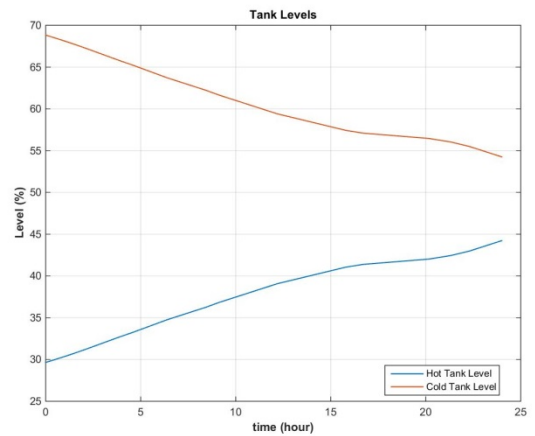
Figure 6.23: Hot and Cold Tank Levels

6.2.3   Winter Day

The coupled reactor – TES system was run for the typical winter day demand profile given in Figure 6.24. The system was again able to meet electric demand while maintaining constant reactor power as shown in Figure 6.25 and Figure 6.26.

65
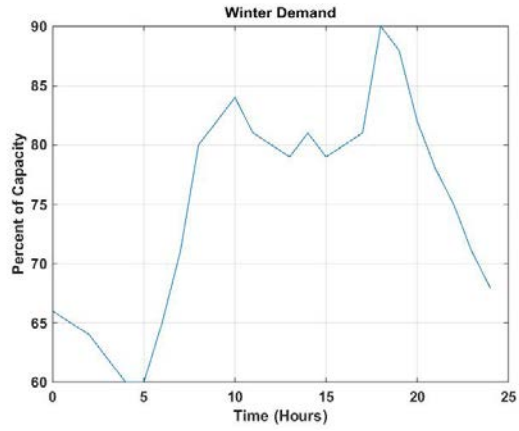
Figure 6.24: Winter Day Demand Profile
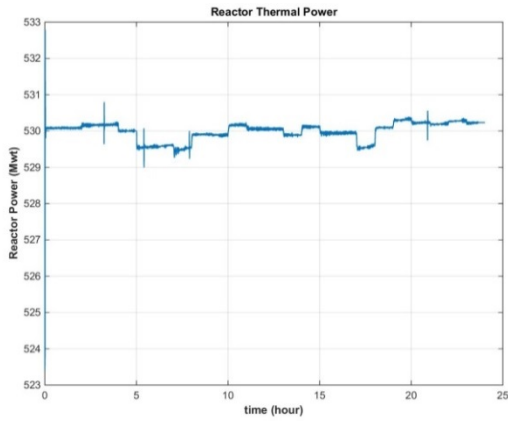
Figure 6.25: Reactor Power
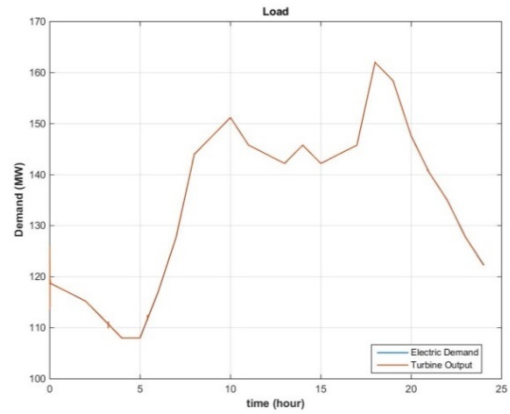
Figure 6.26: Turbine Load and Output
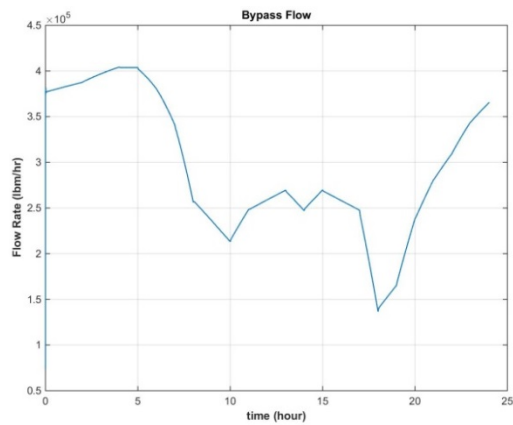
Figure 6.27: Auxiliary Bypass Flow
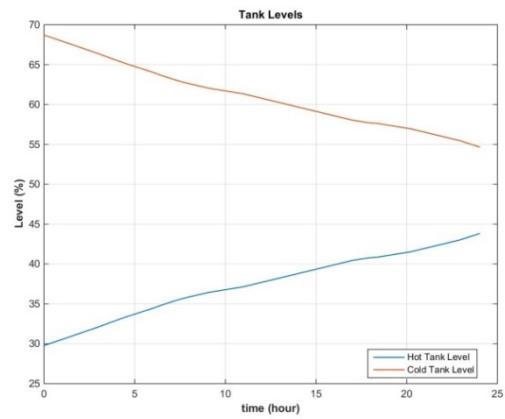
Figure 6.28: Hot and Cold Tank Levels

66

Chapter 7   Conclusions and Future Work

7.1 Conclusions

The results presented demonstrate the feasibility of using TES systems coupled to Small Modular Reactors to minimize power swings during periods of variable electric load. If SMRs are to be deployed in conjunction with intermittent power sources such as wind and solar, these load variations can be significant. Through the use of a sensible heat storage system, it has been shown thermal energy can be stored during periods of low demand, to be recovered at a later time for either electric generation or process heat applications. With the implementation of a TES system, decreases in capacity factor and increased stresses on plant components associated with load follow operation can be minimized, improving economic return over the lifespan of the reactor.

7.2 Future work

Future development will focus on the development and implementation of the models and control strategies necessary to implement the discharge mode. Once the discharge mode is running, studies will be done on how to best optimize system parameters for size and desired ancillary applications. Development will also focus on the design of a high fidelity time-dependent balance of plant. The inclusion of a time-dependent balance of plant system will allow for a more in-depth look at the overall system efficiency associated with thermal energy storage systems.

Chapter 8   Bibliography

[1]   "Renewable Energy and Electricity," 20 June 2016. [Online]. Available: http://www.world-nuclear.org/information-library/energy-and-the-environment/renewable-energy-and-electricity.aspx. [Accessed 08 July 2016].

[2]   "Western Wind and Solar Integration Study Dataset," [Online]. Available: http://www.nrel.gov/electricity/transmission/wind_integration_dataset.html. [Accessed 19 March 2015].

[3]   J. Pollak, "California's New Desalination Plant Wins International Award," 24 April 2016. [Online]. Available: http://www.breitbart.com/california/2016/04/24/san-diego-desalination-plant-wins-international-award/. [Accessed 25 June 2016].

[4]   P. Rogers, "Nation's largest ocean desalination plant goes up near San Diego; Future of the California coast?," 29 May 2014. [Online]. Available: http://www.mercurynews.com/science/ci_25859513/nations-largest-ocean-desalination-plant-goes-up-near. [Accessed 25 June 2016].

[5]   International Atomic Energy Agency, "Introduction of Nuclear Desalination : A Guidebook," Vienna, 2000.

[6]   "How Desalination by Multi-stage Flash Distillation Works," brighthubengineering.com, 23 December 2009. [Online]. Available: http://www.brighthubengineering.com/power-plants/29623-how-desalination-by-multi-stage-flash-distillation-works/. [Accessed 25 June 2016].

[7]   "How Does Reverse Osmosis Plant Work?," 23 December 2009. [Online]. Available: http://www.brighthubengineering.com/power-plants/29624-how-does-reverse-osmosis-plant-work/. [Accessed 25 June 2016].

[8]   M. A. Darwish and N. M. Al-Najem, "Energy consumption by multi-stage flash and reverse osmosis desalters," *Applied Thermal Engineering,* pp. 399-416, 2000.

[9]   "Hydrogen Production: Natural Gas Reforming," Office of Energy Efficiency and Renewable Energy, [Online]. Available: http://energy.gov/eere/fuelcells/hydrogen-production-natural-gas-reforming. [Accessed 27 June 2016].

[10] D. Ingersoll, Z. Houghton, R. Bromm, C. Desportes, M. McKellar and R. Boardman, "EXTENDING NUCLEAR ENERGY TO NON-ELECTRICAL APPLICATIONS," in *The 19th Pacific Basin Nuclear Conference (PBNC 2014)*, Vancouver, 2014.

[11] Office of Energy Efficiency & Renewable Technology, "Hydrogen Production: Electrolysis," [Online]. Available: http://energy.gov/eere/fuelcells/hydrogen-production-electrolysis. [Accessed 11 July 2016].

[12] California Energy Commision, "Renewables Portfolio Standard (RPS)," 22 April 2016. [Online]. Available: http://www.energy.ca.gov/portfolio/. [Accessed 27 June 2016].

[13] National Renewable Energy Laboratory, "Ivanpah Solar Electric Generating System," 20 November 2014. [Online]. Available: http://www.nrel.gov/csp/solarpaces/project_detail.cfm/projectID=62. [Accessed 27 June 2016].

[14] K. Fagan, "Desalination plants a pricey option if drought persists," 15 February 2014. [Online]. Available: http://www.sfgate.com/news/article/Desalination-plants-a-pricey-option-if-drought-5239096.php. [Accessed 27 June 2016].

[15] H. Cooley and M. Heberger, "Key Issues for Seawater Desalination in California: Energy and Greenhouse Gas Emissions," Pacific Institute, 2013.

[16] DriveClean, "Hydrogen Fuel Cell," California Air Resources Board, [Online]. Available: http://www.driveclean.ca.gov/Search_and_Explore/Technologies_and_Fuel_Types/Hydrogen_Fuel_Cell.php. [Accessed 27 June 2016].

[17] Electric Light and Power, "SDG&E energizes 117 mile, 500,000 volt transmission line," 18 June 2012. [Online]. Available: http://www.elp.com/articles/2012/06/sdg-e-energizes-117-mile-500-000-volt-transmission-line.html. [Accessed 27 June 2016].

[18] C. McDaniel, "Solar Energy in Yuma a boon for electric grid," 18 January 2015. [Online]. Available: http://www.yumasun.com/business/solar-energy-in-yuma-a-boon-for-electric-grid/article_46f6652c-9d44-11e4-a3be-efafa287ff9e.html. [Accessed 18 July 2016].

[19] F. Weaver, "The unprecedented water crisis of the American Southwest," theweek.com, 01 February 2014. [Online]. Available: http://theweek.com/articles/451876/unprecedented-water-crisis-american-southwest. [Accessed 25 June 2016].

[20] S. Bragg-Sitton, R. Boardman, J. Collins, M. Ruth, O. Zinaman and C. Forsberg, *Integrated Nuclear-Renewable Energy Systems: Foundational Workshop Report,* Idaho National Laboratory, 2014.

[21] "Iowa: State Profile and Energy Estimates," U.S. Energy Information Administration, 17 March 2016. [Online]. Available: http://www.eia.gov/state/analysis.cfm?sid=IA. [Accessed 25 June 2016].

[22] "Coal Plant Retirements," [Online]. Available: http://www.sourcewatch.org/index.php/Coal_plant_retirements. [Accessed 08 July 2016].

[23] K. Powell and T. Edgar, "Modeling and control of a solar thermal power plant with thermal energy storage".," *Chemical Engineering Science,* vol. 71, pp. 138-145, 2012.

[24] S. Kuravi, J. Trahan, D. Y. Goswami, M. Rahman and E. Stefanakos, "Thermal energy storage technologies and systems for concentrating solar power," *Progress in Energy and Combustion Science,* vol. 39, pp. 285-319, 2013.

[25] Solutia: Applied Chemistry, Creative Solutions, *Therminol 66: High Performance Highly Stable Heat Transfer Fluid.*

[26] Solutia: Applied Chemistry, Creative Solutions, *Therminol 68: Highly Stable Low Viscosity Heat Transfer Fluid.*

[27] Solutia, *Therminol 75: Synthetic, Aromatic, High-temperature Heat Transfer Fluid.*

[28] J. Doster, "Brent's Algorithm," [Online]. Available: http://www4.ncsu.edu/~doster/NE400/Computing/Brent.pdf. [Accessed 08 July 2016].

[29] International Atomic Energy Agency, "Advances in Small Modular Reactor Technology Developments," IAEA, Vienna, 2014.

[30] J. Doster, *SMR Simulator,* Raleigh, 2016.

[31] D. Ingersoll, C. Colbert, Z. Houghton, R. Snuggerud, J. Gaston and M. Empey, "Can Nuclear Power and Renewables Be Friends?," *Proceedings of ICAPP,* pp. 3129-3137, 2015.

[32] "IVANPAH," BrightSource Limitless, [Online]. Available: http://www.brightsourceenergy.com/ivanpah-solar-project#.V28rz_krJD-. [Accessed 25 June 2016].

[33] C. McDaniel, "Solar Energy in Yuma a boon for electric grid," 18 January 2015. [Online]. Available: http://www.yumasun.com/business/solar-energy-in-yuma-a-boon-for-electric-grid/article_46f6652c-9d44-11e4-a3be-efafa287ff9e.html. [Accessed 18 July 2016].

APPENDIX

9.1 Aggressive Load Profile 100MWt reactor

The system was designed to handle 85% steam dump from a 100Mwt system for upwards of a day. To accommodate this demand, large storage tanks were installed. To ensure that neither tank over pressurizes the combined amount of TES fluid in both the hot and cold tanks is slightly less than what either one could hold on their own. System design parameters are given in Table 9.1.

Table 9.1: System Design Parameters

Parameter	Value
TES Fluid	Therminol®-66
Hot tank Volume	$1,000,000$ ft^3
Cold Tank Volume	$1,000,000$ ft^3
IHX reference Exit Temperature	500F
Number of TBV's	4
TES maximum steam accommodation	85% Nominal conditions of NuScale size reactor
Pressure Relief Valve Upper Setpoint	780 psi
Pressure Relief valve Lower Setpoint	730 psi
Condenser Pressure	1 psi
Turbine Header Pressure	825 psi
Shell Side (outer loop) IHX Volume	566.58 ft^3
Number of tubes	12190
Length of tubes	40 ft
Tube Inner Diameter	0.044 ft
Tube Outer Diameter	0.058 ft
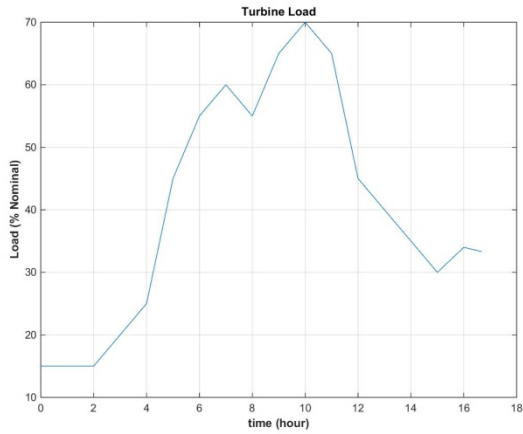
Figure 9.1: Work of the main system turbine.
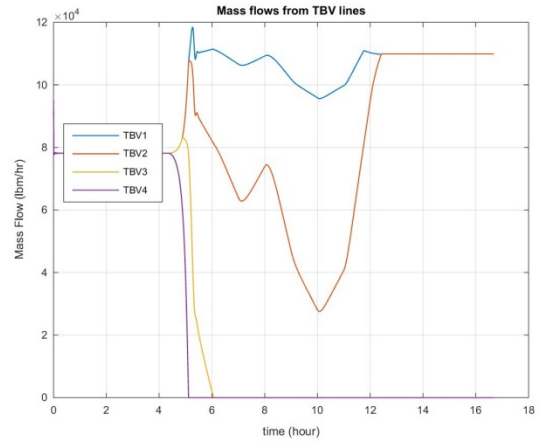
Figure 9.2: Mass flow rates through auxiliary bypass valves into the IHX.
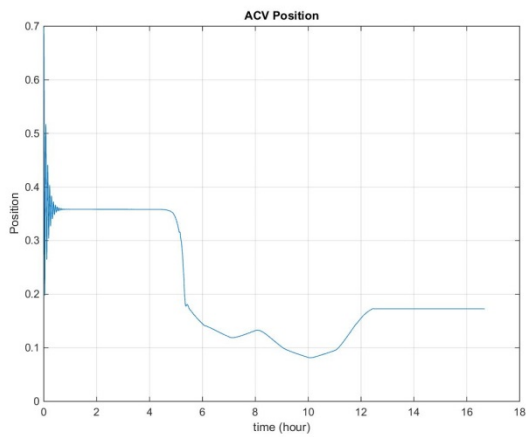
Figure 9.3: Position of the Auxiliary Control Valve.
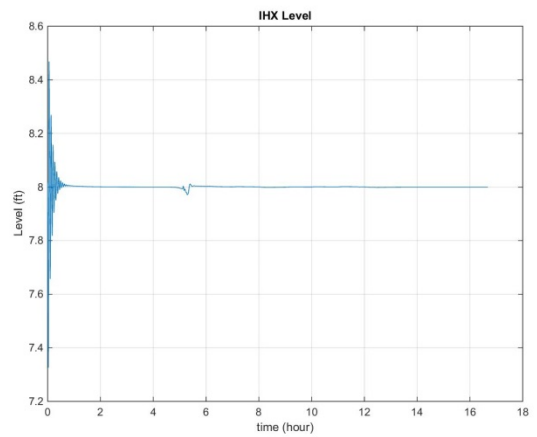
Figure 9.4: Level in the Intermediate Heat Exchanger.

73
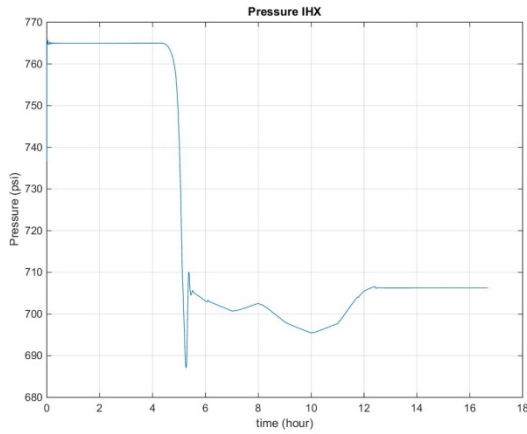
Figure 9.5: Pressure in the Intermediate Heat Exchanger.
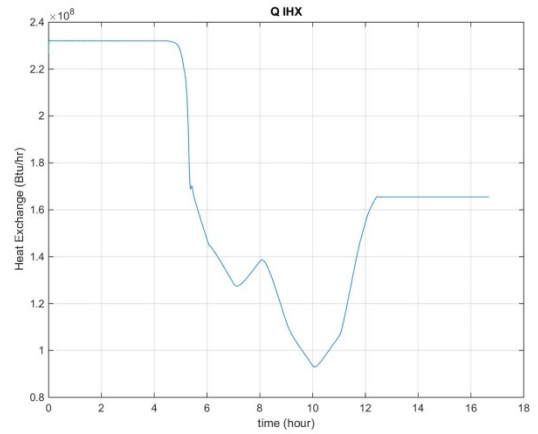
Figure 9.6: Heat transfer rate across the inner and outer loop of the IHX.
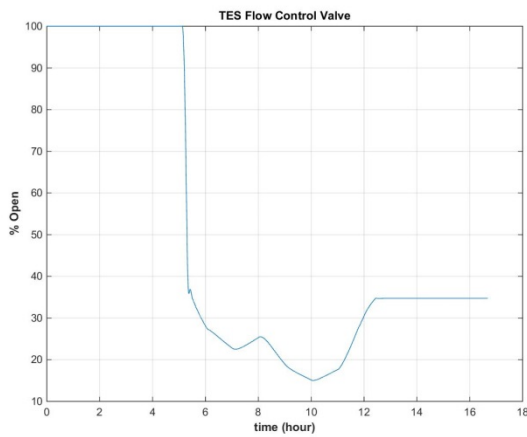
Figure 9.7: Flow Control Valve that regulates flow from the cold tank to the hot tank.
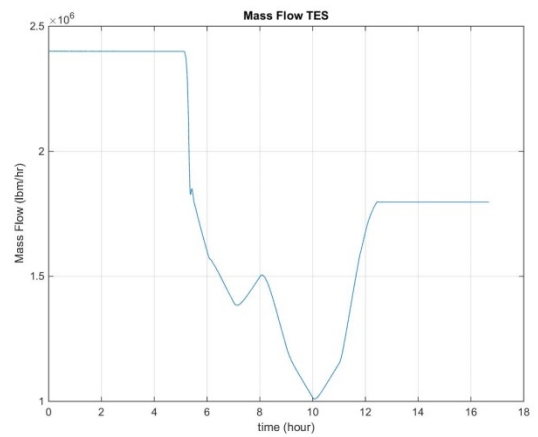
Figure 9.8: Mass Flow of the Therminol-66 from the cold tank to the hot tank.

74
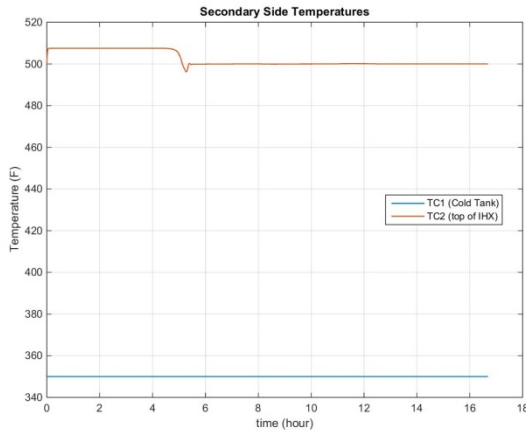
Figure 9.9 Temperature at exit of IHX for the inner loop entering the hot tank
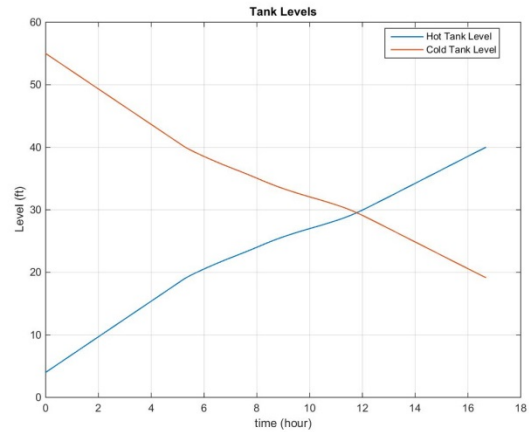
Figure 9.10: Tank Levels for the hot and cold tanks.

The system has a nominal output of ~100 MWth. As seen in Figure 4.1 the system initially starts with about 15% load on the turbine. This small turbine load means that the TES system is in full charging mode as 85% of the net reactor capacity is being pushed through the TES system. At this demand level all four of the auxiliary turbine bypass valves are open to allow steam into the IHX.

With such a large amount of steam dump into the IHX the FCV opens quickly and the mass flow rate of the TES inner loop is at full capacity as shown in Figure 9.7. Since the FCV is responsible for maintaining the TES fluid exit temperature from the IHX at a preset point, with the valve in its full open position the exit temperature will increase above the set point value. From a practical standpoint this is not a major concern as long as the TES fluid temperature remains below its maximum design limit.

As the turbine load increases the bypass valves begin to close and subsequently the heat transfer rate to the inner loop decreases. When the heat transfer rate decreases so does the TES fluid exit temperature causing the FCV to close to keep the temperature above the set point value. The closing of the FCV reduces the charging rate between the hot and cold tanks as seen in Figure 9.8. At the end of the run the cold tank has gone from 91% full down to about 33% full while the hot tank has gone from 8% full up to about 66% full.

75

9.2 Additional Graphs for Stand-alone system

9.2.1 mPower

9.2.1.1. Typical Summer Day
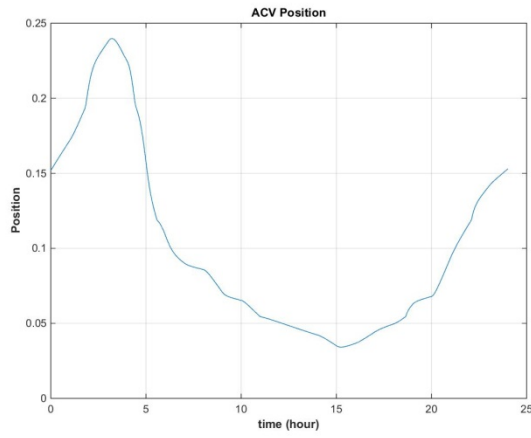
Figure 9.11: Auxiliary Control Valve Position
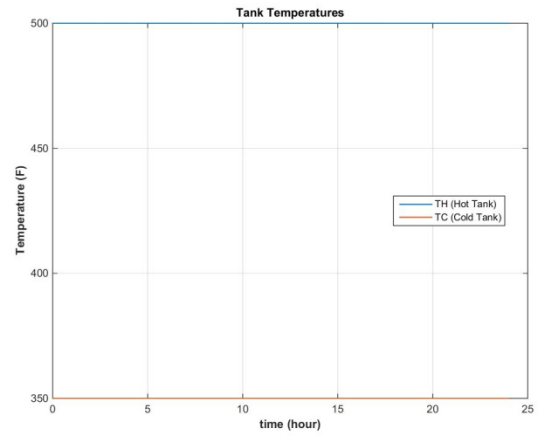
Figure 9.12: Tank Temperatures
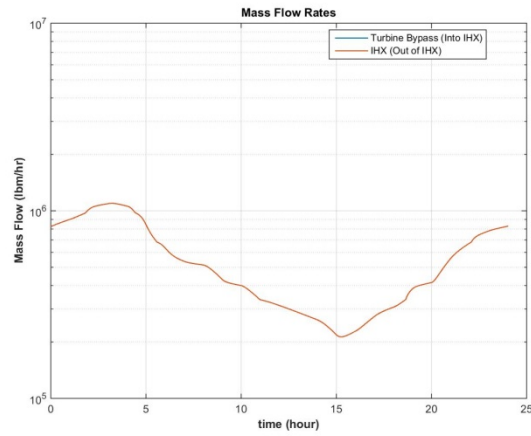
Figure 9.13: Mass flows in and out of shell side of IHX
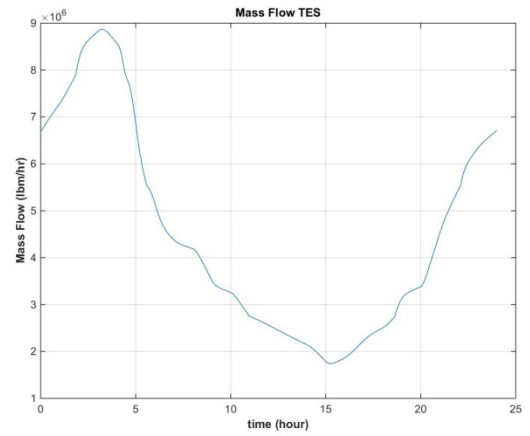
Figure 9.14: TES fluid mass flow

76

9.2.1.2. Typical Winter Day
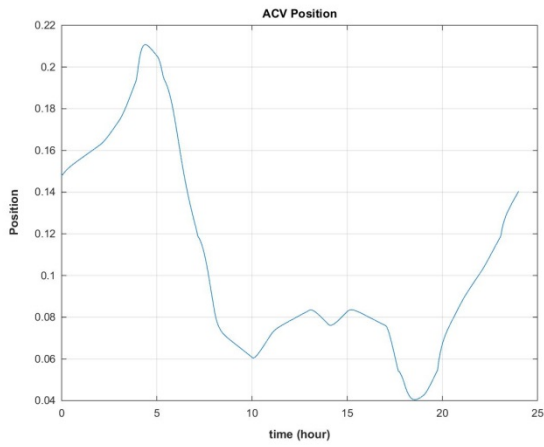
Figure 9.15: Auxiliary Control Valve Position
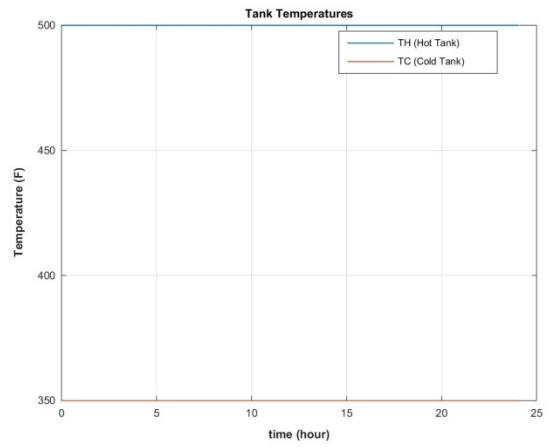
Figure 9.16: Tank Temperatures
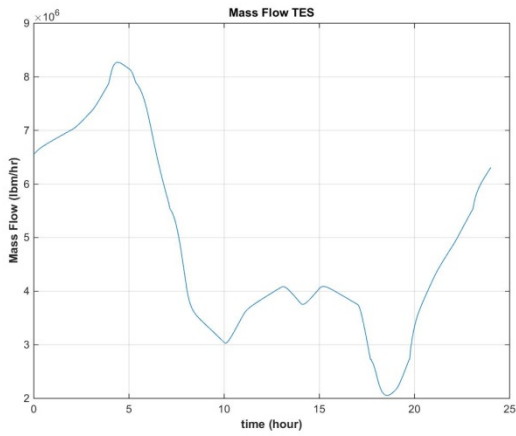
Figure 9.17: TES fluid mass flow
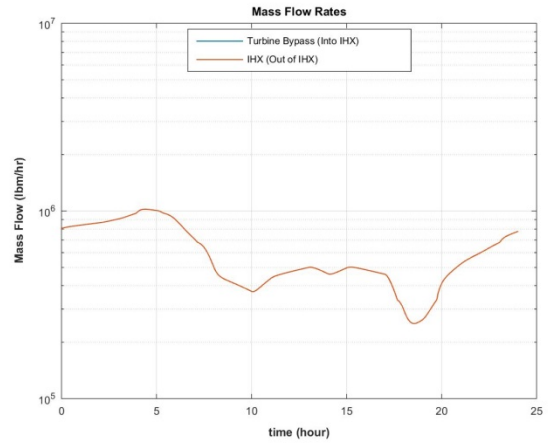
Figure 9.18: Mass flow in and out of shell side of IHX.
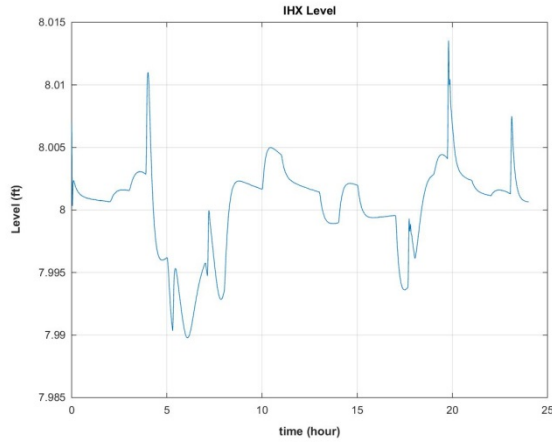
Figure 9.19: Intermediate Heat Exchanger Level
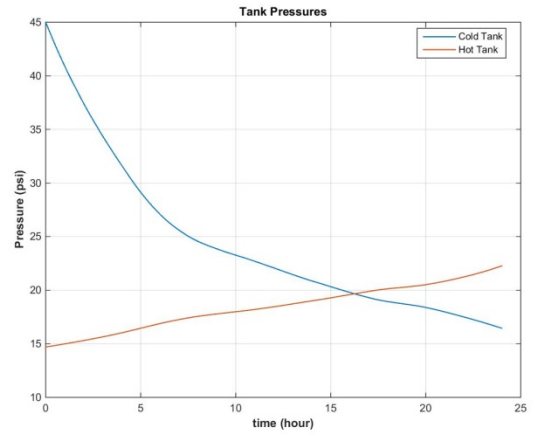
Figure 9.20: Tank Pressures

9.2.1.3. Summer Day –Including Solar
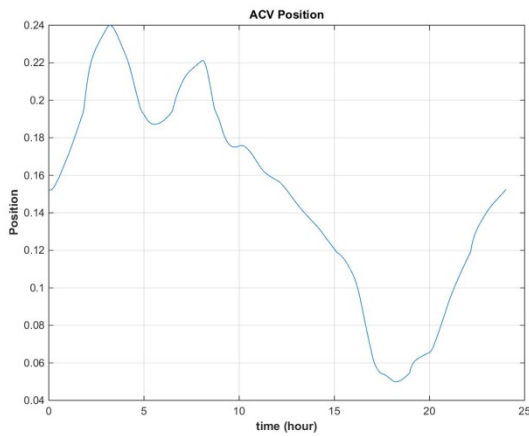
Figure 9.21: Auxiliary Control Valve Position
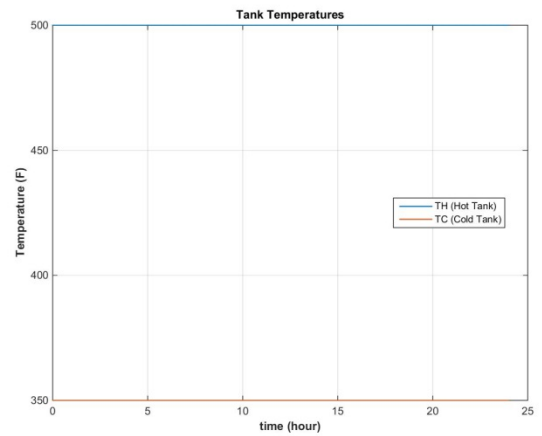
Figure 9.22: Tank Temperatures

78
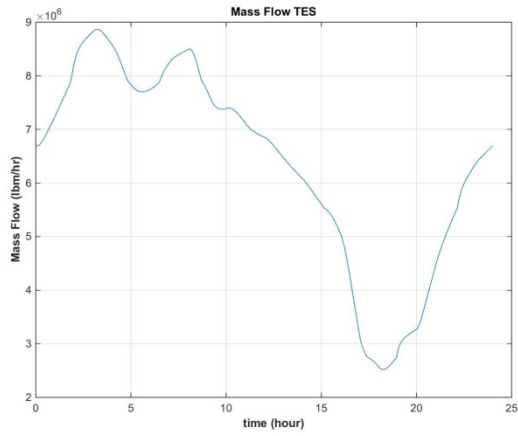
Figure 9.23: TES fluid mass flow rate
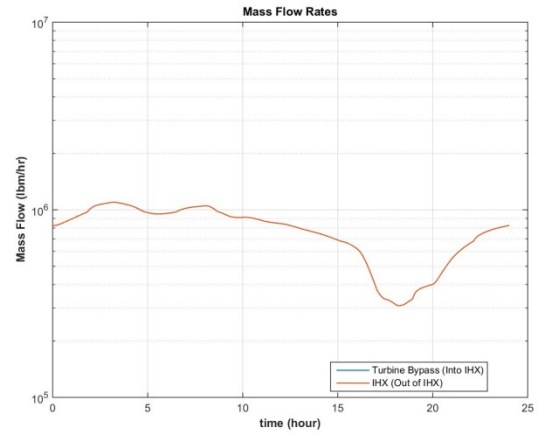
Figure 9.24: Mass flows in and out of shell side of IHX.
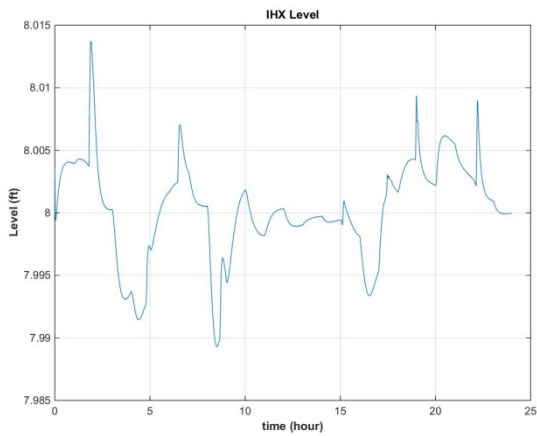
Figure 9.25: Intermediate Heat Exchanger Level
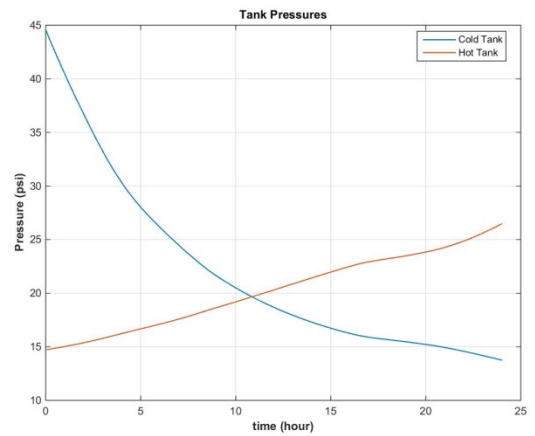
Figure 9.26: Tank Pressures

9.2.1.4. Summer Day –Including Wind
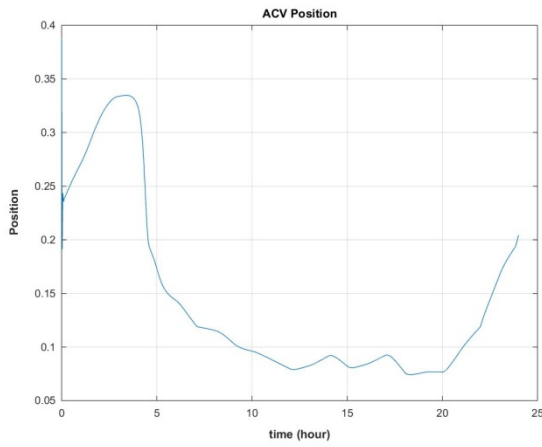
Figure 9.27: Auxiliary Control Valve Position
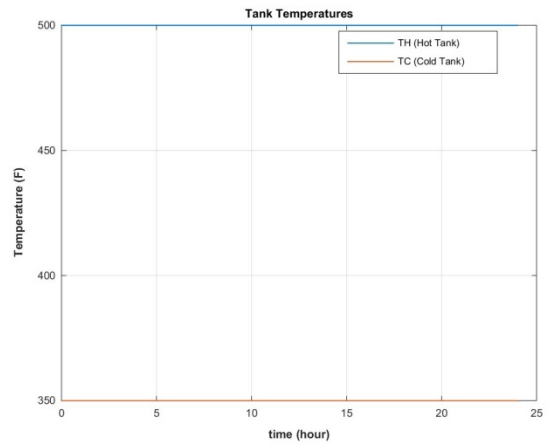
Figure 9.28: Tank Temperatures
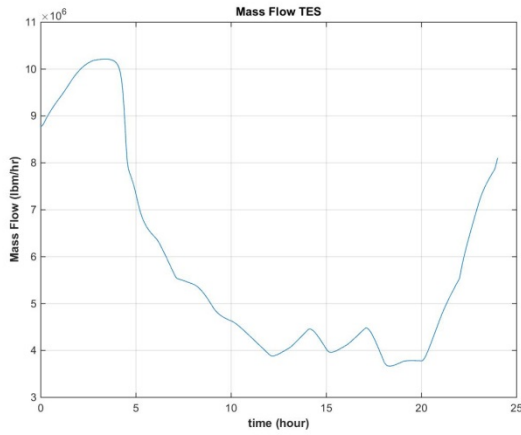
Figure 9.29: TES fluid flow rate
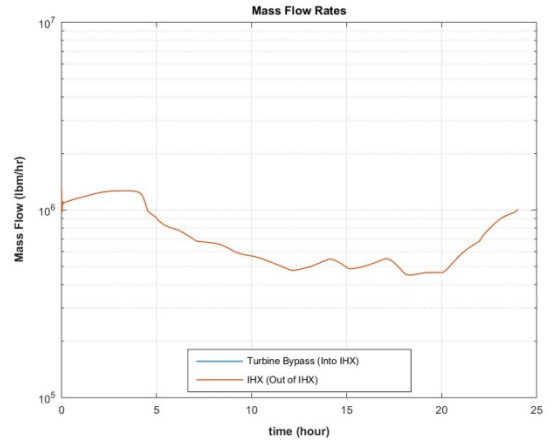
Figure 9.30: Mass flow in and out of shell side of IHX.

80
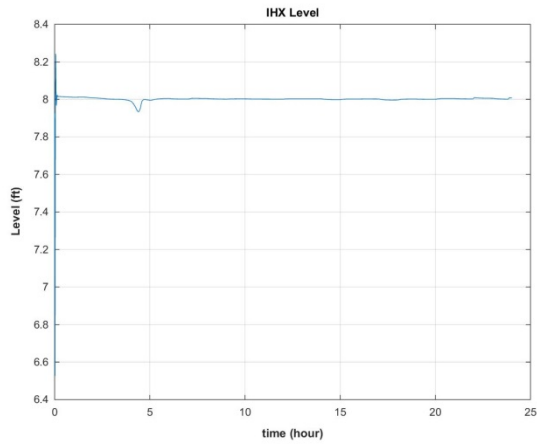
Figure 9.31: Intermediate Heat Exchanger Level
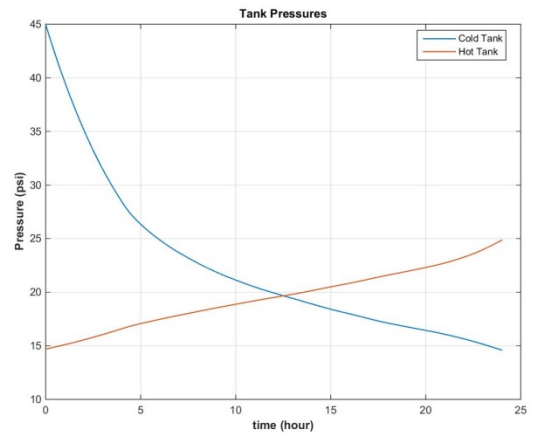
Figure 9.32: Tank Pressures

9.2.1.5. Summer Day - Including Wind and Solar
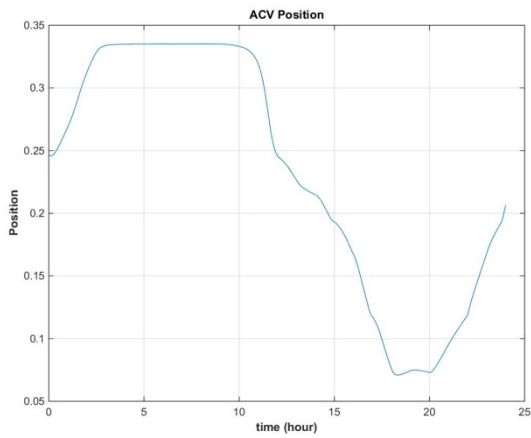
Figure 9.33: Auxiliary Control Valve Position
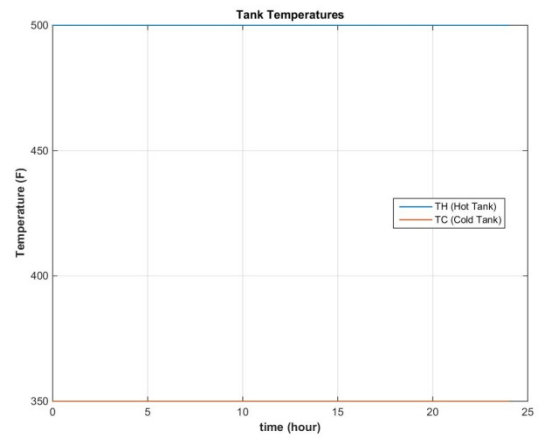
Figure 9.34: Tank Temperatures

81
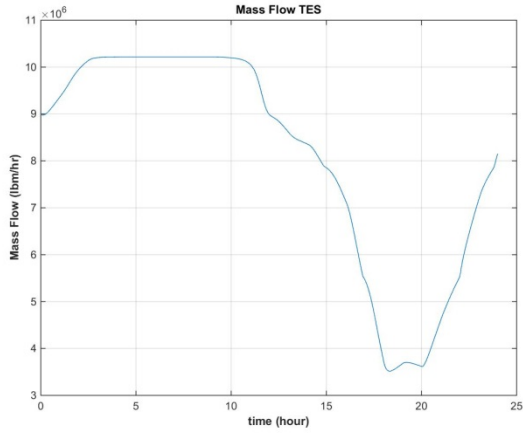
Figure 9.35: TES fluid flow rate
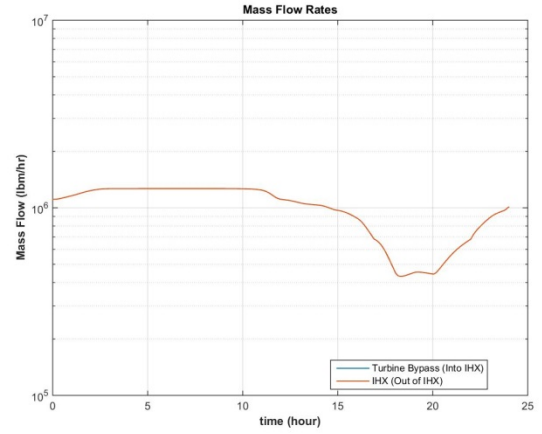
Figure 9.36: Mass flows in and out of shell side of IHX.
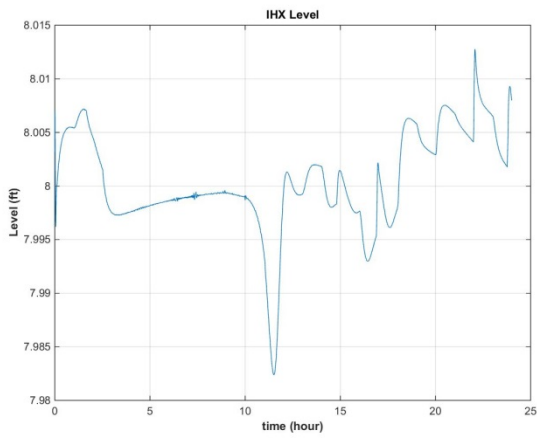
Figure 9.37: Intermediate Heat Exchanger Level
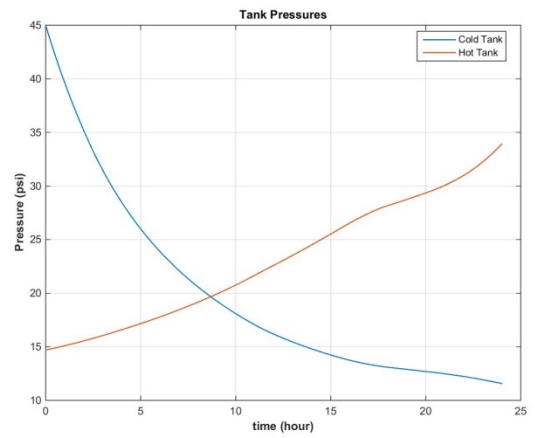
Figure 9.38: Tank Pressures

9.3 Additional Graphs for Stand-alone Reactor Response

9.3.1 mPower

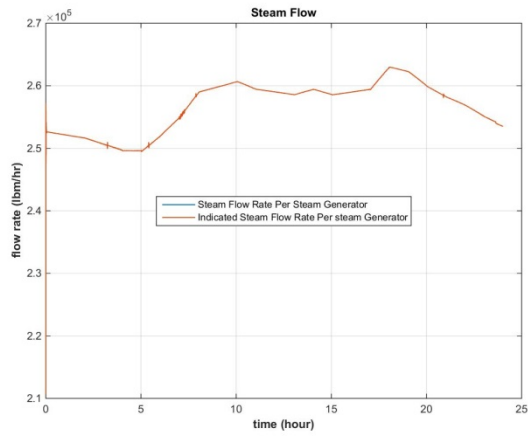### 9.3.1.1. Typical Summer Day
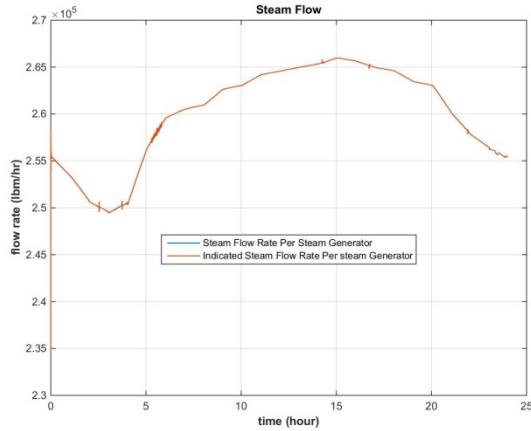
Figure 9.39: Steam Flow out of Steam Generator
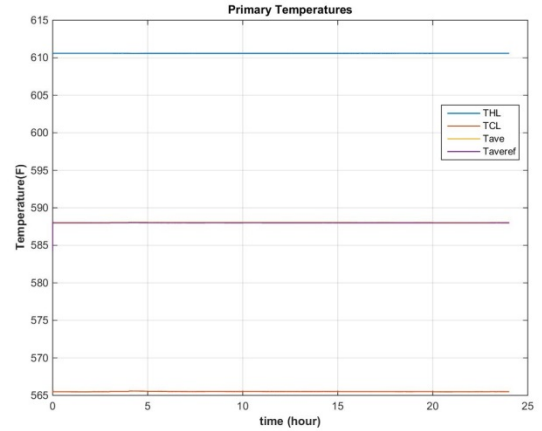
Figure 9.40: Primary Side Temperatures
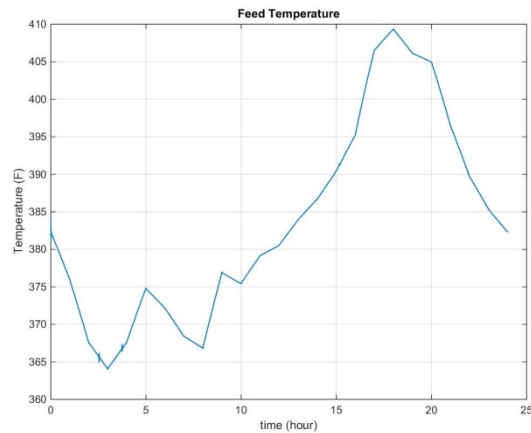
Figure 9.41: Feed Train Temperature
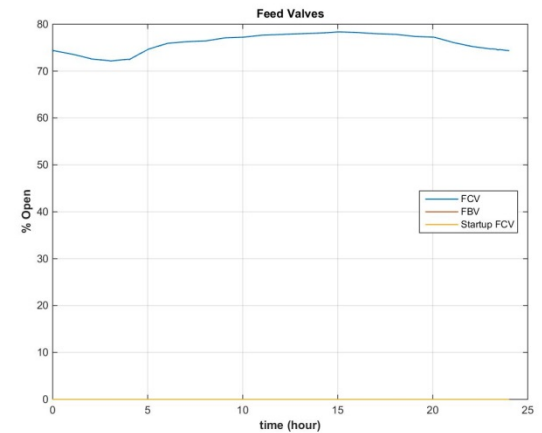
Figure 9.42: Feed Control Valve Position
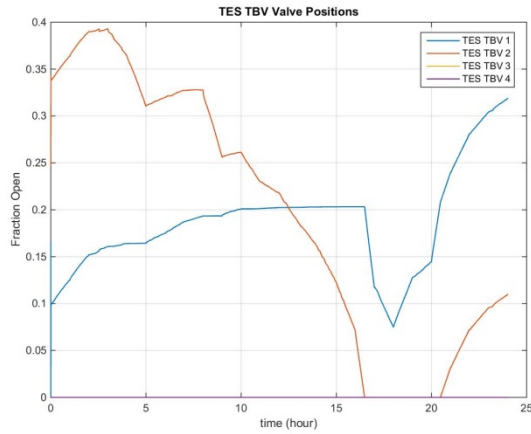
Figure 9.43: Auxiliary Bypass Valve Positions
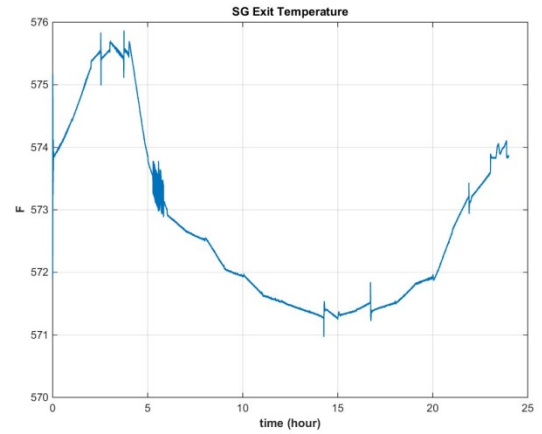
Figure 9.44: Steam Generator Exit Temperature

9.3.1.2. Typical Winter Day
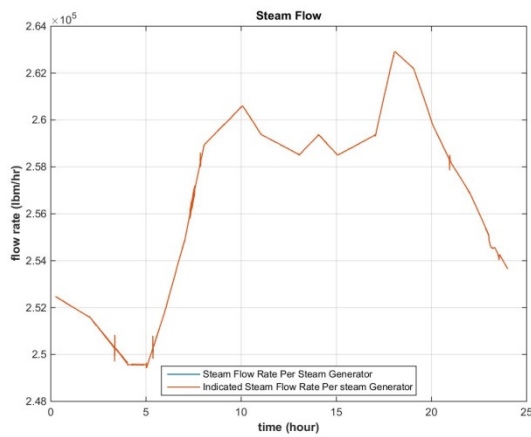
Figure 9.45: Steam Flow out of Steam Generator
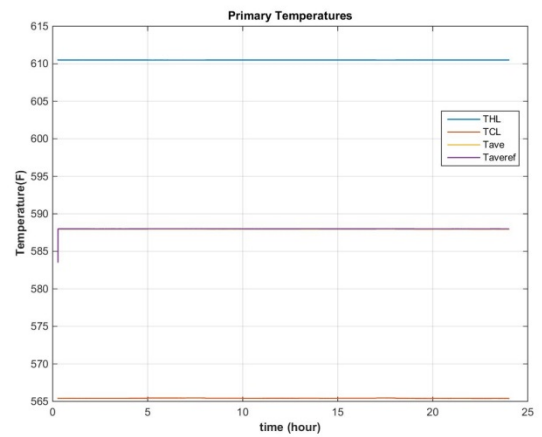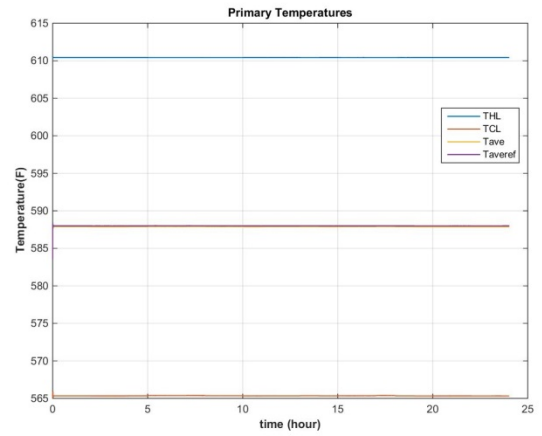

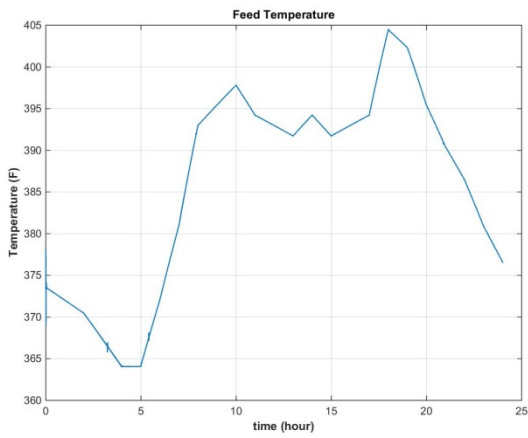**Figure 9.46: Primary Side Temperatures**

84
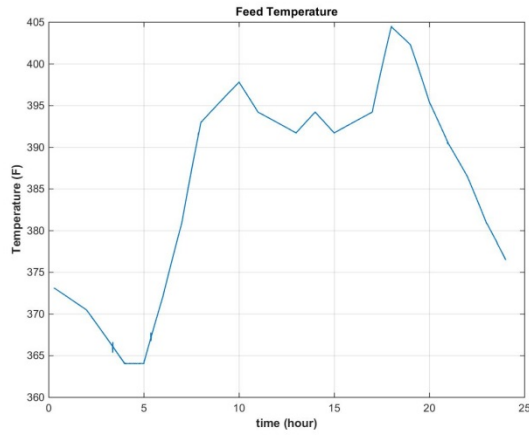
Figure 9.47: Feed Train Temperatures
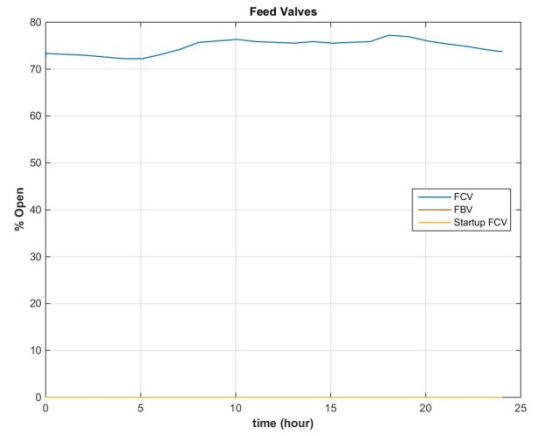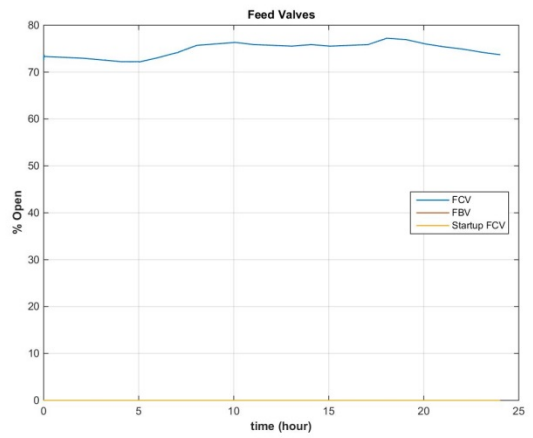

Figure 9.48: Feed Control Valve Position
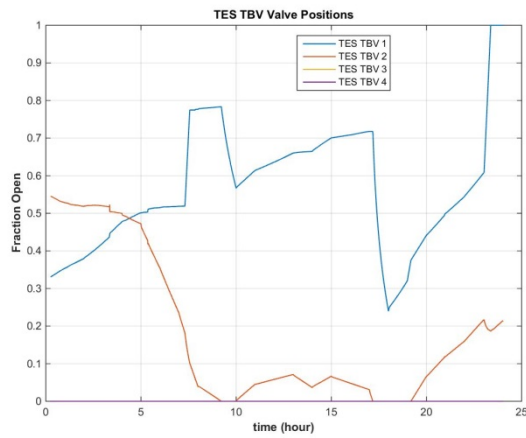
Figure 9.49: Auxiliary Bypass Valve Position
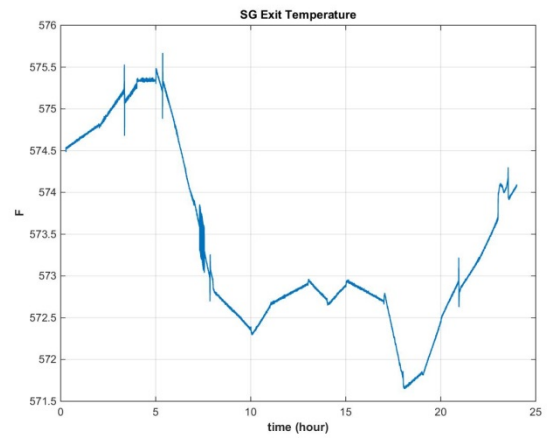
Figure 9.50: Steam Generator Exit Temperature

9.4 Additional graphs for full Reactor-TES simulations

9.4.1 Summer day – Including Solar
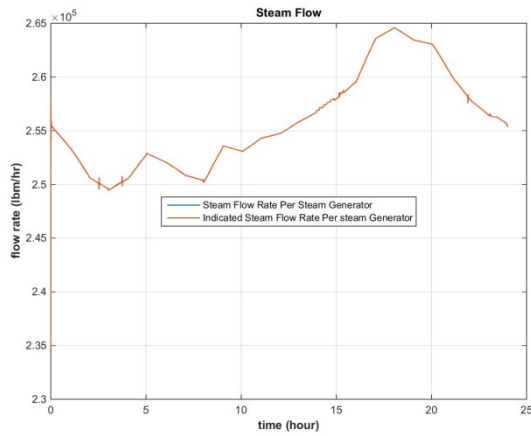
Figure 9.51: Steam Flow from Steam Generator
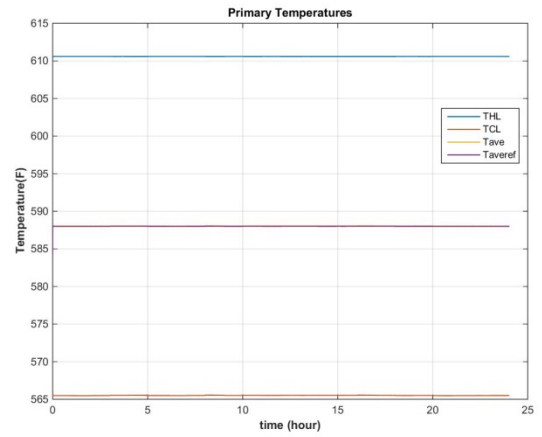
Figure 9.52: Primary side temperatures
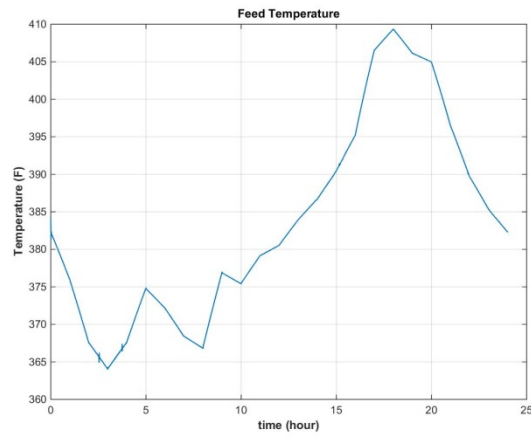
Figure 9.53: Feed Train Temperature
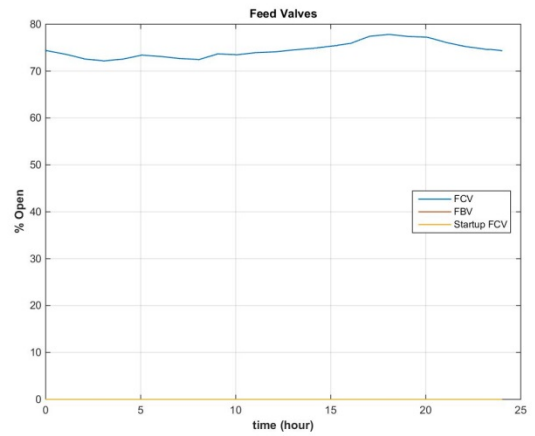
Figure 9.54: Feed Control Valve Position
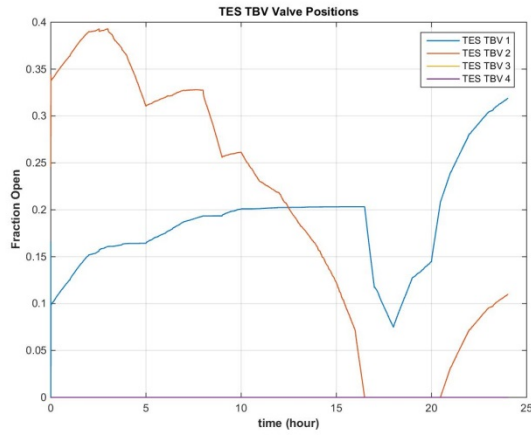
Figure 9.55: Auxiliary Bypass Valve Position
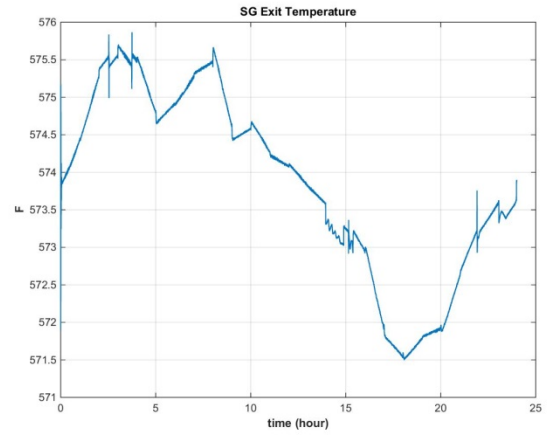
Figure 9.56: Steam Generator Exit Temperature
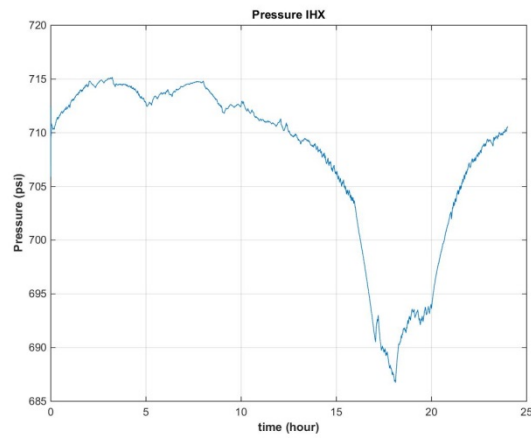
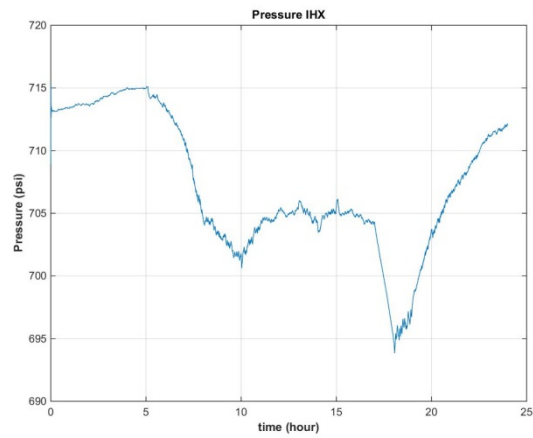**Figure 9.57: Pressure of Intermediate Heat Exchanger**
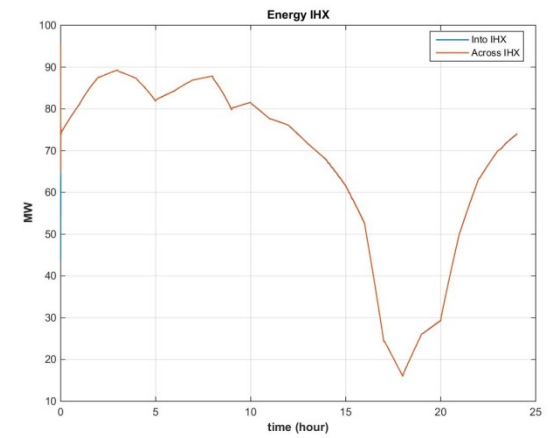
Figure 9.58: Energy dump into and across IHX.
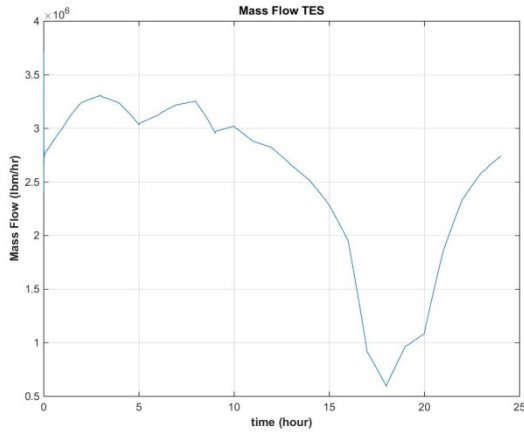
Figure 9.59: TES fluid flow rate
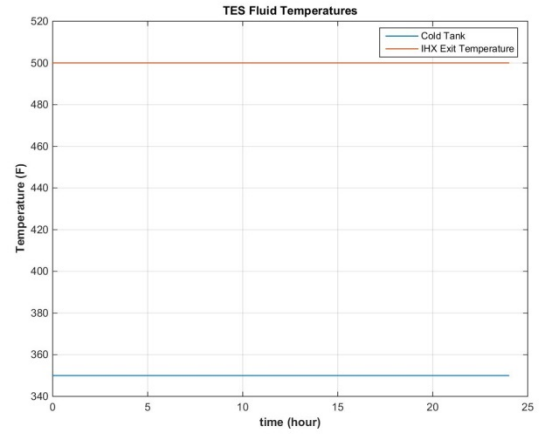
Figure 9.60: TES Fluid Temperature Leaving IHX.
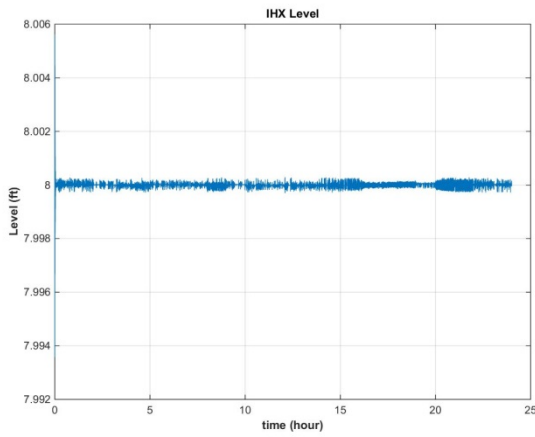
Figure 9.61. Intermediate Heat Exchanger Level
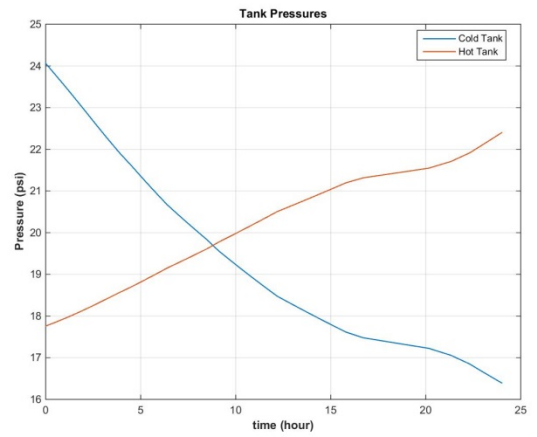
Figure 9.62: Tank Pressures.

88

9.4.2 Typical Winter Day

Figure 9.63: Steam Flow leaving Steam Generator

Figure 9.64: Primary side temperatures

Figure 9.65: Feed Train Temperatures

Figure 9.66: Feed Control Valve Position

89
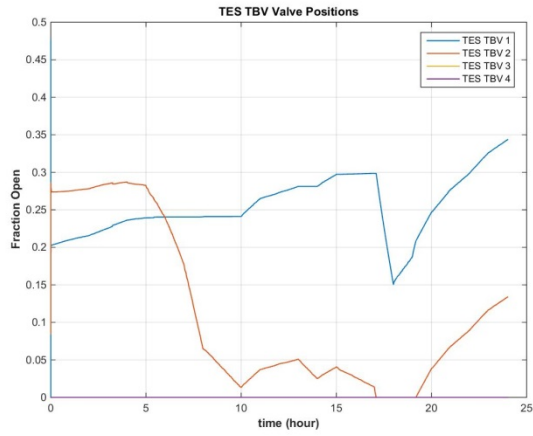
Figure 9.67: Auxiliary Bypass Valve Positions
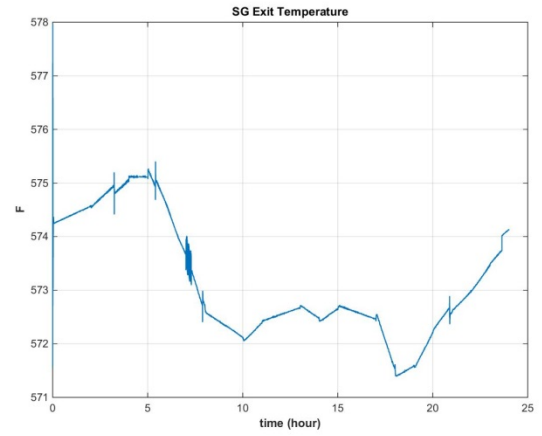
Figure 9.68: Steam Generator Exit Temperature
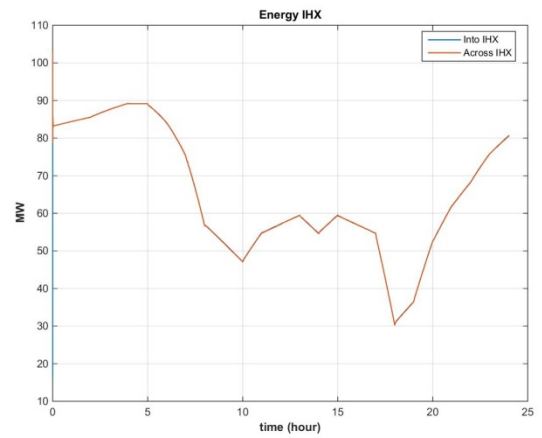

Figure 9.69: Intermediate Heat Exchanger Pressure
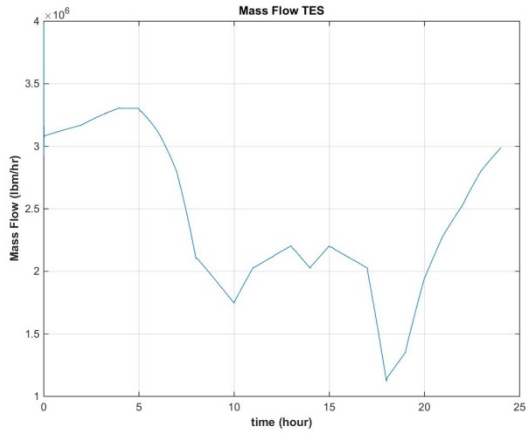

Figure 9.70: Energy dump into and across IHX.

90

Figure 9.71: TES Fluid Flow Rate

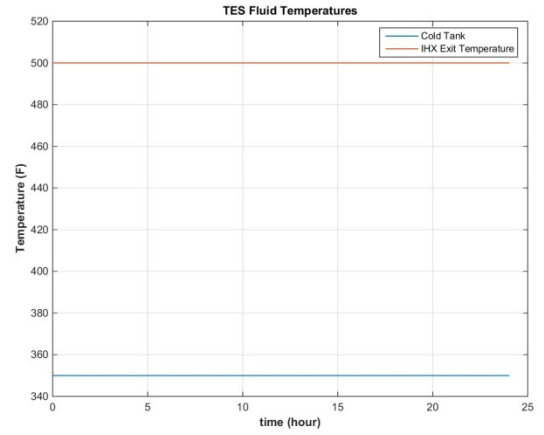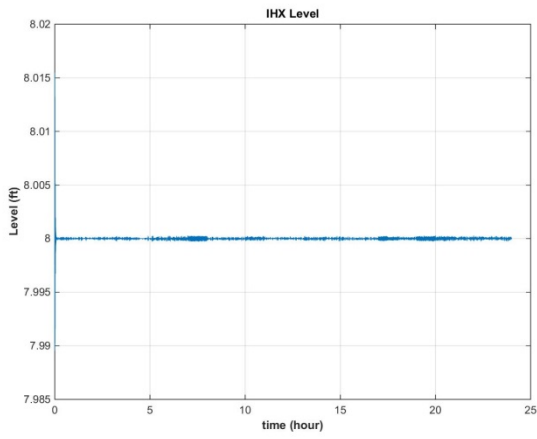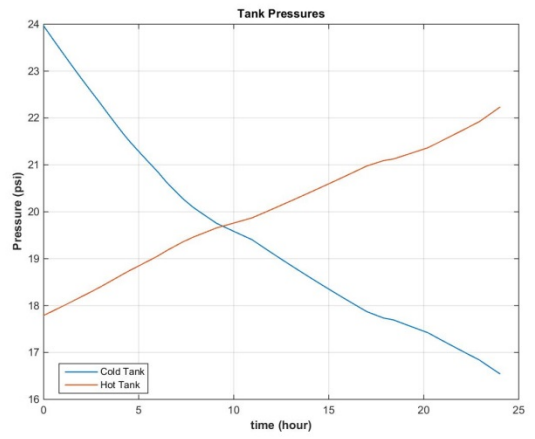**Figure 9.72: TES Fluid Temperature Leaving IHX.**

Figure 9.73: Intermediate Heat Exchanger Level

Figure 9.74: Tank Pressures.

91